

**Draft**

Draft Progress Report

Texas Environmental Research Consortium Project H-13

**Variable Industrial VOC Emissions and their impact on  
ozone formation  
in the Houston Galveston Area**

**Submitted by:**

**David Allen, Cynthia Murphy, Yosuke Kimura, William Vizueté, and Thomas Edgar  
Center for Energy and Environmental Resources  
The University of Texas  
Austin, Texas**

**and**

**Harvey Jeffries, Byeong-Uk Kim, Mort Webster and Michael Symons  
Department of Environmental Sciences and Engineering  
The University of North Carolina  
Chapel Hill, North Carolina**

**Submitted to:**

Texas Environmental Research Consortium

April 9, 2004

## Draft

### I. Executive Summary

The Houston-Galveston area (HGA) is designated as a severe ozone non-attainment region, and the State of Texas is charged with developing a State Implementation Plan (SIP) for reducing emissions that lead to ozone formation. A first step in developing the SIP is to characterize and quantify the emissions that lead to high ozone concentrations. In the HGA, developing inventories of emissions that lead to high ozone concentrations is more complicated than in many other urban areas because of the extensive industrial operations in the region.

Emissions from industrial facilities (point sources) are generally assumed, for SIP development purposes, to be continuous and at a nearly constant level. Emissions from Electricity Generating Units (EGUs) are the exception, and the State of Texas, and most other regions of the United States, use continuously collected data on emissions to characterize the role of EGUs in ozone formation. For petroleum refineries, chemical manufacturing facilities, and other industrial operations (non-EGUs), however, SIP analyses generally assume emissions are constant and continuous. This assumption is made because many non-EGUs operate 24 hours per day, 7 days per week, and their material throughput is nearly constant.

Recent evidence, from a variety of sources, demonstrates that while some types of emissions of volatile organic compounds from non-EGU point sources are constant, others are not. The evidence includes emission event reports, air pollutant measurements made by aircraft, air pollutant measurements made by ground monitors, and industrial process measurements. Daily emissions from a single facility can vary from annual average emissions by a factor of 10-1000. Variations of this magnitude at any single facility typically occur only a few times per year, but because there are so many facilities in the HGA, on many days, there is likely to be a facility experiencing significant emission variability.

Air quality measurements taken in recent field studies have also found evidence of localized regions with elevated concentrations of highly reactive volatile organic compounds (HRVOC). These regions with elevated HRVOC concentrations are frequently associated with very rapid ozone formation, leading to exceedances of the ozone air quality standard.

This report documents the evidence for HRVOC emission variability from non-EGU point sources, characterizes the nature of the variability and assesses the impact of variability on ozone formation processes in the HGA. The analyses presented in the report are summarized in a series of Findings.

**Finding 1: Variability in HRVOC emissions from point sources is significant and is due to both variability in continuous emissions and discrete emission events<sup>1</sup>.** *Roughly 3 times per month in 2003, reported emission events caused single facilities to have HRVOC emissions that were greater than 10,000 lb/hr (the total annual average emissions of HRVOCs, from all industrial point sources in the Houston-Galveston region is approximately 5,000 - 10,000 lb/hr). Roughly 3 times per week in 2003, reported emission events caused single facilities to have HRVOC emissions that were greater than 1,000 lb/hr. Roughly once a day in 2003, reported emission events caused single facilities to have HRVOC emissions that were greater than 100 lb/hr. Variability in continuous emissions is more difficult to quantify than emission variability due to reported emission events, but preliminary modeling indicates that variations in continuous (as opposed to discrete) HRVOC emissions could cause localized emissions of HRVOCs to double as frequently as once per month.*

*2-3 times per month HRVOC emissions variability > 10,000 lb/hr  
2-3 times per week HRVOC emissions variability > 1,000 lb/hr  
daily HRVOC emissions variability > 100 lb/hr*

The impact of emission variability on ozone formation can take multiple forms. If the emission variability is large enough, and the meteorological conditions are sufficiently ozone conducive, the variability in emissions may be sufficient to cause an exceedance of the National Ambient Air Quality Standard (NAAQS) for ozone (concentrations averaged over 1-hour) that would not have occurred in the absence of the emission event. Documentation, from TCEQ, is provided in the report for a 6700 pound release of ethylene that caused ozone NAAQS exceedances at multiple monitors.

As noted in Finding 1, however, very large variations in emissions are less common than smaller variations in emissions. While very large variations in emissions might lead to ozone NAAQS exceedances directly, more frequent, smaller variations in emissions have the potential to marginally increase the magnitude of ozone concentrations. If the HRVOC emission variability occurs at critical times and locations, it can marginally increase the peak ozone concentration that might be expected in the Houston-Galveston area.

Air quality modeling analyses were performed to assess the changes in peak, region-wide ozone concentrations that might be expected from HRVOC emission variability in the range of 100-5000 lb/hr.

**Finding 2: HRVOC emission variability in the range of 100-1000 lb/hr, which has been reported daily in the Houston-Galveston area, can increase peak, region-wide ozone concentrations, if the emission variability occurs in regions upwind of the location of the peak, region-wide ozone concentration.** *The magnitude of the increase in ozone concentration depends on the location of the emission variability, the time of day when the emission variability occurs and the magnitude of the non-variable ozone precursor emissions. Increases of 1-4 ppb in peak ozone concentration per 1000 lb/hr of HRVOC emission variability are expected at times and locations that are sensitive to emission variability. This sensitivity may increase as non-variable HRVOC emissions decrease and NO<sub>x</sub> emissions increase.*

**Finding 3: Emission variability of roughly 1000 lb/hr should be expected in the regions upwind of peak, region wide ozone concentration at least once per year in the Houston-Galveston area.** *This finding is based on estimates of the frequency of ozone conducive conditions and the frequency and magnitude of HRVOC emission events reported through a TCEQ database. This expected value could potentially be decreased by imposing short term limits on HRVOC emission variability.*

<sup>1</sup>Reportable emission events are defined by Texas Administrative Code (TAC) Title 30 Chapter 101. Section 101.1, paragraph (83) defines a reportable emissions event as “Any emissions event which, in any 24-hour period, results in an unauthorized emission equal to or in excess of the reportable quantity...”. The reportable quantity for HRVOCs is 100 lb. Emission variability, either discrete, or routine, may not in all cases result in a reportable emission event.

## Draft

## Contents

I.	Executive Summary	2
II.	Introduction	6
III.	Emission Inventories for air quality modeling in southeast Texas	7
IV.	Variability in emissions from industrial sources	15
	a.) Event emissions	
	b.) Continuous emissions	
V.	Ozone formation potential of variable emissions	37
	a.) Observational data	
	b.) Air quality modeling analyses	
VI.	Modeling tools for characterizing the ozone formation potential of variable emissions	52
	a.) Computationally efficient sub-domain models	
	b.) Combining 3-D photochemical and sub-domain models	
VII.	Characterizing the impact of variable emissions on attaining the NAAQS for ozone	88
	a.) Estimating the probability of emission events and impacts on peak ozone concentrations	
	b.) Impact of short term limits and other control scenarios on emission event magnitudes	

## II. Introduction

The Houston-Galveston area (HGA) is designated as a severe ozone non-attainment region, and the State of Texas, through the Texas Commission on Environmental Quality (TCEQ), is charged with developing a State Implementation Plan (SIP) for reducing emissions that lead to ozone formation in the HGA. A first step in developing the SIP is to characterize and quantify emissions of volatile organic compounds (VOCs) and oxides of nitrogen (NO<sub>x</sub>) that lead to ozone formation, especially the emissions of ozone precursors that produce the highest ozone concentrations.

Emissions are characterized and quantified in emissions inventories, and emission inventories are used for a variety of purposes. For example, emission inventories are used to establish state-wide and nation-wide trends in air quality. They are used to determine which categories of emission sources are most important in specific geographical areas. They are also used as inputs to models that attempt to predict air quality on specific days. The type of information that is required in an emission inventory depends on the way in which the inventory will be used. Emission inventories that are used to establish air quality trends at regional or national scales need only have information about average emission rates. However, emission inventories that will be used in models that predict air quality on specific days, or that are used to predict the likelihood of extremes in air pollutant concentrations, must consider both average emission rates and the daily variability in emissions.

The concept that daily, even hourly, variability in emissions must be accounted for in air quality modeling of specific days, or analyses used to predict extremes in air pollutant concentrations, is well established for certain categories of emissions. For example, when considering biogenic emissions (compounds released by vegetation) or the vaporization of fuel from vehicles, inventories used to establish national trends report emissions developed for average “ozone season days”. Temperatures and the intensity of sunlight, which influence these emissions, are based on average data or data from representative days. In contrast, when an emission inventory is to be used for modeling air quality on a specific day or days, the temperatures and sunlight intensities for those specific days are used. Emission rates on specific days can be significantly different than on average days.

This same concept is also applied to some, but not all, emissions from large industrial facilities (commonly referred to as point sources). For electricity generating units (EGUs) that emit largely NO<sub>x</sub> and sulfur oxides (SO<sub>x</sub>), emissions inventories are used in defining rules that limit acid precipitation. These inventories are based on annual or seasonal emission rates. In contrast, when emissions from EGUs are needed to evaluate ozone formation on specific days, hourly emission rates on those days are used in models designed to predict air quality.

For petroleum refineries, chemical manufacturing facilities, and other industrial operations (non-EGUs), however, emissions, even those used to predict air quality on specific days, are generally assumed to be continuous and at a nearly constant level. A large body of observational evidence from the Houston-Galveston area indicates that these emissions are not constant and can have variability that has a significant impact on the prevalence of extreme ozone concentrations. This report documents the evidence for emission variability from non-EGU point sources,

## Draft

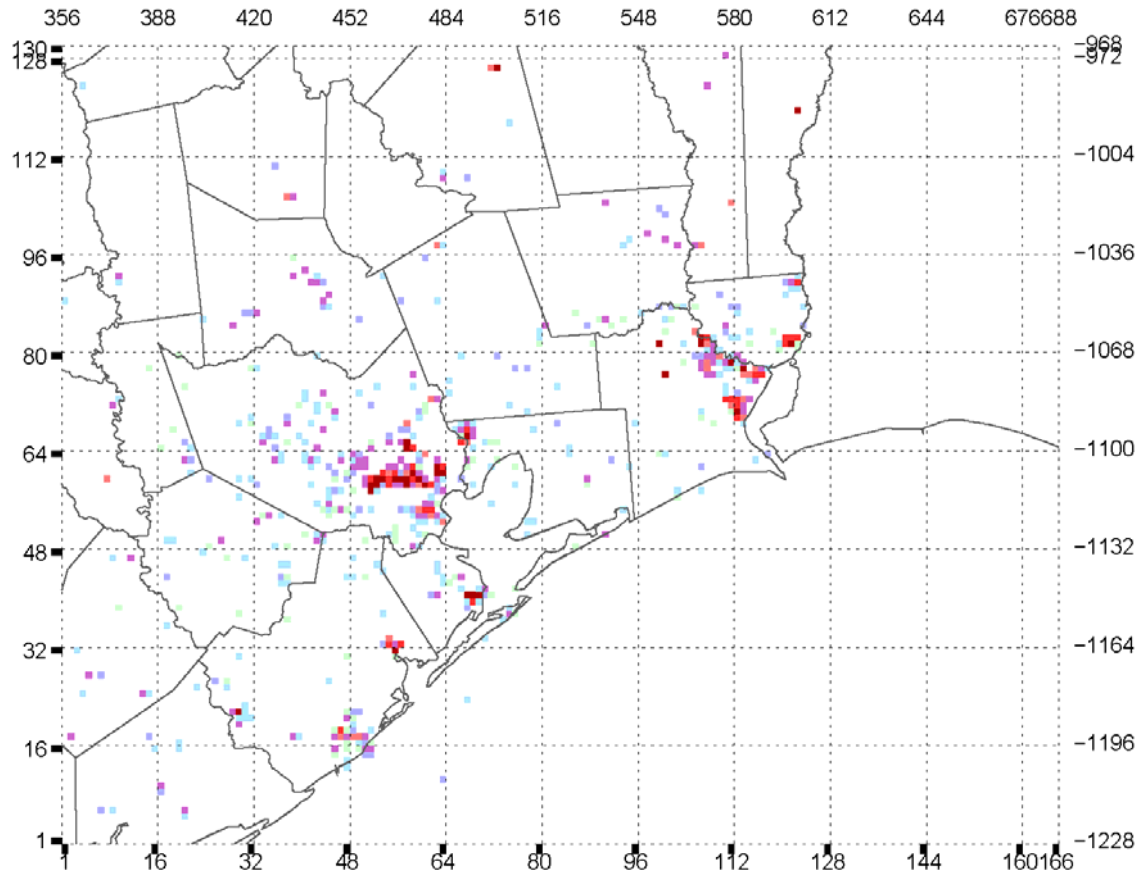
characterizes the nature of the variability and assesses the impact of variability on ozone formation processes in the HGA.

### III. Emission inventories for air quality modeling in southeast Texas

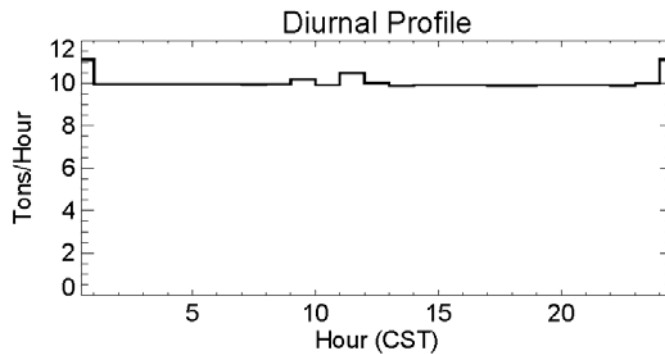
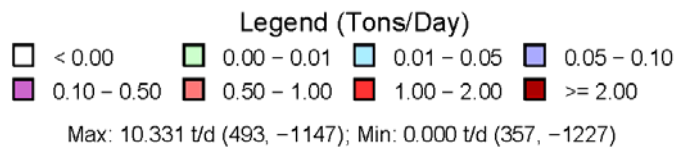
Inventories of the emissions that lead to ozone formation in the HGA have been continually updated and reviewed for decades (for a review, see Allen, et al., 2003), and the emission inventories developed by the State of Texas for air quality modeling are among the most detailed that have ever been assembled. In the summer of 2000, however, a large air quality field program was undertaken in southeast Texas and the unique measurements that were deployed during that field program provided new insights into the magnitude and variability of ozone precursor emissions, especially the emissions of VOCs from industrial facilities (point sources). Subsequent measurements and analyses, especially at industrial facilities, have further defined the features of point source emissions in the HGA.

Figure 1 summarizes one of several sets of point source VOC emissions that have been used to simulate air quality for August 25, 2000. The emissions, as a function of time of day, shown in the lower right portion of the Figure, clearly indicate that for this emission inventory point source VOC emissions are treated as nearly constant. Figure 2 shows that for this, and other point source VOC emission inventories, most of the emissions are calculated or estimated, rather than directly measured.

Draft



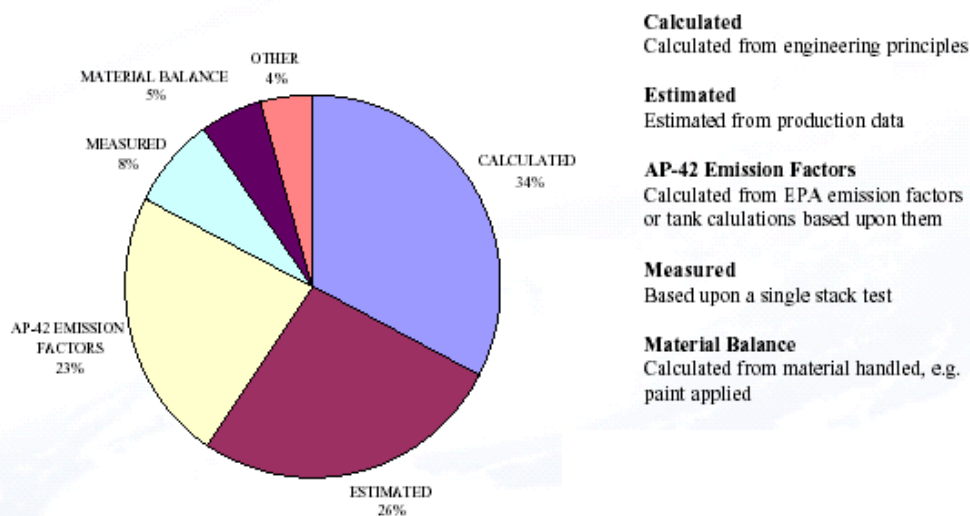
Emissions Plotted	
County	Tons/Day
Brazoria	16.59
Chambers	7.40
Fort Bend	1.34
Galveston	28.87
Harris	107.48
Liberty	1.49
Montgomery	2.00
Waller	0.41
HG SUBTOTAL:	165.57
Hardin	1.66
Jefferson	44.01
Orange	15.83
BPA SUBTOTAL:	61.50
MAP TOTAL:	240.40



**Figure 1.** Example of one set of point source VOC emissions used in TCEQ’s air quality model for August 25, 2000. Note the nearly constant diurnal profile to apportion the daily emission to hour of the day.



## 2000 HG VOC Emissions by EI Method



Dataset: Oracle.psd\_b\_alloc\_2000\_v15

**Figure 2.** The Houston-Galveston Year 2000 VOC Point Source Emissions by method used to determine the emission magnitudes. (Cantu, 2004)

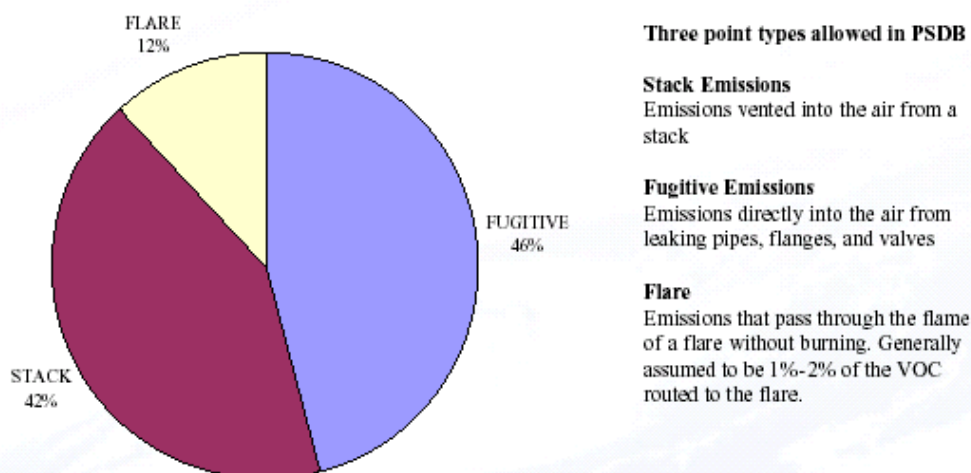
The data in Figures 1 and 2 summarize information on point source VOC emissions from approximately 30,000 distinct sources, called FINs, in the Houston-Galveston area. These FINs are connected to atmospheric emission points (called EPNs) that are classified by “point type”. The point source emission database has historically had three major types of EPNs, but others are being added. The types of EPNs used historically are:

- **FL** – flares
- **FU** – fugitive emissions
- **ST** – stacks

Figure 3 shows the contribution of these emission point types to the HGA inventory.



## 2000 HG VOC Emissions by PSDB Point Type



Dataset: Oracle.psdh\_alloc\_2000\_v15

**Figure 3.** The contribution of emission point types to Houston-Galveston Year 2000 VOC Point Source Emissions (Cantu, 2004)

Work is underway to add additional point types such as

- **CT** – cooling towers
- **PV** – polymer vents
- **TK** – tanks
- **ELF** – equipment leak fugitives
- **COM** – combustion device
- **CD** – control device
- **WW** – waste water fugitives

Another important component of VOC emission inventories are the “speciation profiles” that characterize the composition and therefore the atmospheric reactivity of the VOC emissions. Each of the tens of thousands of FINs in the inventory is assigned a profile, resulting in approximately 10,000 distinct speciation profiles. The overall composition of the the VOC inventory (in a historically used inventory) is summarized in Figure 4.

Because certain hydrocarbons are highly reactive in the atmosphere, and can play a significant role in the rapid ozone formation that is observed in the Houston-Galveston area, a group of highly reactive VOCs (HRVOCs) in the inventory merits special attention. These HRVOCs include ethene, propene, butenes, and 1,3-butadiene, and they are among the compounds

identified in Figure 4. Ambient observations from a variety of sources are being used to revise the estimated emissions of these compounds, so the emissions of HRVOCs shown in Figure are subject to considerable adjustment.

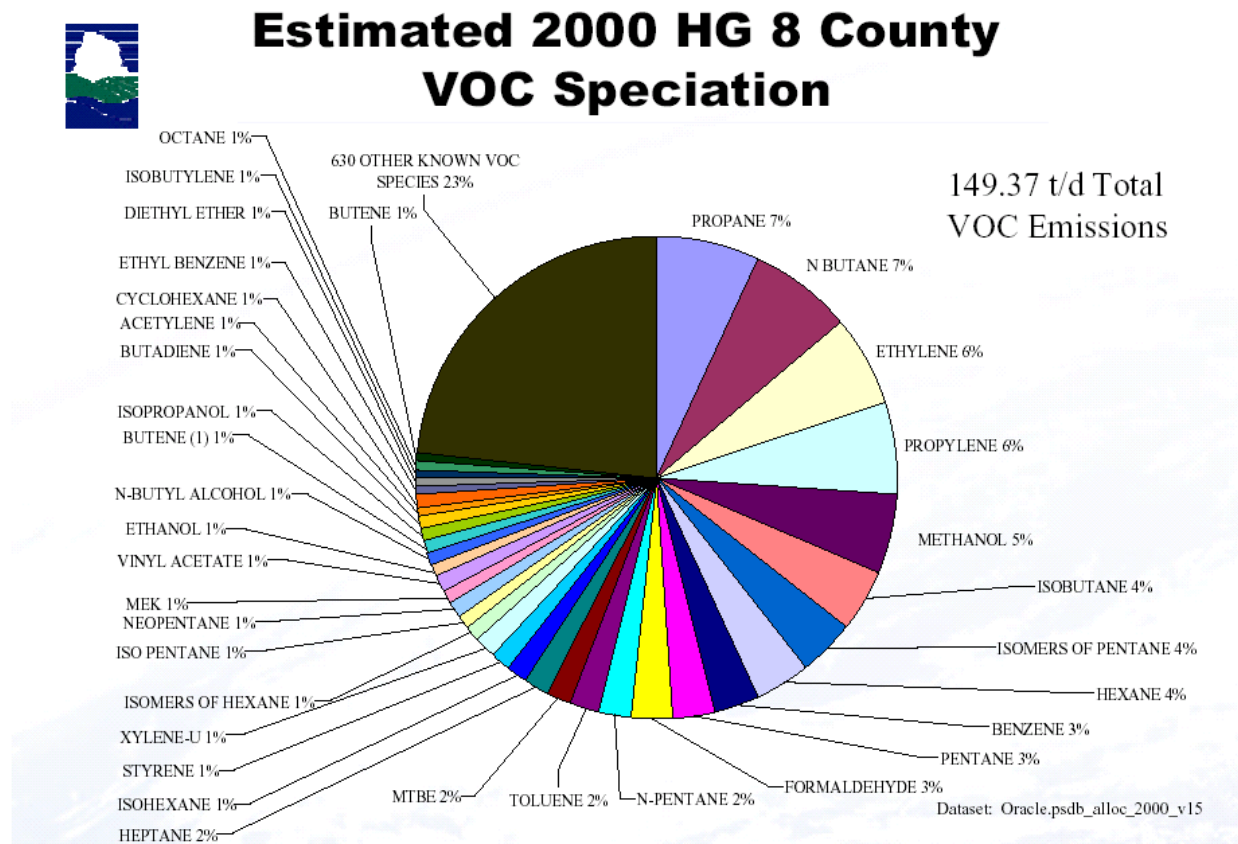


**Figure 4.** The fractional contribution of major VOC species to Houston-Galveston Year 2000 VOC Point Source Emissions. (Cantu, 2004)

Regardless of the absolute magnitude of the point source HRVOC emissions, the emissions of highly reactive volatile organic compounds (HRVOCs, which include ethene, propene, butenes and 1,3-butadiene) are dominated by a small number of source categories. Shown in Table 1 is a list of the major emission source categories for ethene. A small number of source categories account for the majority of the emissions. Even within major source categories, such as chemical manufacturing, a small number of unit processes can lead to the majority of the emissions. Figure 5 shows that fugitive emissions, and emissions from flares, vents and cooling towers dominate the inventory of routine emissions of HRVOCs from point sources in the Houston-Galveston area.

**Draft**

**Table 1.** Fractions of the ethylene point source inventory assigned to source categories (based on historical inventory data)

Industrial Processes	Chemical Manufacturing	Plastics Production	0.244
Industrial Processes	Chemical Manufacturing	Fugitive Emissions	0.137
Industrial Processes	Chemical Manufacturing	Butylene, Ethylene, Propylene, Olefin Production	0.126
Industrial Processes	Chemical Manufacturing	General Processes	0.108
Industrial Processes	Chemical Manufacturing	Other Not Classified	0.057
Industrial Processes	Chemical Manufacturing	Fuel Fired Equipment	0.044
Industrial Processes	Petroleum Industry	Fugitive Emissions	0.041
Industrial Processes	Cooling Tower	Process Cooling	0.032
Industrial Processes	Petroleum Industry	Cooling Towers	0.030
Industrial Processes	Petroleum Industry	Flares	0.021
Industrial Processes	Oil and Gas Production	Natural Gas Production	0.019
Industrial Processes	Petroleum Industry	Petroleum Products - Not Classified	0.013
Internal Combustion Engines	Industrial	Natural Gas	0.012
Petroleum and Solvent Evaporation	Petroleum Liquids Storage (non-Refinery)	Bulk Terminals	0.011
Petroleum and Solvent Evaporation	Organic Solvent Evaporation	Miscellaneous Volatile Organic Compound Evaporation	0.011
Industrial Processes	Chemical Manufacturing	Vinyl Acetate	0.011
Industrial Processes	Petroleum Industry	Blowdown Systems	0.010
Industrial Processes	Miscellaneous Manufacturing Industries	Miscellaneous Manufacturing Industries	0.009
Petroleum and Solvent Evaporation	Petroleum Liquids Storage (non-Refinery)	Petroleum Products - Underground Tanks	0.007
Industrial Processes	Chemical Manufacturing	Ethylene Glycol	0.007
Industrial Processes	Oil and Gas Production	Fugitive Emissions	0.007
Industrial Processes	Chemical Manufacturing	Ethylene Oxide	0.005

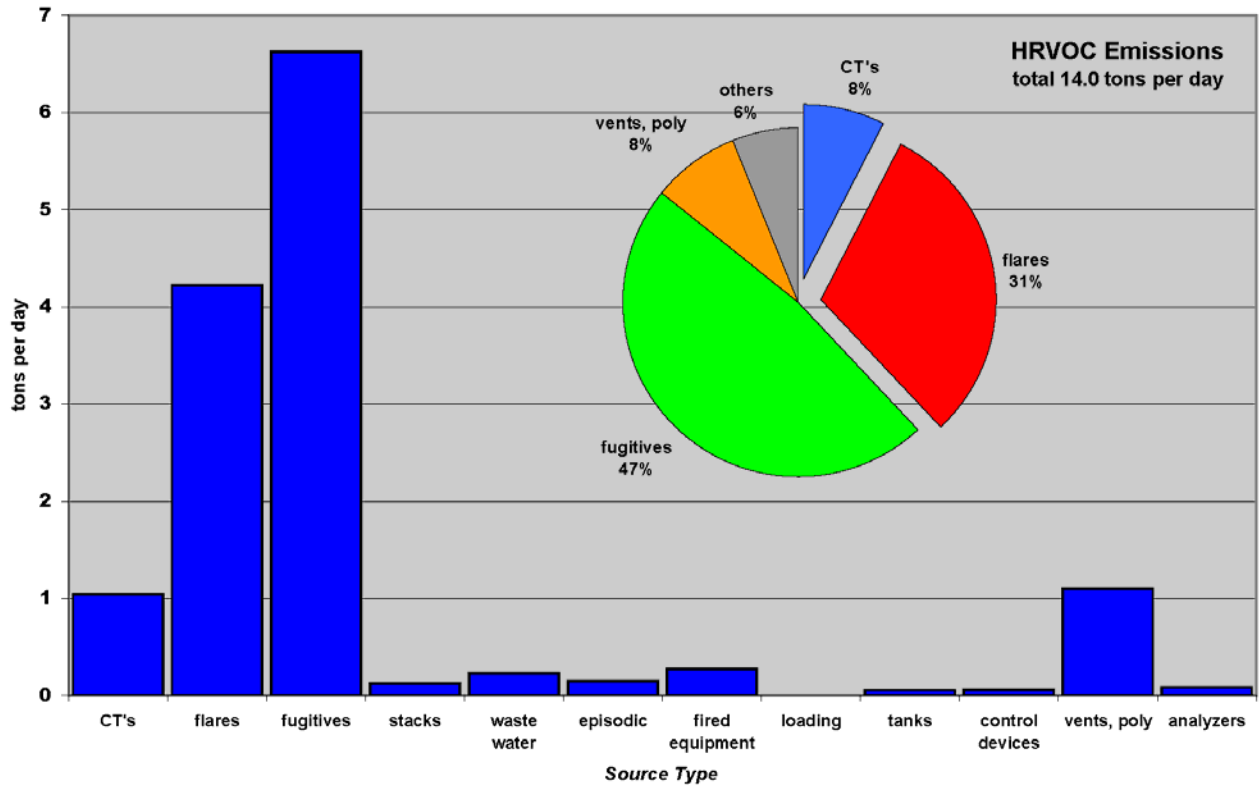


**Figure 5.** Sources of emissions of highly reactive volatile organic compounds (ethene, propene, butanes and 1,3-butadiene) from point sources in the Houston-Galveston area

Finally, even among the source categories with large emissions and the unit operations within those source categories with large emissions, a small number of individual units account for a large fraction of the emissions. For example, Figure 6 shows that less than 5% of the total flares in the HGA account for 50% of the total flare emissions.

To summarize, there are tens of thousands of point sources of VOC emissions in the Houston-Galveston area. These VOC emissions include significant quantities of HRVOCs emitted by flares, cooling towers and as fugitives, and a small number of sources contribute the bulk of the HRVOC emissions. Point source VOC and HRVOC emissions have generally been assumed to be continuous and constant, but data, summarized in the next section, indicates that the emissions can have substantial variability.

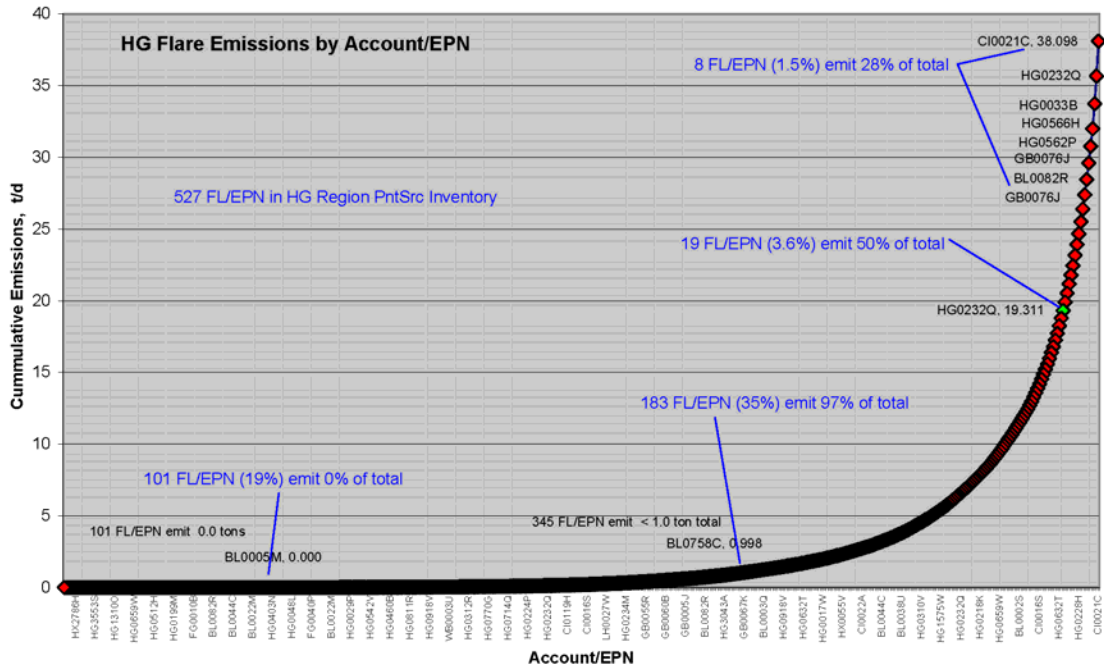


Figure 6. Emissions from flares sorted by emission rate; 19 flares (3.6% of 527) account for the majority of the total flare emissions

## IV. Variability in emissions from industrial sources

Emissions from industrial sources can be divided into four major categories:

- Emissions released at a constant rate due to continuous process operation (nearly constant emissions)
- Emissions released at a variable rate due to fluctuations in process operations (routinely variable emissions)
- Episodic emissions that lead to a significant increase in daily emission rate, yet are below the maximum daily permit level (allowable episodic emission events)
- Emergency releases and other event driven emissions that lead to daily emissions greater than permitted levels (large episodic emission events)

This section describes data available on each of these potential sources of variability in emissions, beginning with large, episodic emission events.

### IV a. Event Emissions

Prior to late 2002, emission events above permitted levels were not recorded on a regular basis unless a reportable emission of greater than 5000 pounds in a 24-hour period was released. Both lack of data and the lack of easy access to the data has made it difficult to quantitatively and accurately determine whether the magnitude and or frequency of event emissions appreciably affects ozone concentrations and rates of ozone formation, and if so how they are most effectively addressed in photochemical modeling and policy development.

Effective September 12, 2002, per Texas Administrative Code (TAC) Title 30 Chapter 101 (TAC, 2002), reporting requirements were changed and reportable quantities were reduced from 5000 lbs. to 100 lbs. for most compounds in the Houston/Galveston ozone non-attainment area. Section 101.1, paragraph (83) defines a reportable emissions event as “Any emissions event which, in any 24-hour period, results in an unauthorized emission equal to or in excess of the reportable quantity...”. Alkanes remain at the 5000 lb limit provided they contain less than 0.02% of ethene (ethylene), propene (propylene), butene (butylenes), toluene, acetaldehyde, or oxides of nitrogen, and less than 2.0% of any other reportable compound. In addition, Texas House Bill (HB) 2912 requires that air emission incidents be filed electronically and be posted in a publicly accessible database (TCEQ, 2002; Texas House, 2003). This has resulted in the availability of on-line data for events beginning January 31, 2003 (2003b). These newly available data provide new insight into the magnitude and variability of emission events, especially those of highly reactive volatile organic compounds. The data will be used to address two key questions:

Question 1: *Are the magnitudes of emission events, singularly and collectively, significant relative to that of continuous emissions?* The effect of individual events is examined by calculating flow rates (pounds per hour) of oxides of nitrogen (NO<sub>x</sub>), volatile organic compounds (VOC), and HRVOC during events and comparing these against annual average flow rates.

**Draft**

Question 2. *What are the characteristics of the events in terms of time, space, and composition?* The facilities, types of facilities, and/or facility locations that have the largest (greatest mass), most frequent, and most persistent events are identified.

In order to answer these questions, data have been collected from the Texas Commission on Environmental Quality (TCEQ) Air Emission Event Reports, which can be downloaded from the Internet through an on-line reporting system (TCEQ, 2003b). The data were imported into a relational Microsoft Access® database developed by the University of Texas at Austin and data for analysis are selected and aggregated by enacting queries within the database. The database is described in the Appendix.

As of December 31, 2003, a total of 1727 events occurring in TCEQ Region 12 (which includes the Houston-Galveston area) and beginning on or after January 31, 2003 had been posted on the TCEQ web site (TCEQ, 2003b). A summary of these events is presented in Table 2. The release of HRVOCs was involved in approximately 40% (711) of these events. Significant HRVOC event emissions, both in terms of frequency and mass are limited to four counties, Harris, Brazoria, Galveston, and Chambers; 709 out of 711 (99.72%) events and 1,666,540 lbs out of 1,667,009 lbs (99.97%) occur in these four counties.

**Table 2.** TCEQ Region 12 events posted between January 31, 2003 and December 31, 2003

County	All Events	HRVOC Events	Event HRVOCs		Point Source HRVOCs TPY (2000)**	Point Source VOCs TPY (2001)*
			lbs	tons		
Harris	934	423	816,961	408	4,736	28,992
Brazoria	331	187	759,853	380	1,433	6,251
Galveston	329	86	69,229	35	515	8,342
Chambers	53	13	20,497	10	112	1,788
<b>4 County Total</b>	<b>1,647</b>	<b>709</b>	<b>1,666,540</b>	<b>833</b>	<b>6,796</b>	<b>45,373</b>
Fort Bend	40					798
Montgomery	19					730
Liberty	1	1	558	<1		475
Waller	2					205
<b>HGA Total</b>	<b>1,709</b>	<b>710</b>	<b>1,667,098</b>	<b>833</b>	<b>6,796</b>	<b>47,581</b>
Matagorda	11	1	1	<1		290
Colorado	4					170
Wharton	2					525
Walker	1					16
Austin	0					458
<b>Region 12 Total</b>	<b>1,727</b>	<b>711</b>	<b>1,667,099</b>	<b>833</b>	<b>6,796</b>	<b>49,040</b>

\*TCEQ Point Source Database (TCEQ, 2003c)

\*\*TCEQ Special Inventory (TCEQ, 2003d)

It can be seen from Table 2 that the mass of emitted HRVOCs is relatively low when considered on an annual time-scale and over a broad geographic region (i.e., at the county level). The mass of HRVOCs emitted as events, relative to annual VOC emissions, is less than 2%; relative to annual HRVOC emissions HRVOC event emissions constitute about 12% of the total. However, events are extremely limited in time and space and thus event emissions have the potential to be

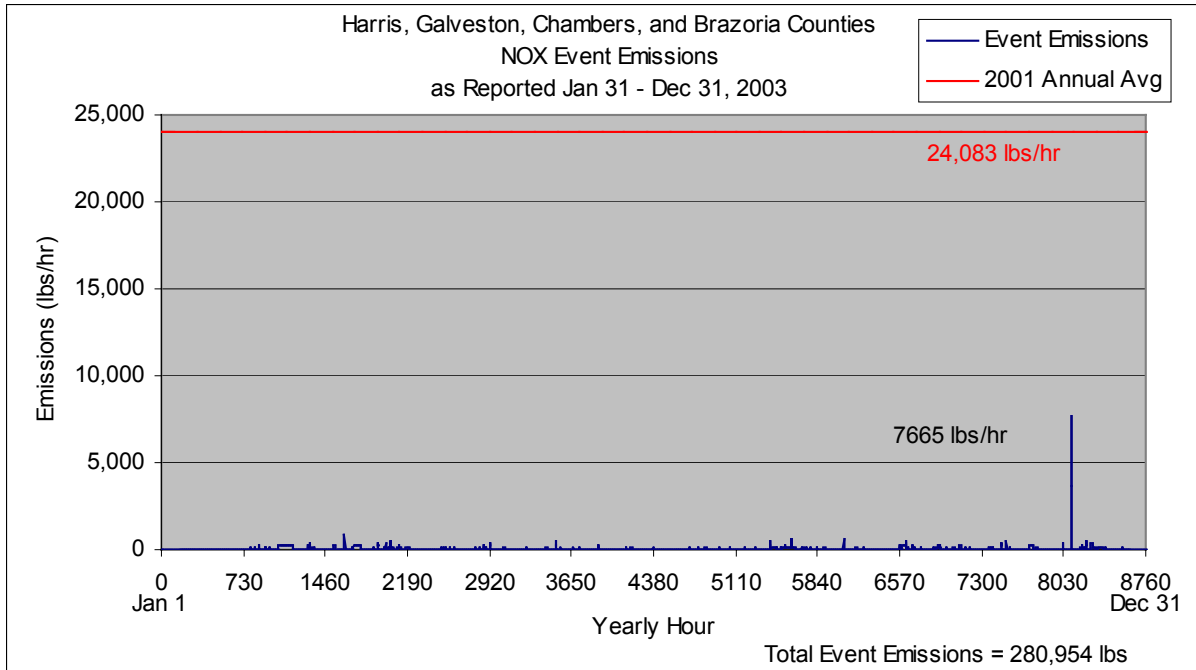
## Draft

extremely concentrated. This characteristic is critical to development of an accurate HGA emissions inventory and consequently to understanding and modeling the formation of ground-level ozone.

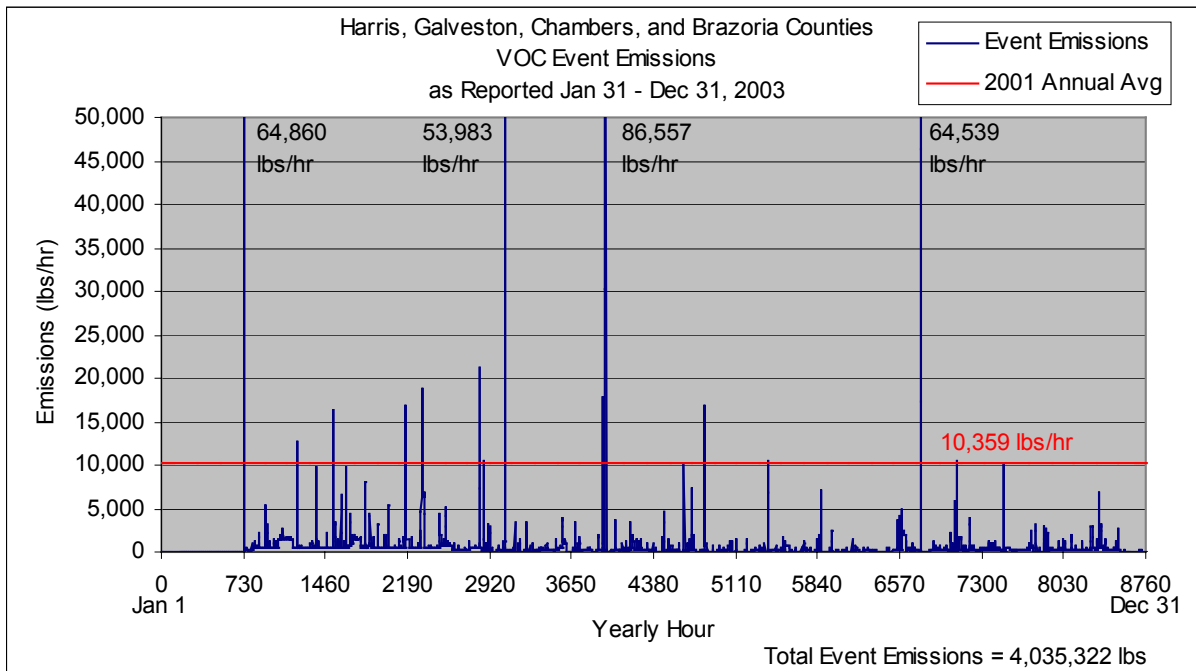
When the data summarized in Table 2 are presented as emission rates for each hour, over the course of a year (an annual time series), the temporal pattern of the emissions becomes clearer (Methods used in developing the time series are described in the Appendix). Figure 7 presents a time series of NO<sub>x</sub> event emissions facilities in a 4 county region (Brazoria, Harris, Galveston and Chambers counties). To provide a point of comparison for the event emissions, the average annual flow rate in pounds per hour for all facilities in the 4 county region has been calculated from the 2001 TCEQ Point Source Database (TCEQ, 2003c) and is graphed as a horizontal line at 24,083 lbs/hr. As can be seen in the figure, only one event exceeds a NO<sub>x</sub> flow rate of 1000 lbs/hr and that event, at 7665 lbs/hr is less than a third of the annual average, routine emissions. In the case of NO<sub>x</sub> emissions, it appears that individual events do not significantly add to the magnitude of the inventory. Furthermore the total mass of NO<sub>x</sub> contributed by events is only 140 tons (280,954 lbs) per year or 0.1% of the 105,482 tons per year emitted by point sources located within the four counties. Thus the magnitude of NO<sub>x</sub> from events appears not to be significant relative to that of routine emissions, either singularly or collectively.

Figure 8 presents a time series of VOC event emissions in the same format as the NO<sub>x</sub> event emissions. The average annual flow rate for routine emissions for all of the facilities in the 4 county region, 10,359 lbs/hr based on historical inventories, appears as a horizontal line. In contrast to NO<sub>x</sub>, there are 14 times during the eleven-month period in which VOC event emissions exceed the annual average. The time involved is 18 hours. In four instances, the flow rate of event emissions is more than five times the annual average with a maximum of 86,557 lbs/hr. The total mass of greater than 4 millions pounds (2018 tons) contributes 4% to the 45,373 tons of VOC emitted during a single year from point sources in the four counties. Therefore, if event reports are complete and reasonably accurate, individual VOC events may have an impact on the magnitude (total mass) of the inventory when considered locally and over limited amounts of time, but collectively they do not add significantly to the annual, regional inventory.

The frequency of these events warrants further investigation. Many of the events involve unspiciated VOCs and it is unknown whether these many involve significant amounts of HRVOCs. In addition, VOCs that have lower reaction rates than the four identified HRVOC species may be of interest because of their large total mass and persistence. However, a larger examination of VOCs is out of the scope of the current effort.



**Figure 7.** NO<sub>x</sub> emissions (lbs/hr) from events and as an annual average (from 2001) are presented in a time series using 8760 one-hour time blocks for a single year. NO<sub>x</sub> event emissions exceed 1000 lbs/hr only once and never exceed the total 2001 annual average for all facilities in the 4 county area. Event emission data are from TCEQ (2003b) and point source data are from TCEQ (2003c).



**Figure 8.** VOC emissions (lbs/hr) from events and as an annual average (from 2001) are presented in a time series using 8760 one-hour time blocks for a single year. There are 14 times during a roughly eleven-month time period when VOC event emissions exceed the total 2001 annual average of 10,359 lbs/hr for all facilities in the 4 county area. Event emission data are from TCEQ (2003b) and point source data are from TCEQ (2003c).

## Draft

A time series for HRVOC emissions is shown in Figure 9. The annual average of routine HRVOC emissions is calculated from the 2000 special inventory (TCEQ, 2003d), which is the only generally available TCEQ inventory that contains speciated HRVOC emissions. The flow of HRVOC event emissions exceeds the 1500 lb/hr annual average 29 times during the eleven-month period (almost 3 times per month), impacting a total of 115 hours. There are 7 times (8 hours) when the flow exceeds 5 times that of the annual average, with a maximum of 39,340 lbs/hr. HRVOC event emissions also account for an estimated 12% of the total HRVOC mass emitted over the year based on the 828 tons (1.6 million pounds) emitted in 2003. Therefore, if event reports are complete and reasonably accurate, HRVOC events have a significant impact on the magnitude (total mass) of the inventory when considered both individually and collectively. In addition, the frequency is such that they have a marked effect on the temporal profile.

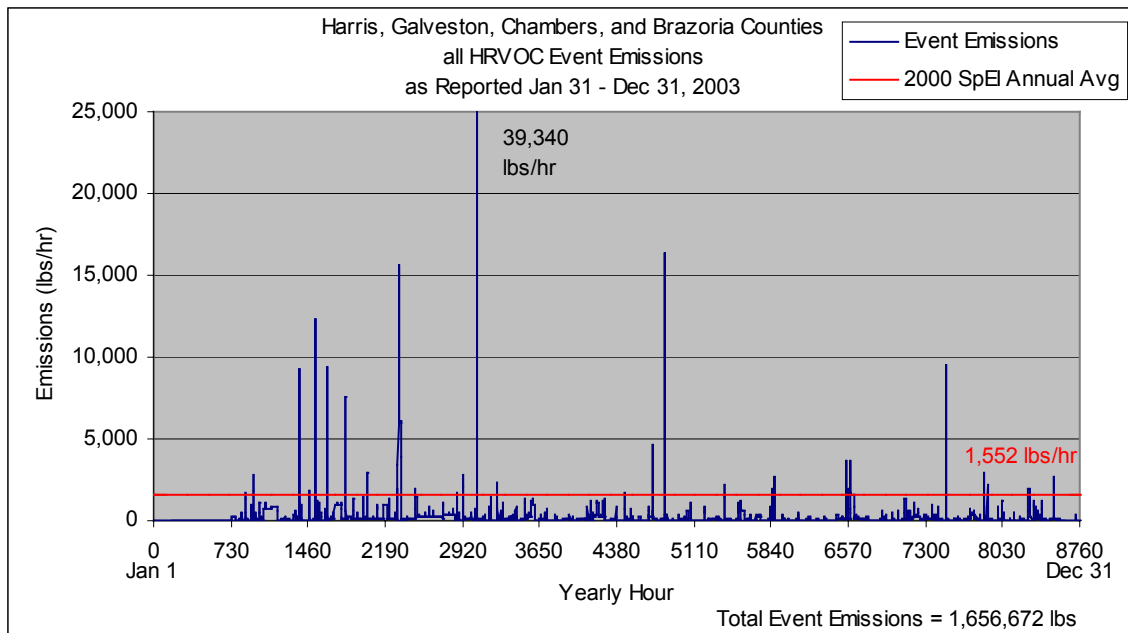


**Figure 9.** HRVOC emissions (lbs/hr) from events and as an annual average (from 2001) are presented in a time series using 8760 one-hour time blocks for a single year. There are 29 times during a roughly eleven-month time period when HRVOC event emissions exceed the 2000 annual average of 1,552 lbs/hr. Event emission data are from TCEQ (2003b) and point source data are from TCEQ (2003d).

Four species, or groups of species have been designated as HRVOCs; these are 1,3-butadiene, all isomers of butene, propene (propylene), and ethene (ethylene). For events beginning January 31, 2003 and posted through December 31, 2003, the total 1,3-butadiene event mass is 53,383 pounds, the total butene event mass is 105,089 pounds, the total propene (propylene) mass is 543,783, and the total ethene (ethylene) mass is 954,418 pounds. Time series for event emissions for each of these have been developed and are given in Figures 10, 11, 12, and 13.

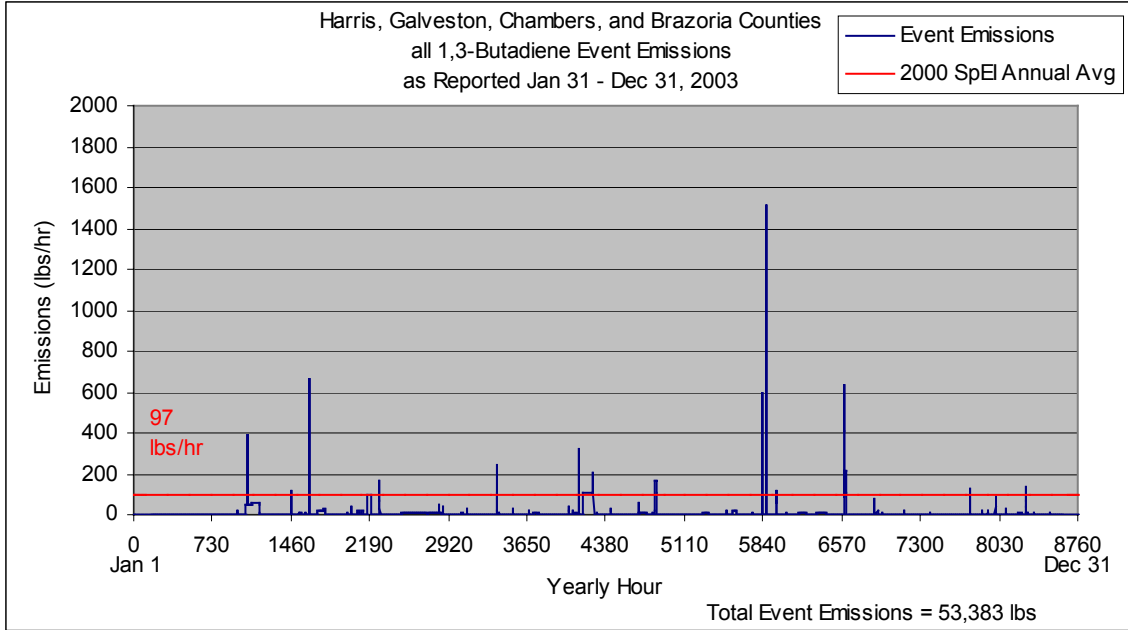


**Figure 10.** 1,3-butadiene emissions (lbs/hr) from events and as an annual average are presented in a time series using 8760 one-hour time blocks for a single year. Over an 11-month period there are 17 times (affecting 206 hours) when 1,3-butadiene emissions event emissions exceed the 2000 annual average of 97 lbs/hr. Event emission data are from TCEQ (2003b) and point source data are from TCEQ (2003d).

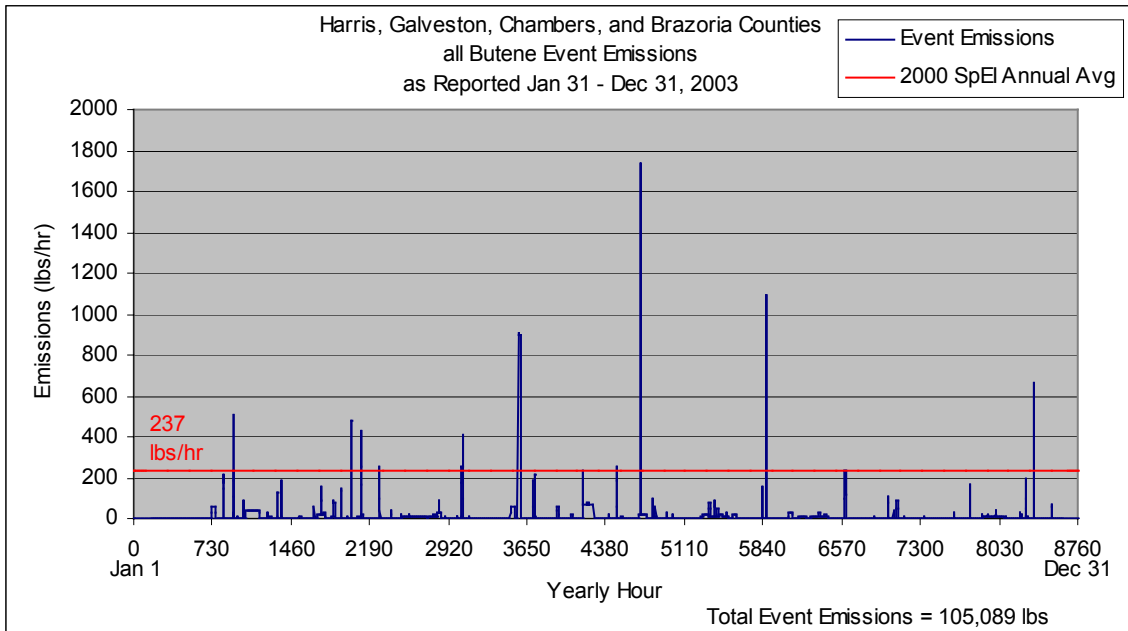


**Figure 11.** Butene emissions (lbs/hr) from events and as an annual average are presented in a time series using 8760 one-hour time blocks for a single year. Over an 11-month period there are 10 times (affecting 64 hours) when butene emissions event emissions exceed the 2000 annual average of 237 lbs/hr. Event emission data are from TCEQ (2003b) and point source data are from TCEQ (2003d).

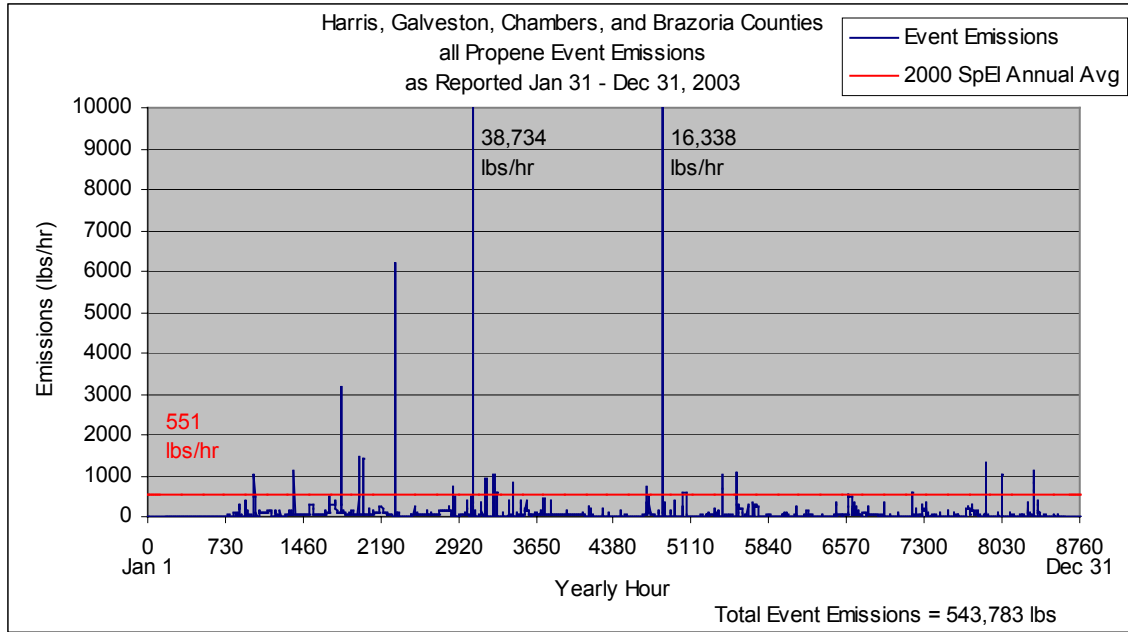


**Figure 12.** Propene emissions (lbs/hr) from events and as an annual average are presented in a time series using 8760 one-hour time blocks for a single year. Over an 11-month period there are 21 times (affecting 87 hours) when propene emissions event emissions exceed the 2000 annual average of 551 lbs/hr. Event emission data are from TCEQ (2003b) and point source data are from TCEQ (2003d).

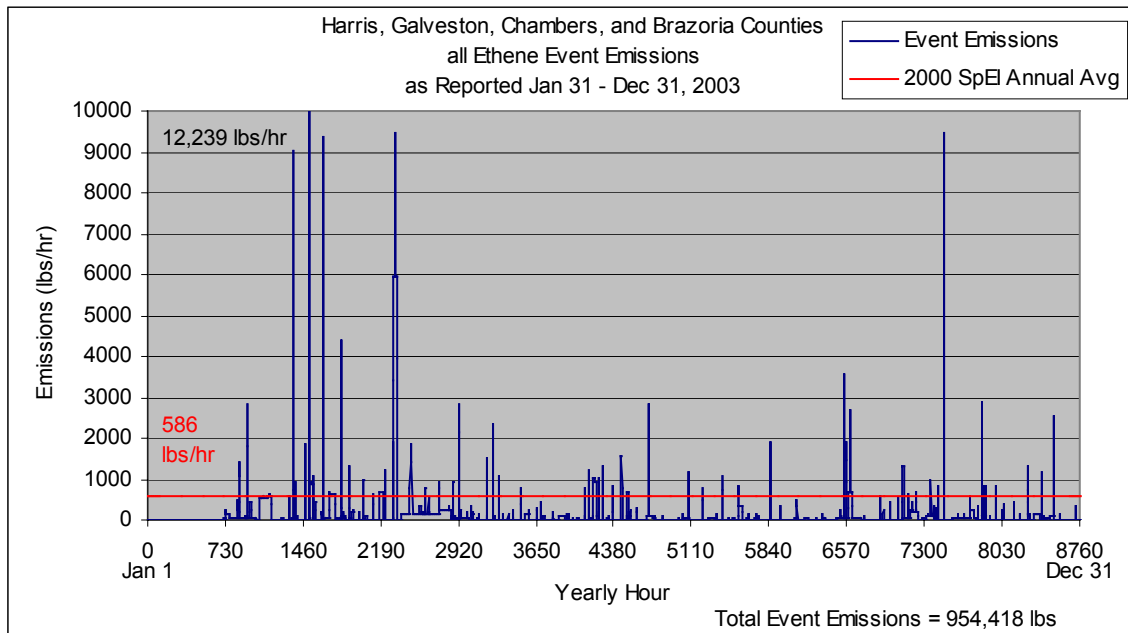


**Figure 13.** Ethene (ethylene) emissions (lbs/hr) from events and as an annual average are presented in a time series using 8760 one-hour time blocks for a single year. Over an 11-month period there are 58 times (affecting 395 hours) when ethylene event emissions exceed the 2000 annual average of 586 lbs/hr. Event emission data are from TCEQ (2003b) and point source data are from TCEQ (2003d).

Ethene (ethylene) exhibits the most significant frequency and magnitude of event emissions. Over an 11-month period there are 58 times (affecting 395 hours) when ethylene event emissions exceed the 2000 annual average for all point sources in the region of 586 lbs/hr and 7 times (affecting 44 hours) when event emissions exceed 5 times the annual average. Next most significant is propene (propylene). Over the same period of time there were 21 instances (affecting 87 hours) where event emissions exceeded the 2000 annual average of 551 lbs/hr. In 4 cases (affecting 8 hours), the amount was 5 times the annual average. 1,3-butadiene contributes only about half the total mass to event emissions when compared to butene, however it has nearly double the number of instances where event emissions exceed the 2000 annual average (17 for 1,3-butadiene vs. 10 for butene) and four times the number of events where the amount is 5 times the annual average (4 for 1,3-butadiene vs. 1 for butene).

Visual analysis of the time series plots (Figures 9 –13) suggests that the length of the events is relatively short. Quantitative evaluation reveals that of the 711 events involving the release of HRVOCs, 523 events (74%) last 24 hours or less (Figure 14). 175 events (25%) last one hour or less and 82 events (12%) last 10 minutes or less. The distribution of event durations for events of up to one hour is shown in Figures 15 and 16 for all HRVOC events and for those emitting greater than 1000 pounds of HRVOC. All 27 of the events lasting less than one hour and emitting more than 1000 pounds of HRVOC are unscheduled. More than half (17) last less than 10 minutes. The average release during these large events (greater than 1000 lbs) lasting 10 minutes or less was 2588 pounds of HRVOC. The average release of large events lasting 60 minutes or less was 3771 pounds of HRVOC.

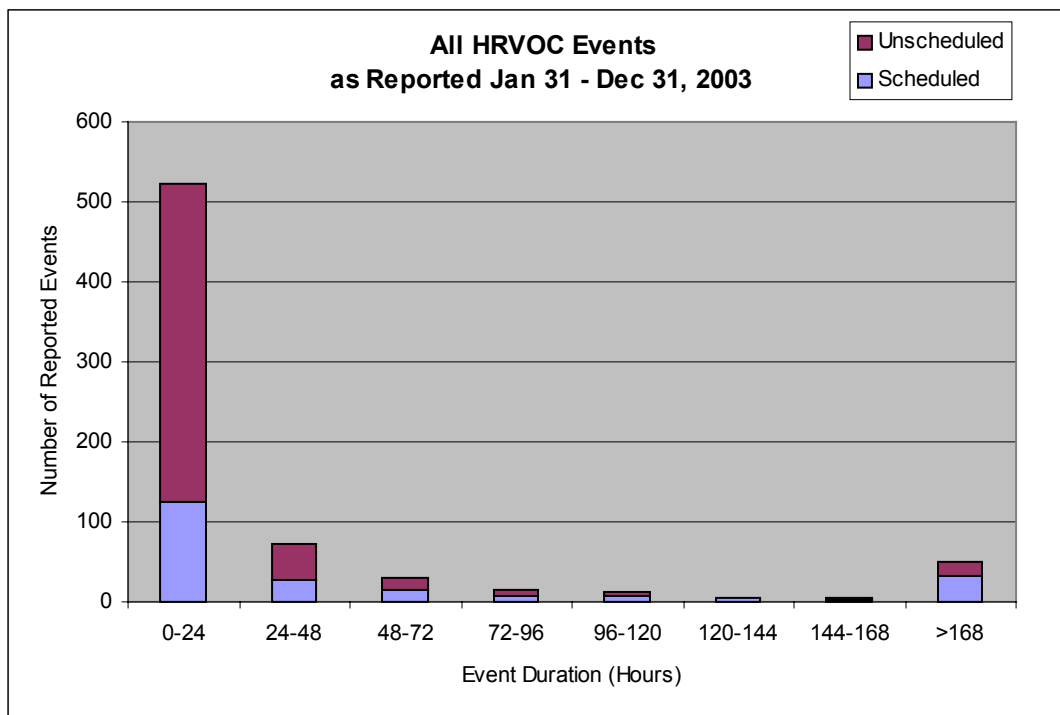


**Figure 14.** Most events, both scheduled and unscheduled, last less than 24 hours. More than 50% of events that last more than two days (48 hours) are scheduled.

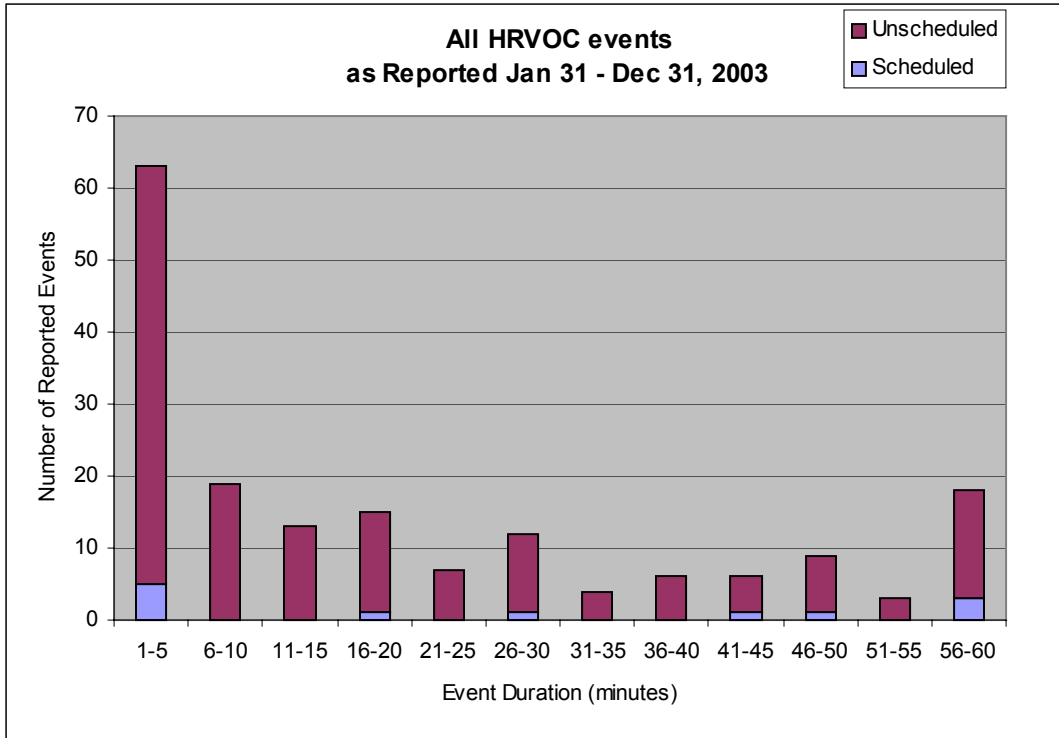


**Figure 15.** Of the 711 HRVOC events 175 (25%) last one hour or less and 82 (12%) last ten minutes or less. Increased frequency in the 30, 45, and 60-minute bins is probably an artifact of reporting estimates.

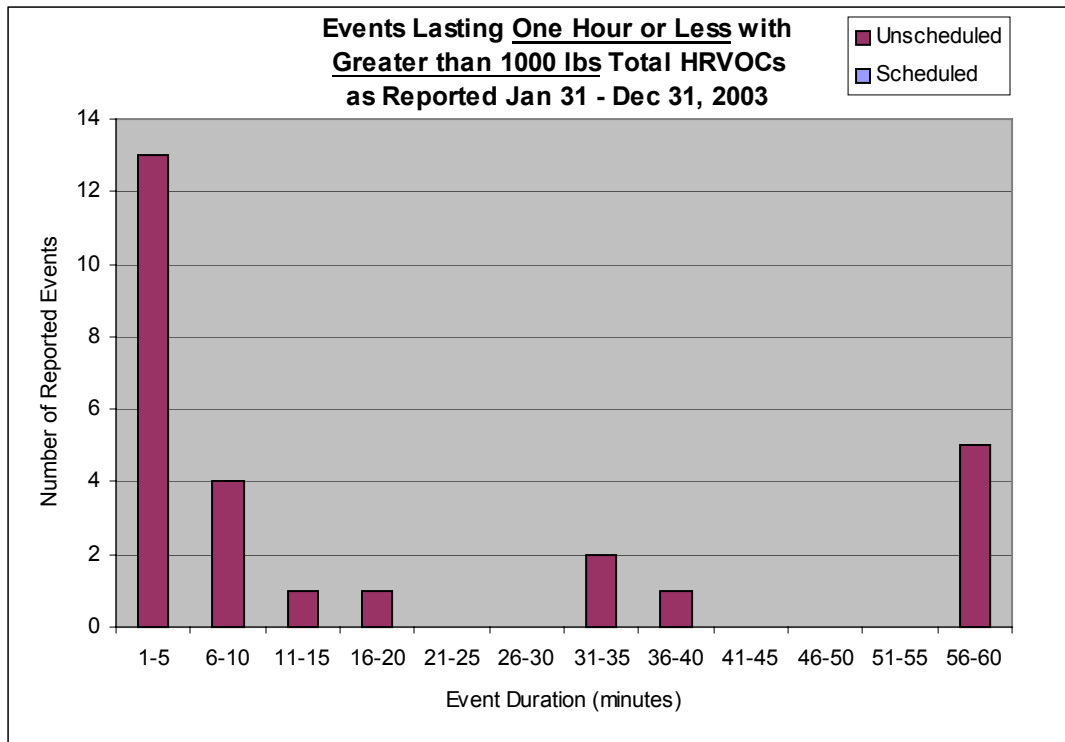
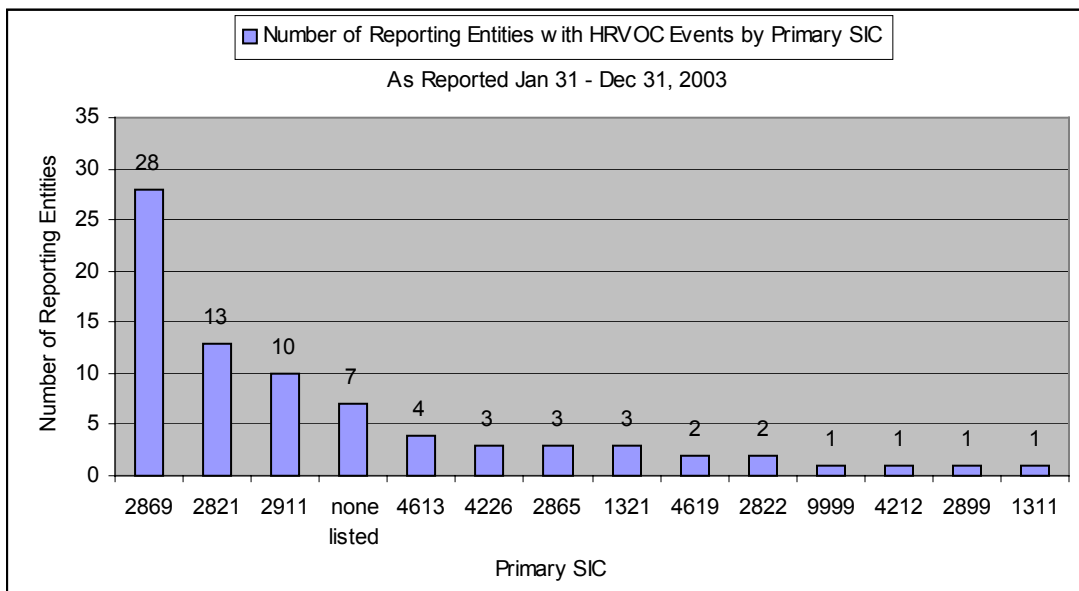


**Figure 16.** All 27 of the events lasting less than one hour and emitting more than 1000 pounds of HRVOC are unscheduled. More than half (17) last less than 10 minutes.

**Draft**

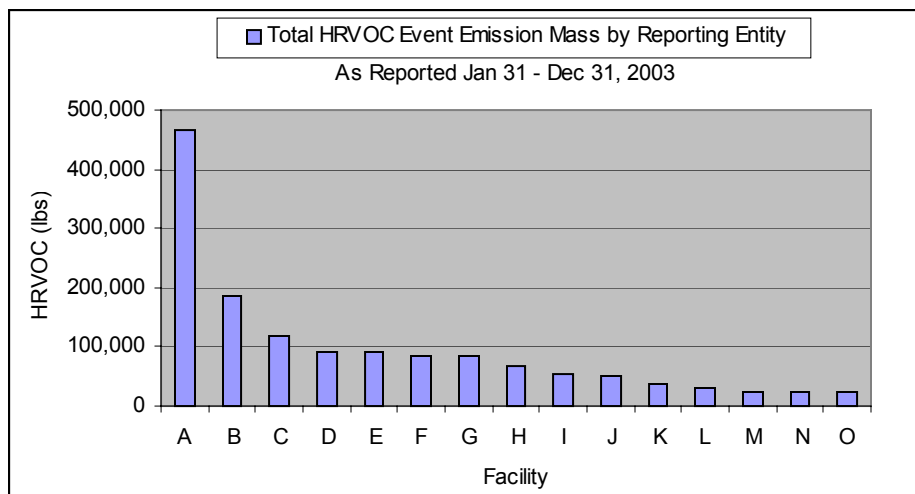
Figures 14-16 differentiate between scheduled and unscheduled events. Scheduled events are due to scheduled start-up, shut-down and maintenance activities. Unscheduled events are due to a wide range of causes and may result in an unplanned shut-down. The data in Figures 14-16 show that unscheduled event emissions tend to dominate.

As of December 31, 2003 a total of 79 entities had reported events with HRVOC emissions beginning on or after January 31, 2003. Approximately one third of these entities are identified in the TCEQ Central Registry (TCEQ, 2003e) with a primary standard industrial code (SIC) of 2869, Industrial Organic Chemicals. Just under 20% (13) entities have the primary SIC 2821, Plastics Materials. 10 entities are petroleum refineries (SIC 2911) and at least 8 are pipelines (SICs 4613 and 4619 plus some of the entities for which no SIC is listed). The distribution of HRVOC event emitting entities by primary SIC is shown in Figure 17.



SIC	SIC Description	SIC	SIC Description
2869	Industrial Organic Chemicals	1321	Natural Gas Liquids
2821	Plastics Materials	4619	Pipelines
2911	Petroleum Refining	2822	Synthetic Rubber (Vulcanizable Elastomers)
none listed*	*includes some pipelines	9999	Nonclassifiable Establishments
4613	Refined Petroleum Pipelines	4212	Local Trucking Without Storage
4226	Special Warehousing and Storage	2899	Chemicals and Chemical Preparations
2865	Cyclic Organic Crudes and Intermediates	1311	Crude Petroleum and Natural Gas

**Figure 17.** There were 79 reporting entities representing 14 different primary standard industrial codes (SICs) reporting HRVOC event emissions in the last 11 months of 2003. 28 of the entities (35%) had a primary SIC of 2869, Industrial Organic Chemicals.



Reporting Entity	Primary SIC	SIC Description	Total HRVOC lbs
A Dow Texas Operations Freeport	2869	Industrial Organic Chemicals	467,138
B Equistar Chemicals Channelview Complex	2869	Industrial Organic Chemicals	186,813
C Equistar Chemicals Chocolate Bayou Complex	2869	Industrial Organic Chemicals	117,498
D BP Amoco Chemical Chocolate Bayou Plant	2869	Industrial Organic Chemicals	90,366
E Equistar Chemicals La Porte Complex	2869	Industrial Organic Chemicals	89,763
F Lyondell Chemical Channelview	2869	Industrial Organic Chemicals	83,596
G Lyondell-Citgo Refining	2911	Petroleum Refining	83,017
H Sunoco Inc R & M Bayport Polypropylene	2821	Plastics Materials	67,148
I Chevron Phillips Chemical Sweeny Complex	2911	Petroleum Refining	54,451
J Chevron Cedar Bayou Chemical Plant	2869	Industrial Organic Chemicals	51,583
K Exxon Mobil Baytown Facility	2911	Petroleum Refining	36,045
L Union Carbide Texas City Operations	2869	Industrial Organic Chemicals	31,034
M Shell Oil Deer Park	2911	Petroleum Refining	25,059
N BP Solvay Polyethylene NA	2821	Plastics Materials	23,319
O BP Products North America Texas City	2911	Petroleum Refining	22,414

**Figure 18.** The top 15 reporting entities for 2003 in terms of total HRVOC event emissions mass account for nearly 90% of the total HRVOC event emissions mass in Harris, Brazoria, Galveston, and Chambers Counties. The top 6, all with a primary SIC of 2869 (Industrial Organic Chemicals) emitted 951,579 lbs and thus contributed approximately 60% of the four county total.

While only 35% of the reporting entities had a primary SIC code of 2869, this industrial sector accounts for more than 1 million of the 1.6 million pounds of HRVOC event emissions reported for the last eleven months of 2003. In addition, the top six facilities in terms of total HRVOC emission mass all fall within this SIC classification (Figure 18). The total mass for these six reporting entities is 951,579 lbs. Figure 18 shows the total mass and corresponding SIC codes for the 15 entities with the largest amounts of HRVOC event emissions. Together these 15 facilities released a total of 1,429,244 lbs or almost 90% of all 79 reporting entities.

The amount of HRVOCs reported as emitted during any single event ranges from one pound to 203,000 pounds. More than half of the events (375 out of 711) emitted between 100 and 1000 lbs (Figure 19). However, the actual number of events with less than 100 lbs of HRVOC is likely to be higher than the reported 160, since 100 lbs is the reporting threshold. Data on these events are available only because a reportable quantity of one or more compounds other than an HRVOC was emitted during the same event.

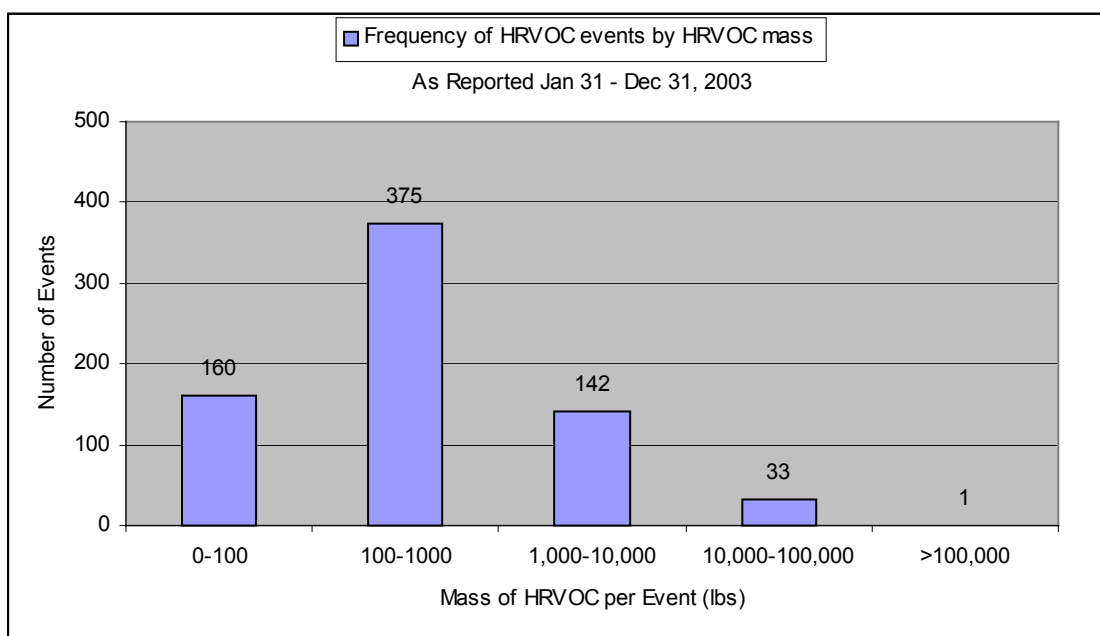


**Figure 19.** The amount of HRVOCs emitted during any single event, as reported in 2003, ranges from one pound to 203,000 pounds. More than half of the events (375 out of 711) are reported to have emitted between 100 and 1000 lbs.

To summarize, if event reports are complete and reasonably accurate, HRVOC events contribute approximately 12% to the total annual HRVOC mass emitted, and large events (those that exceed the annual average) occur on the order of almost three times a month (29 in an 11 month period). More than half of the mass is attributable to ethene and almost one third is due to propene. The remaining 10% consists of isomers of butene and 1,3-butadiene. In addition to dominating the mass, ethene has the most frequent events, with emissions from events exceeding the annual average flow rate for this compound more than once per week.

The length of the events is relatively short. Of the 711 HRVOC events, 523 (74%) last 24 hours or less, 175 (25%) last one hour or less, and 82 (12%) last 10 minutes or less. Despite their short duration, however, the magnitude of the emissions can still be quite large. 27 of the events lasting one hour or less release more than 1000 pounds of HRVOCs.

Roughly two-thirds of the mass is attributable to reporting entities with a primary SIC code of 2869 (Industrial Organic Chemicals) and 90% of the reported mass in 2003 can be assigned to 15 reporting entities. Although the amount of HRVOC event emissions per event in 2003 ranged from one pound to 203,000 pounds, more than half of the events (375 out of 711) emitted between 100 and 1000 lbs.

#### IV b. Continuous emissions

As noted in the introduction to this section, industrial emissions fall into several categories:

- Emissions released at a constant rate due to continuous process operation (nearly constant emissions)
- Emissions released at a variable rate due to fluctuations in process operations (routinely variable emissions)
- Episodic emissions that lead to a significant increase in daily emission rate, yet are below the maximum daily permit level (allowable episodic emission events)
- Emergency releases and other event driven emissions that lead to daily emissions greater than permitted levels (large episodic emission events)

The data in Section IV a. described large episodic emission events; the variability in emissions introduced by routinely variable and allowable episodic emissions are described here and in more detail in the Appendix.

To more clearly define the emission categories, Figure 20 reports the mass flow rate to a flare at an olefins facility, over approximately a year of operation. The flare has constant continuous emissions associated with a mass flow rate of approximately 2000 lb-mol/hr. Variable continuous mass flows add approximately 1000 lb-mol/hr, leading to the actual annual average mass flow rate of 2930 lb-mol/hr (blue line). This is below the average annual permitted mass flow rate of 3430 lb-mol/hr (purple line). Approximately weekly, episodic emissions lead to daily mass flows that are double the annual average (6000 lb-mol-hr). This is well below the daily allowable maximum flow to the flare of 34,700 lb-mol/hr. Twice during the year, large episodic emission events led to exceedances of the daily allowable maximum flow.

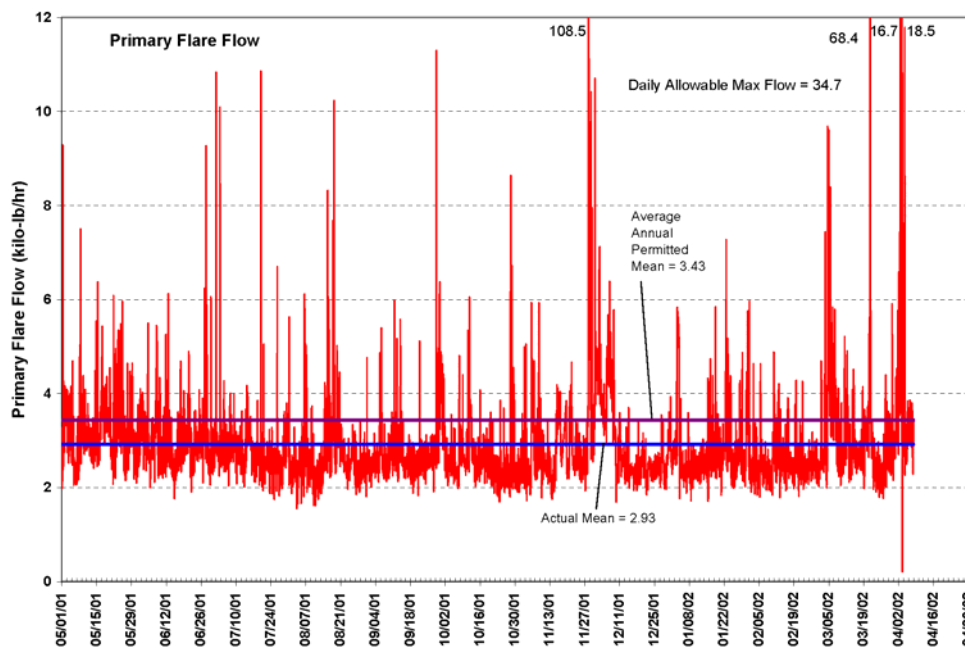
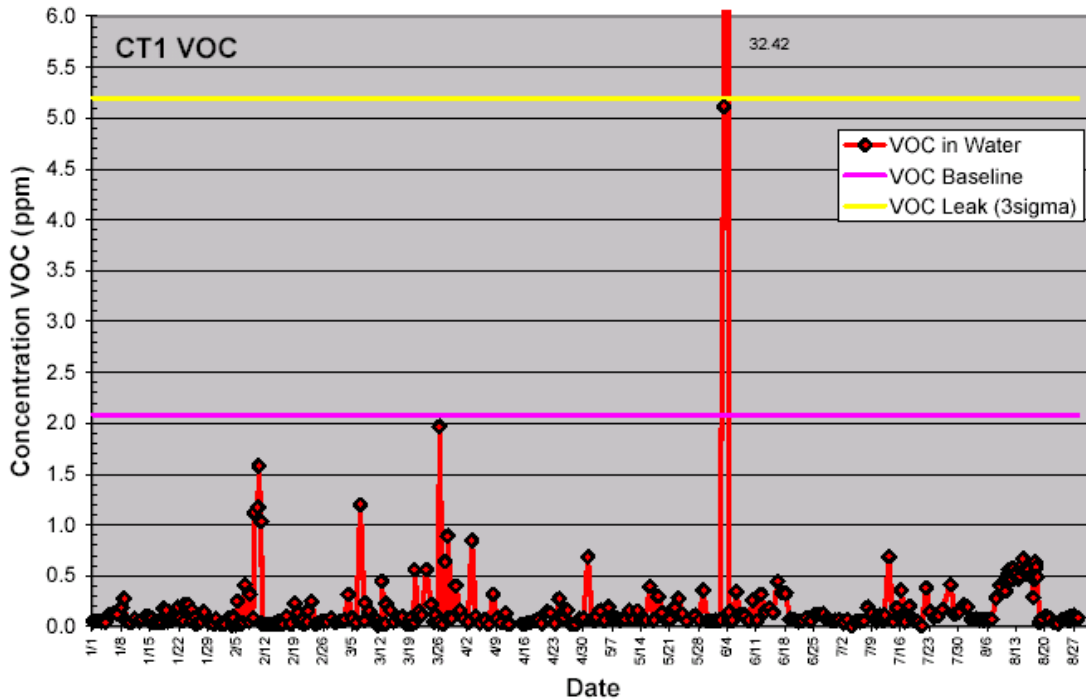


Figure 20. Variability in mass flow rates (a surrogate for emissions) to a flare at an olefins facility

Data related to VOC emissions from cooling towers also exhibit variability. Figure 21 shows the concentrations of VOC in cooling tower water (a surrogate for emissions) over roughly nine months of operation. In this case, constant continuous emissions are very small. Variable continuous emissions are also relatively small, but episodic emissions can be significant.



**Figure 21.** Variability in concentrations of hydrocarbons detected at a cooling tower (a surrogate for emissions)

To adequately describe emissions from units such as the flare of Figure 20 or the cooling tower of Figure 21, each of the four contributions to the total emissions must be accounted for. The first contributor, constant continuous emissions, is straightforward and can be characterized using existing emission estimation techniques. The remaining 3 components are not constant emissions. Quantifying these variable emission rates requires a new approach to characterizing point source emissions, illustrated in Figure 22.

Figure 22 illustrates how the flare flow data of Figure 20 can be characterized using a probability distribution function (PDF). The distribution describes the fraction of the time that the source emits at a particular rate. For example, the PDF on the left hand side of Figure 22 indicates that the probability of the flare having a mass flow rate within the range labeled as  $\delta f$  (roughly 4.9 to 5.1 thousand lb/hr) is the probability density (0.03) multiplied by  $\delta f$ .

### Fitting Probability Density Functions to Flare Flow Data

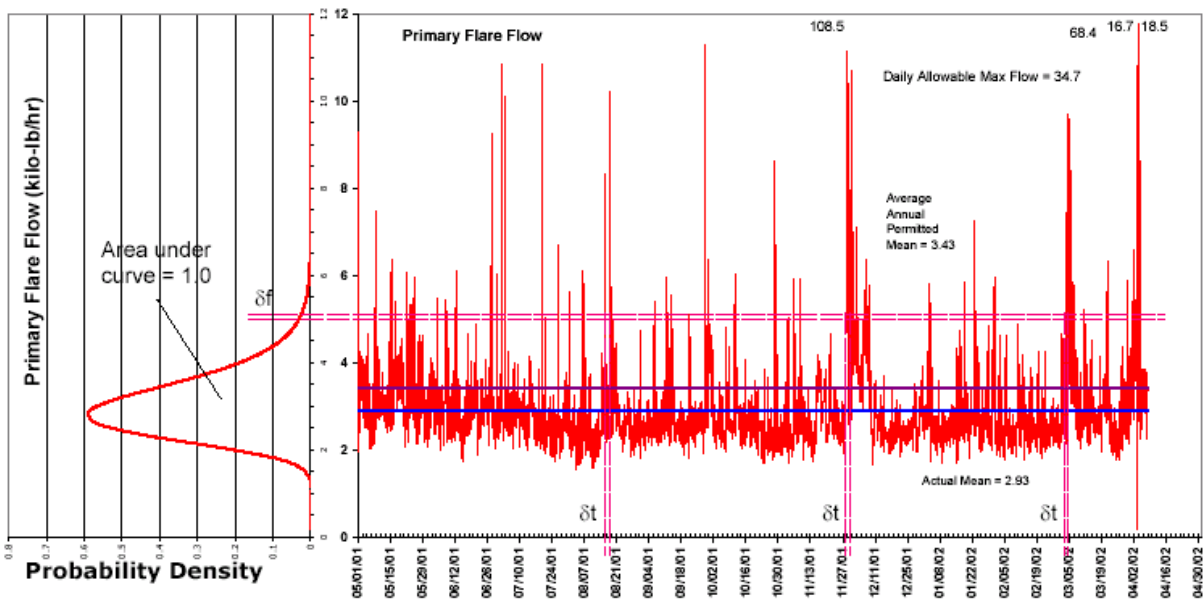


Figure 22. Probability distribution function (PDF) of mass flow rate for a flare at an olefins facility

Figures 20 and 21 illustrate variability for specific flares and cooling towers. The limited data that are available indicate that not all flares, and not all cooling towers, have the same PDFs. For example, Figure 23 shows mass flow data for a different flare than in Figure 20 and Figure 24 shows hydrocarbon concentrations for a different cooling tower than in Figure 21 (additional data are available in the Appendix).

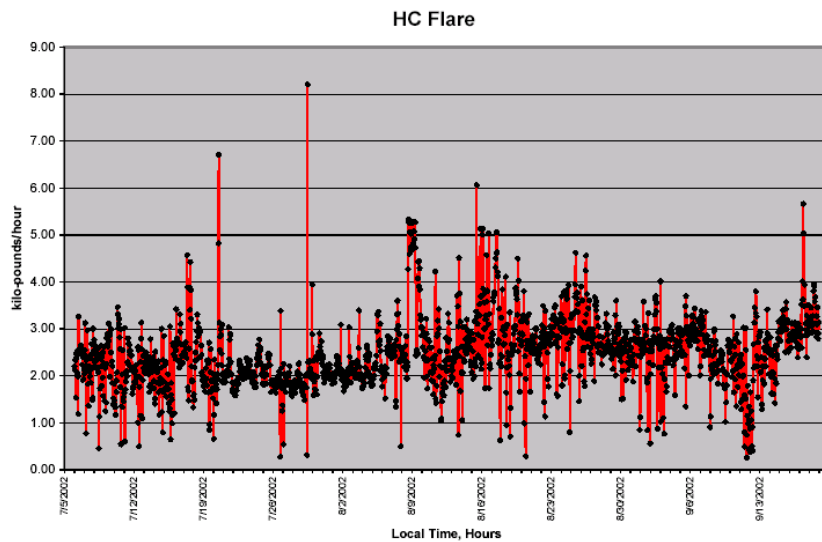
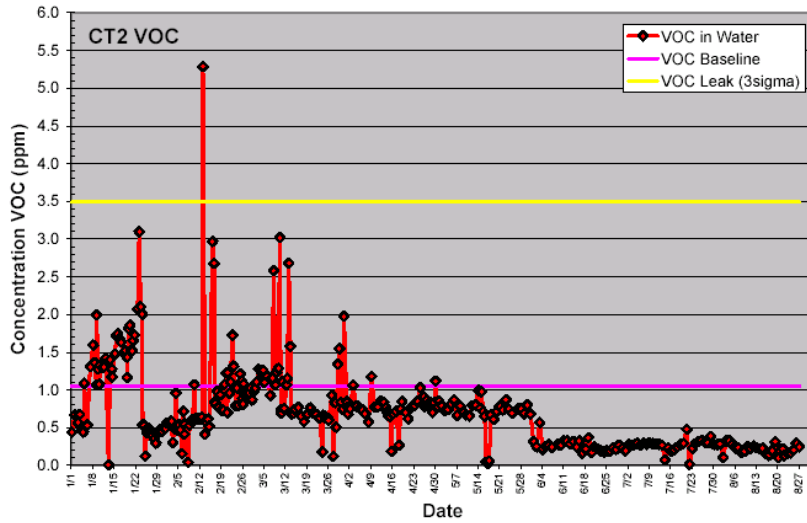


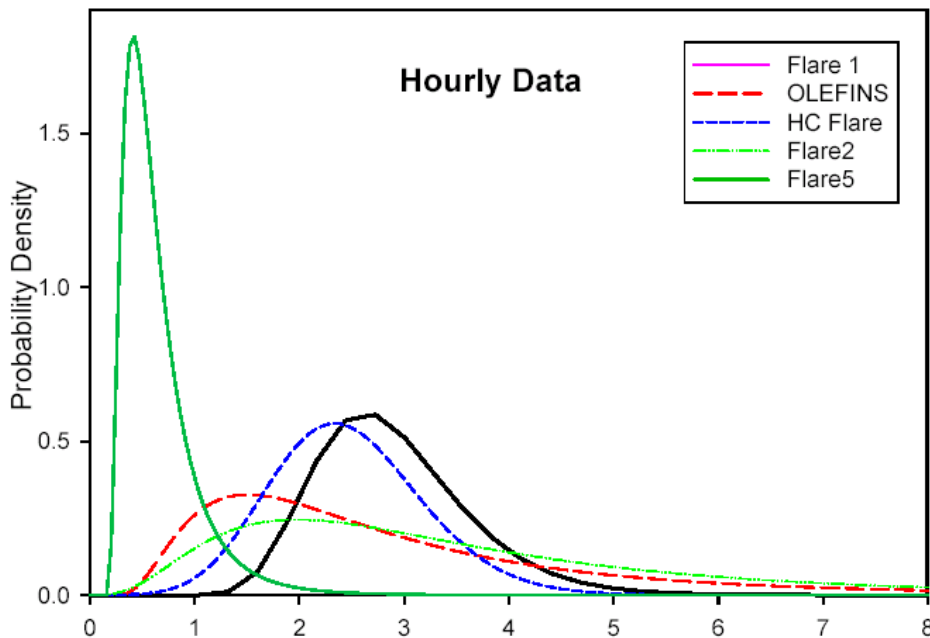
Figure 23. Variability in mass flow rates (a surrogate for emissions) in a flare at a different plant than shown in Figure 20



**Figure 24.** Variability in concentrations of hydrocarbons detected at a cooling tower (a surrogate for emissions) at a different plant than shown in Figure 21

Comparison of Figures 20 and 21 and Figures 23 and 24 indicate that there will be some differences in PDFs of emissions for specific flares, specific cooling towers and other unit operations. Examination of the emerging data on these unit operations, however, suggest that a limited number of PDFs could characterize the major types of emission sources. Thus, the variable emissions from a facility might be characterized by a group of PDFs, as shown in Figure 25.

**Figure 25.** Variable emission sources within a facility could be characterized by a set of PDFs, each representing a particular class of emission sources.

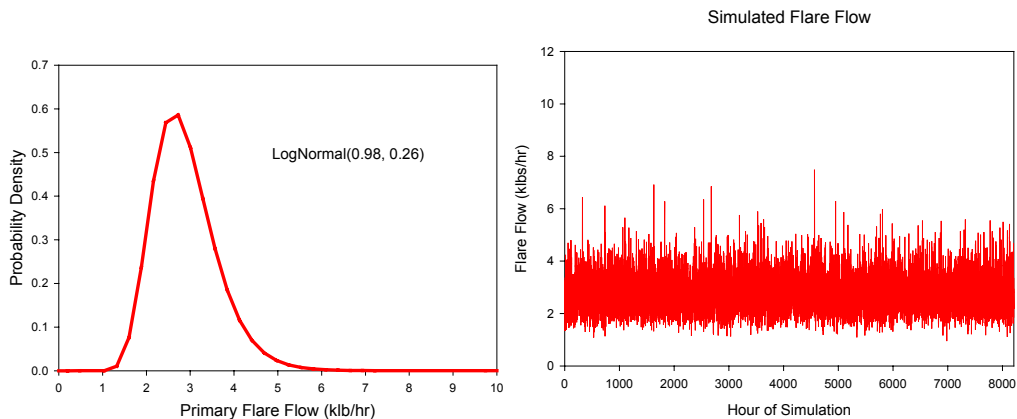


There are a number of advantages to describing variable emissions using PDFs. PDFs describe the full range of possible emission scenarios or emission snapshots. Examining the full range of these snapshots allows for a more comprehensive assessment of the variable emissions that can lead to rapid ozone formation and high ozone concentrations. The PDFs can also be used to forecast future emissions and control strategies can be modeled by varying the PDFs; for example, a strategy designed to reduce large emission could be expressed as a reduced probability of a high emission.

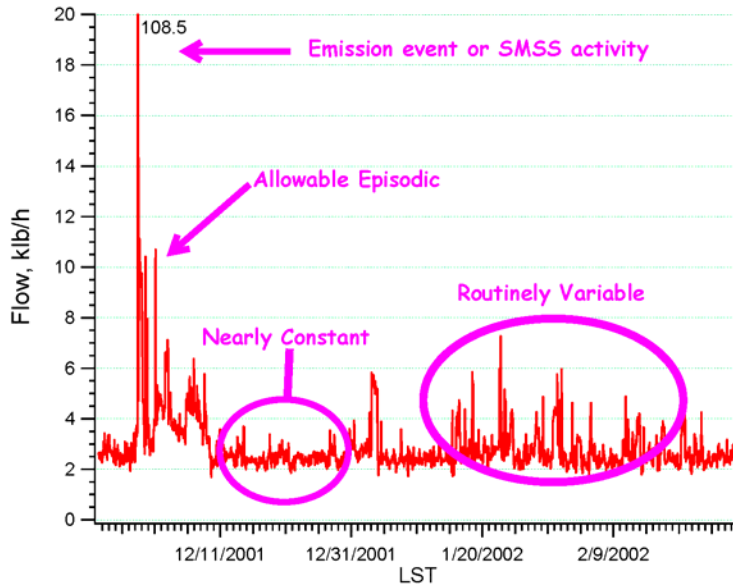
Because of these, and other advantages, PDFs have been used in other types of environmental analyses (e.g., estimation of risks) and there are sophisticated analysis tools for describing and manipulating PDFs. Balancing these advantages are the challenges of assessing the accuracy of PDFs describing emissions, using the PDFs to develop a region wide inventory, and accounting for the ozone formation implications of variable emissions in air quality models.

PDFs describing variability in point source emissions have been based on analyses of historical data of emission surrogates (e.g., mass flow rates to flares). The simplest approach in modeling historical data is to assume that the emission rate or the emission surrogate is due to one type of phenomenon, and therefore can be represented by a single PDF. For example, if all of the mass flow to a flare were due to venting of tanks due to diurnal cycling, then a single PDF representing the range of observed temperature cycling should be sufficient to describe the flow.

Figure 26 shows an attempt to model mass flow rates to a flare using a single PDF. The PDF and a simulated mass flow rate time series are shown. The mass flow rate time series can be compared to the original data in Figure 20. In this case it is clear that a single PDF is not able to characterize the flare flow.

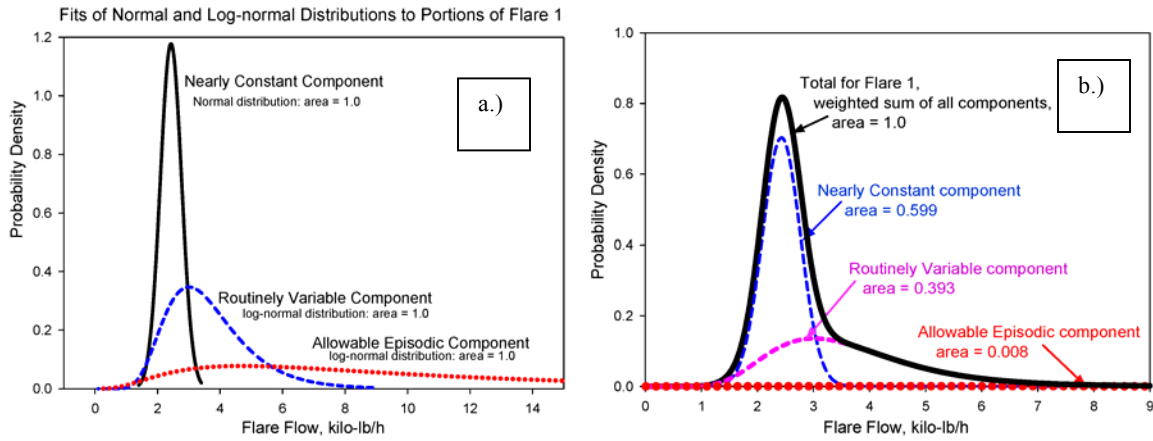


**Figure 26.** Mass flow rates to a flare modeled using a single PDF. The PDF and a simulated mass flow rate time series are shown. The mass flow rate time series can be compared to the original data in Figure 20. In this case it is clear that a single PDF is not able to characterize the flare flow.

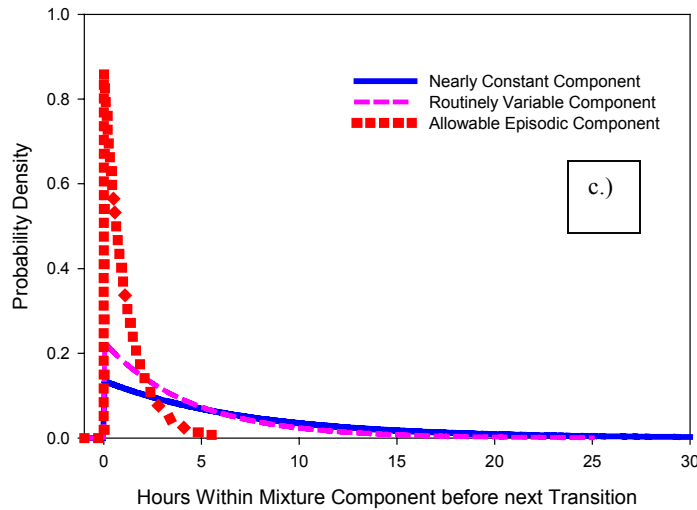


**Figure 27.** Four major types of phenomena that may lead to emission variability

A closer examination of the original data indicates that it is unlikely that a single phenomenon is responsible for the flare flow. Figure 27 shows that there are at least four major types of phenomena that may lead to very different flare flow rates. These are labeled in the Figure as nearly constant, routinely variable, allowable episodic and emission event. Work is currently underway to link physical causes to these different types of phenomena; for example, an emission event may be caused by the failure of a compressor that feeds hydrocarbons to a reactor. This type of event leads to a very different PDF than the diurnal cycling of tanks (a nearly constant or routinely variable emission). Therefore, it should not be surprising that multiple PDFs might be required to represent an emission source. Figure 28 shows the multiple PDFs used to model a flare, and Figure 29 shows a simulated time series of emissions predicted using the multiple PDF model and an actual time series. Data on additional flares and cooling towers are provided in the Appendix.



**Figure 28.** Three PDFs are used to model the emissions from a flare. To simulate an hourly emission, the emission model first randomly selects which flow mode the flare is in, nearly constant, routinely variable or allowable episodic (emission events are handled separately). Then an emission flow rate is selected for that hour, based on the PDF in Figure a. The combination of time in mode and probability of emission rate in each mode can be plotted as a composite PDF, shown in Figure b. For the next hour of emissions, the mode is selected based on the probability that the flare operates in the same mode as the previous hour, or transitions to a new mode – this probability is shown in Figure c.



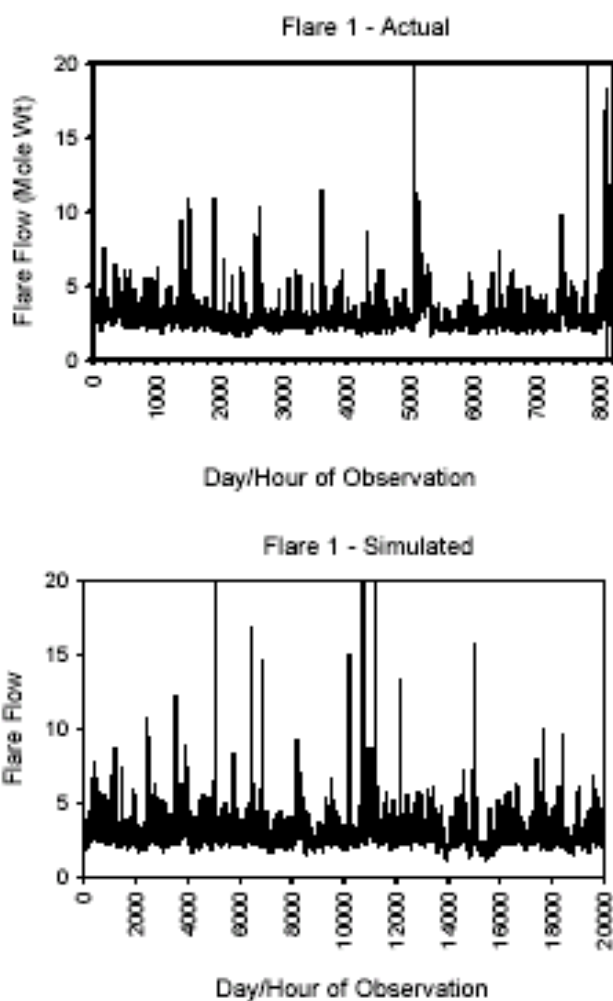


**Figure 29.** Simulated and actual time series of flare flow simulated using the model of Figure 28. Note that the goal is not to represent the exact time series, but to represent the variability in the time series.

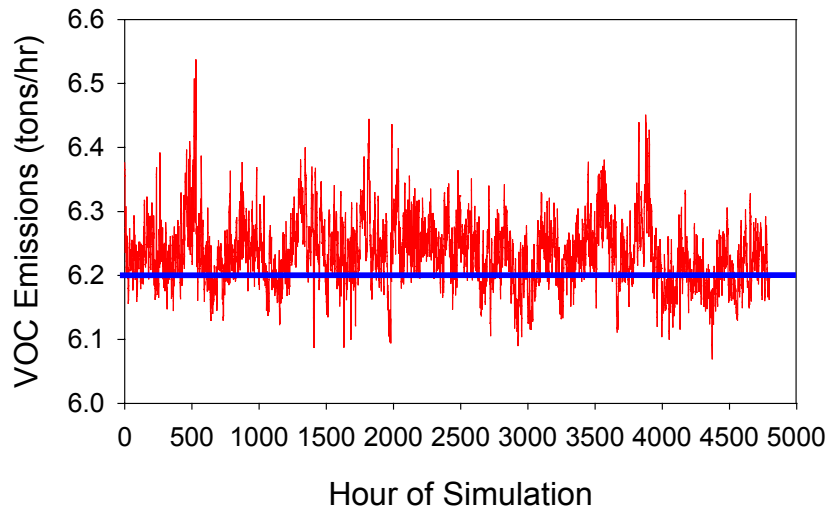
Thus, with multiple PDFs, it is possible to provide a reasonable representation of emission variability from emission sources such as flares. The next step is to apply the variable emissions models to the entire Houston-Galveston area, rather than to just a single emission source. This involves some uncertainties, since the available data indicate that individual sources like flares may have very different emission variabilities, and there is not yet a reasonable basis for assigning specific emission types for every source in the region.

Nevertheless, some preliminary results are shown. The point of presenting these preliminary results is to assess how the overall emission variability will be affected by a large number of independently variable sources.

## Draft

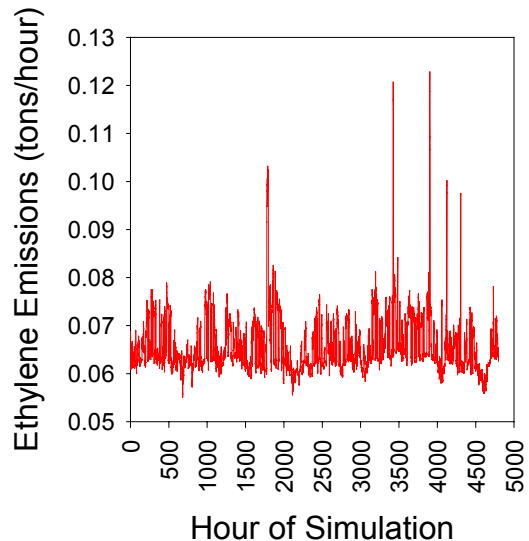
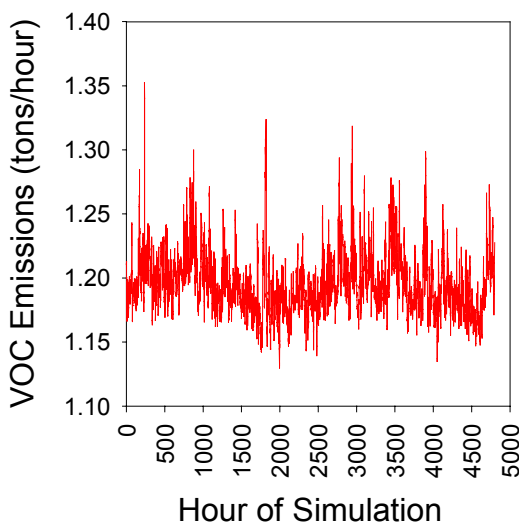
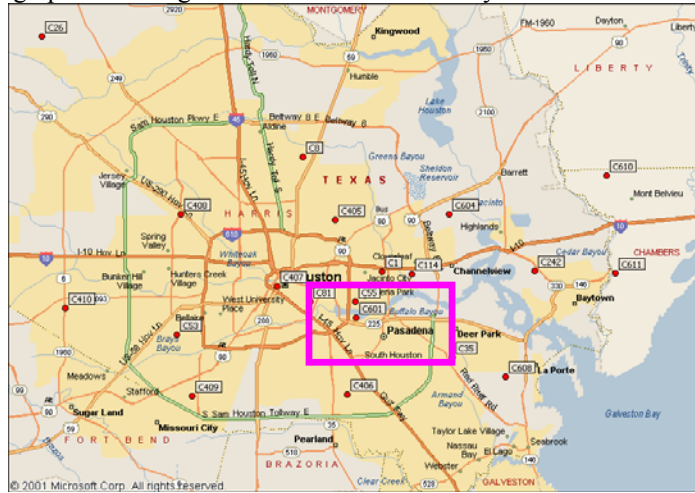
The analysis, described in detail in the Appendix, assumes that total annual emissions remain fixed, but that individual sources exhibit independent variability; so, if one source is in an allowable episodic emission mode, another source might be in a routine variability mode. Using these constraints, and eliminating large episodic events which were described in Section IVa., a time series of the emissions for the entire region can be estimated. Figure 30 shows one possible hourly profile of total VOC emissions for 200 days (not including large emission events described in Section IVa). This is an “instance” or random sample for the aggregate of all point source VOC emissions over all of the Houston Galveston area. Many other instances are possible. Note that the total variability in emissions, summed over the entire domain, is much less than the variability in any single source. The estimates suggest that the mass associated with this combined variability is about 5-10% of the inventory, comparable to the mass due to emission events (which are not included in this time series).

**Figure 30.** One possible hourly profile of total VOC emissions for 200 days. This is an “instance” or random sample for the aggregate of all point source VOC emissions over all of the Houston Galveston area.



To better characterize local impacts of variability in emissions, it is useful to focus on a specific geographic sub-region of interest. As an example, Figure 31 shows an estimated inventory for a region south of the ship channel and including Deer Park. Figure 31 also shows the estimated variability in the emissions in the subregion (ignoring the effects of transport, i.e., considering only emissions released in the subregion; details of the analysis are available in the Appendix).

Figure 31. Geographical subregion and estimated variability in the emissions in that subregion



The variability of total emissions in the subregion (5-10%) is comparable to the variability in total emissions for the entire region, but for specific compounds, such as ethylene, the variability increases because a smaller number of sources is being considered. For ethylene, Figure 31 suggests that variability in emissions could cause emission rates in localized sub-regions to double roughly once per month.

**Finding 1: Variability in HRVOC emissions from point sources is significant and is due to both variability in continuous emissions and discrete emission events.** Roughly 3 times per month in 2003, reported emission events caused single facilities to have HRVOC emissions that were greater than 10,000 lb/hr (the total annual average emissions of HRVOCs, from all industrial point sources in the Houston-Galveston region is approximately 5,000 - 10,000 lb/hr). Roughly 3 times per week in 2003, reported emission events caused single facilities to have HRVOC emissions that were greater than 1,000 lb/hr. Roughly once a day in 2003, reported emission events caused single facilities to have HRVOC emissions that were greater than 100 lb/hr. Variability in continuous emissions is more difficult to quantify than emission variability due to reported emission events, but preliminary modeling indicates that variations in continuous (as opposed to discrete) HRVOC emissions could cause localized emissions of HRVOCs to double as frequently as once per month.

## V. Ozone formation potential of variable emissions

### V a. Observational data *Ground VOC Monitors*

The emission variability documented in the previous section is qualitatively apparent in ambient measurements of hydrocarbon concentrations. Ground monitors, that record the hourly average concentrations of more than 50 individual hydrocarbons at several sites in the HGA, show significant variability in VOC concentrations. Figure 32 shows time series of the hourly average concentrations of ethene, propene and other organic compounds at two sampling sites located near the heavily industrialized Ship Channel. The data are for August 2000, and demonstrate that total hourly averaged non-methane hydrocarbon concentrations can exceed 2000 ppb and concentrations of individual highly reactive hydrocarbons can exceed 100 ppbC on a weekly basis.

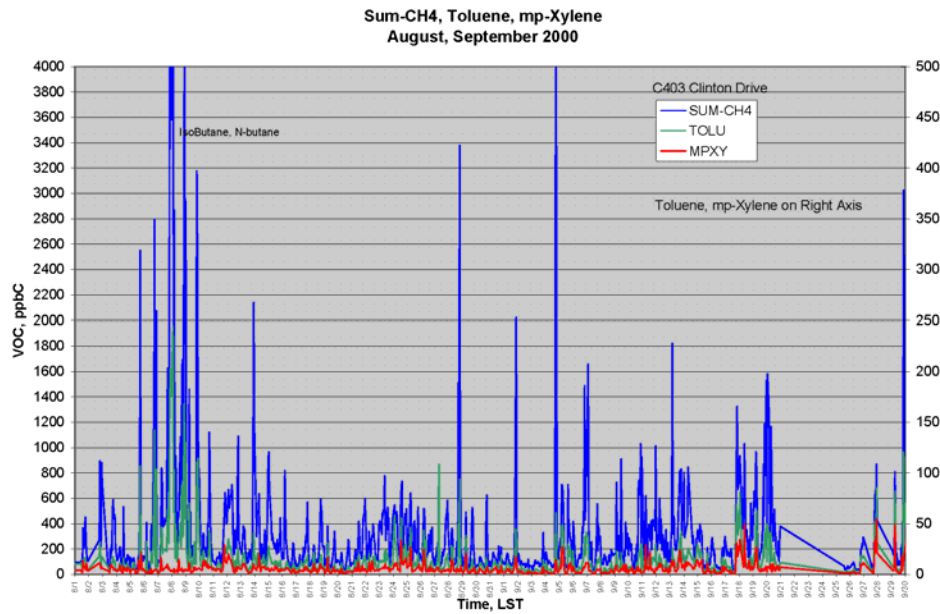
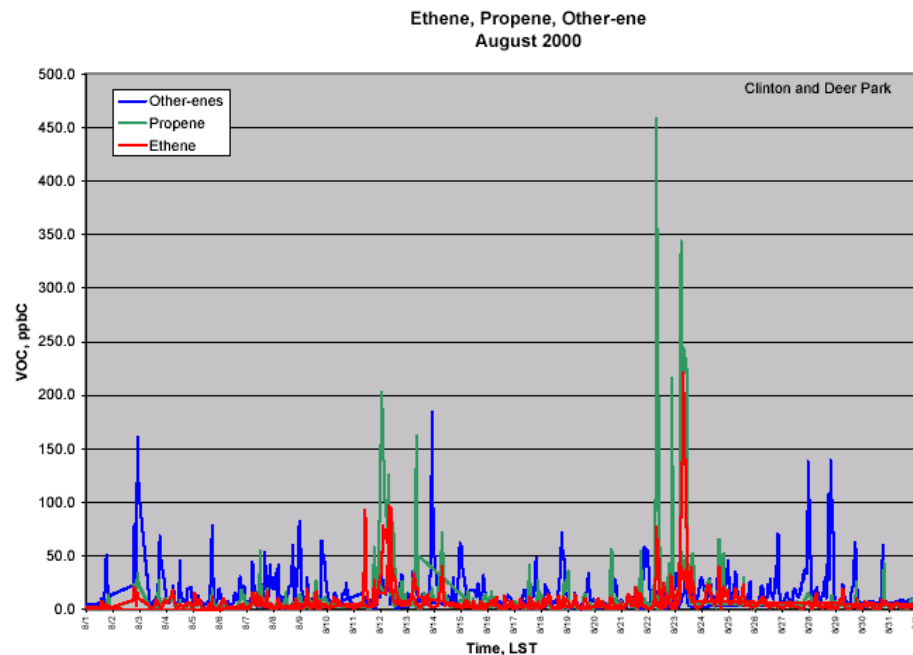


**Figure 32.** Selected ambient reactive VOCs measured hourly for August 2000 at two sites in Houston near the Ship Channel. (Sum-CH4 represents non-methane hydrocarbons)



## Draft

The distributions of concentrations documented in Figure 32 are described in Table 3. Note that the data are hourly measurements, so a measurement at the 99.5 percentile level (equivalent to 1 in 200) occurs approximately weekly (or once every 168 hours).

Table 3. Statistical summary of hydrocarbon concentration distributions

	Sum-CH4 ppbC	Alkanes ppbC	Alkenes ppbC	Aromatics ppbC	Ethene ppbC	Propene ppbC
<b>All Sites</b>						
max	16703.4	16443.6	2357.7	1157.3	536.0	2195.9
99.5th percentile	3242.9	2944.4	420.2	201.4	149.4	264.6
99th percentile	1845.0	1547.3	316.9	168.8	109.0	168.2
95th percentile	763.9	529.8	126.2	96.2	41.9	46.9
90th percentile	523.6	362.4	78.7	68.4	25.6	25.6
50th percentile	131.2	88.0	16.2	17.8	4.8	3.5
average	256.4	187.8	36.0	29.6	11.5	13.3
stddev	571.4	532.5	73.8	36.4	23.2	53.2

The time period of August 2000 is not unique in its record of variable, and at times very elevated concentrations of highly reactive hydrocarbons. Figure 33 (Main, et al, 2001) report concentrations of ethene as a function of time of day at the Deer Park monitoring site (dominated by industrial sources) for the entire year of 2000. Similar data analyses are available for 1,3 butadiene, propene, and other reactive hydrocarbons. Figure 33 indicates that the median ethene hourly concentration is less than about 10 ppbC for all hours and that 75 percent of the concentrations fall below 20 ppbC. However, there are a number of hours when ethene concentrations are significantly greater than 50 ppbC and some approach 300 ppbC.

The data from Deer Park can be contrasted with a similar data set collected at the Aldine monitoring site (largely residential, but at times, downwind of the industrial source region). The Aldine data are shown in Figure 34. For Aldine, ethene concentrations did not exceed 100 ppbC and the frequency of ethylene concentration measurements in excess of 40 ppbC is much lower than at Deer Park, suggesting that many of the extreme values in ambient concentrations are due to proximity to industrial sources.

While Figures 33 and 34 suggest that there is variability in VOC and HRVOC concentrations, the variability can be attributed to both variability in emissions and variability in atmospheric conditions. The data in Figure 33 show that the highest concentrations are observed in the morning hours when mixing heights are low and when hydrocarbons have had the little opportunity to react, indicating that at least some of the ambient concentration variability is due to meteorology.

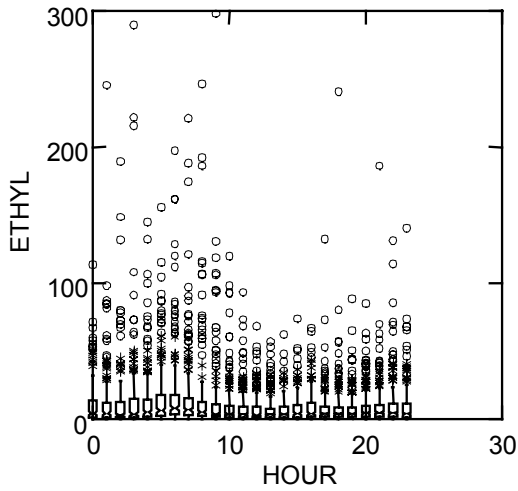


**Figure 33.** Notched box plots of ethene concentrations (ppbC) by time of day in 2000 at the Deer Park monitoring site (Main, et al, 2001).

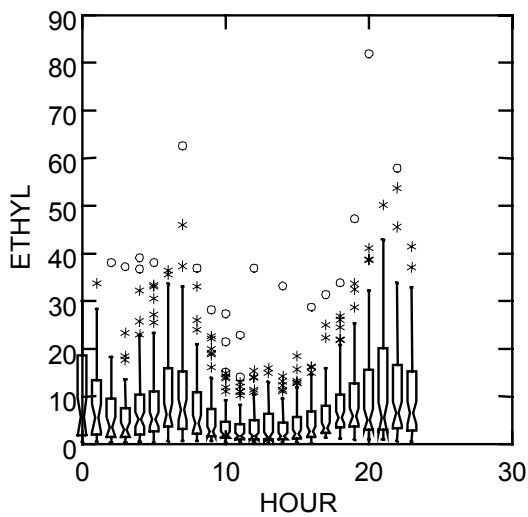
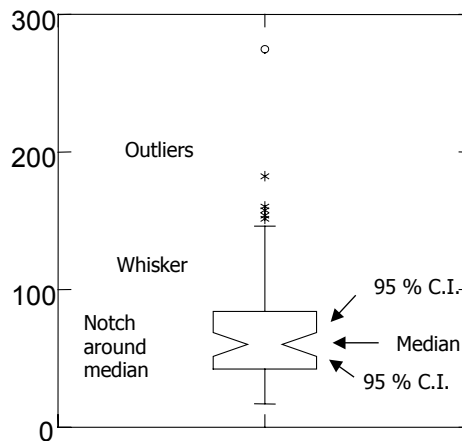
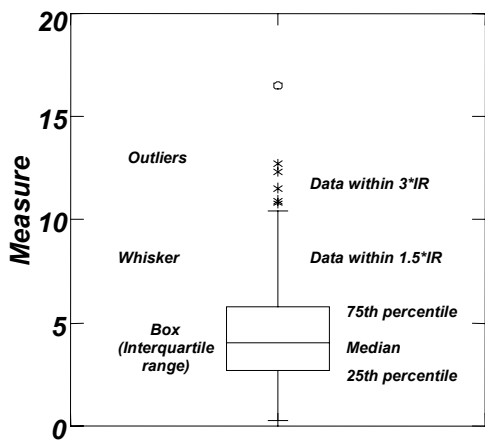


**Figure 34.** Notched box plots of ethene concentrations (ppbC) by time of day in 2000 at the Aldine monitoring site (Main, et al, 2001).

Figures 33 and 34 provide summaries of observed concentration distributions through lines that contain boxes and whiskers, as shown in the diagram. The box shows the 25<sup>th</sup>, 50<sup>th</sup> (median), and 75<sup>th</sup> percentiles. The whiskers have a maximum length equal to 1.5 times the length of the box (the interquartile range). If there are data outside this range, the points are shown on the plot. Asterisks represent points that fall within three times the interquartile range from the end of the box and circles representing points beyond this.



One qualitative method for attempting to separate the effects of meteorology from emissions variability in the concentrations of VOCs observed at ground monitors is to examine time series. Figure 35 shows time series of concentrations, observed at the Clinton monitor, of total VOCs, ethene, and propene. The Figure shows the hourly averaged concentrations at various percentile levels. If meteorology were the sole cause of concentration variability, consistent annual cycles would be expected due to the seasonality of wind direction, and similar time series patterns might be expected for individual pollutants (such as ethene and propene) due to the effects of low mixing heights on certain days. Neither of these patterns is evident in the data.

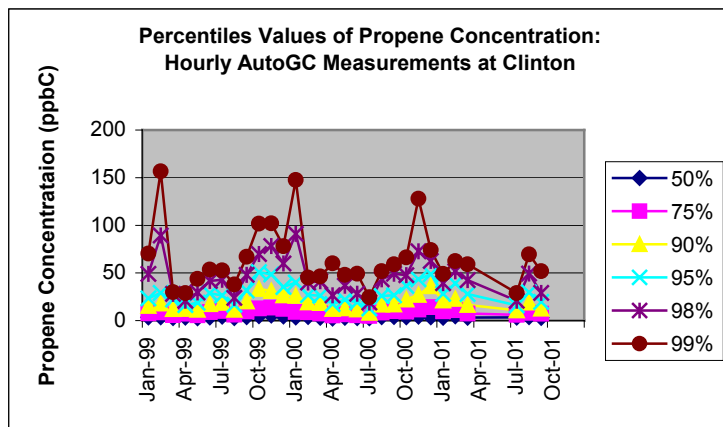
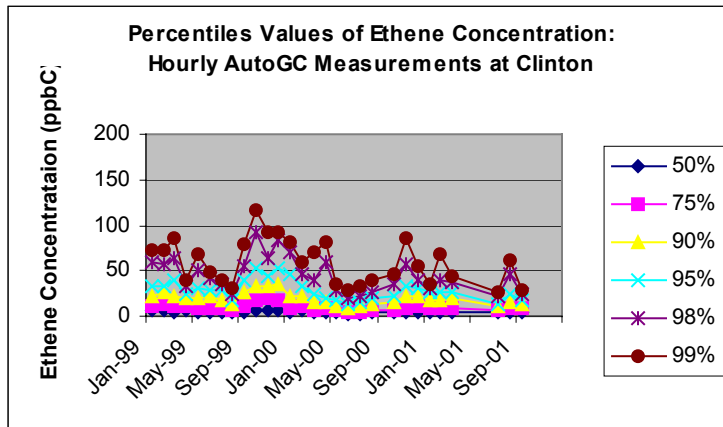
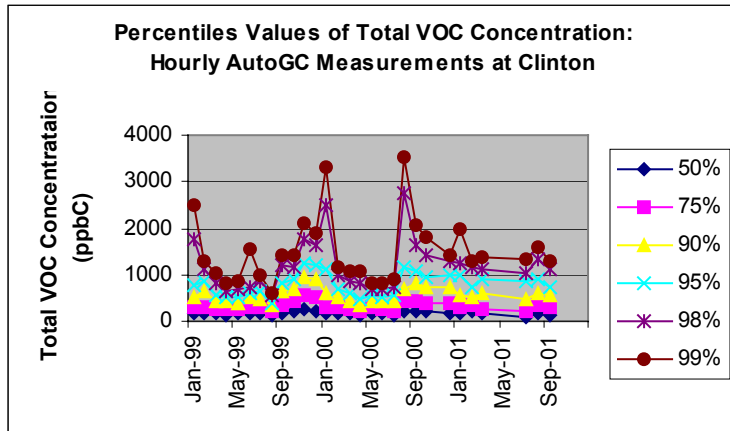
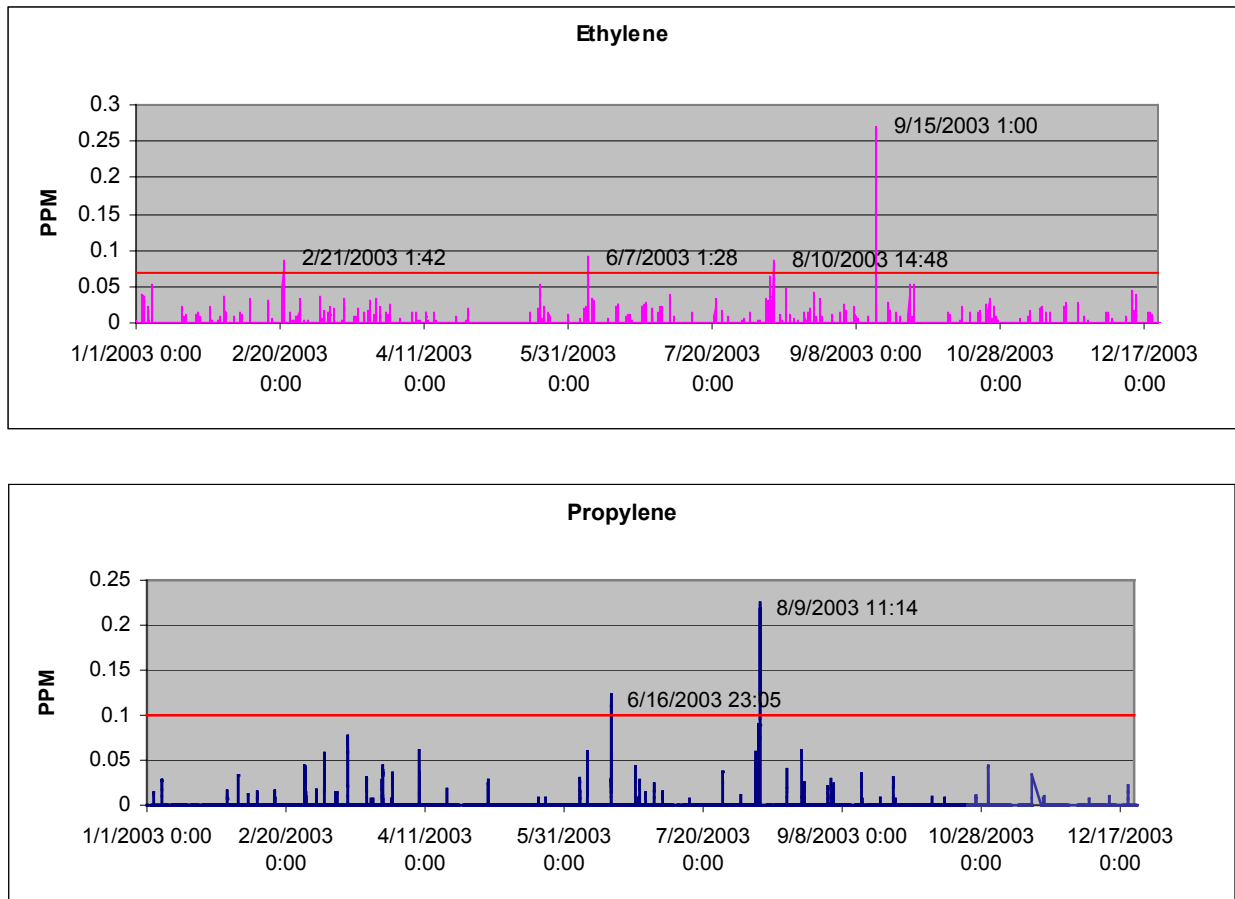


**Figure 35.** Concentration time series, observed at the Clinton monitor, for total VOCs, ethene, and propene. The Figure shows the concentrations at various percentile levels. For example, the line labeled 99% represents the 99<sup>th</sup> percentile or the highest 1% of concentrations recorded each month. If meteorology were the sole cause of concentration variability, consistent annual cycles would be expected due to the seasonality of wind direction, and similar time series patterns might be expected for individual pollutants (such as ethene and propene) due to the effects of low mixing heights on certain days. Neither of these patterns is evident in the data.

## Draft

Further evidence from ground monitors on the role of emissions variability as a factor in driving variability in ambient concentrations comes from FTIR based monitoring. An FTIR monitor is located in the Bayport region on the western coast of Galveston Bay. Shown in Figure 36 are time series of ethene and propene concentrations observed at the monitor in 2003. The data show concentrations above 50 ppb (100 and 150 ppbC for ethylene and propylene, respectively) on a roughly monthly basis.

**Figure 36.** Time series of ethene and propene concentrations observed with an FTIR monitor at the Seabrook site (near Bayport)



These data are consistent with measurements made at other monitoring sites that rely on automatic gas chromatographs (auto-GCs). The new information that this monitor provides is sub-hour time resolution. The auto-GCs provide an hourly average measurement of hydrocarbon concentrations that is based on a sample collected over a 40-minute period – followed by a 20 minute analysis/purge sequence. The IR monitor collects spectra continuously and currently reports 13-14 minute average concentrations. Therefore, the data from the IR monitor provide data on a finer time scale. Those measurements are summarized in Figure 37.

**Figure 37.** Duration of individual events hydrocarbon detection events for ethylene and propene, where the duration is defined as the length of time between the start of detection and the return to a no-detect level (10 ppb for ethylene and 20 ppb for propylene).

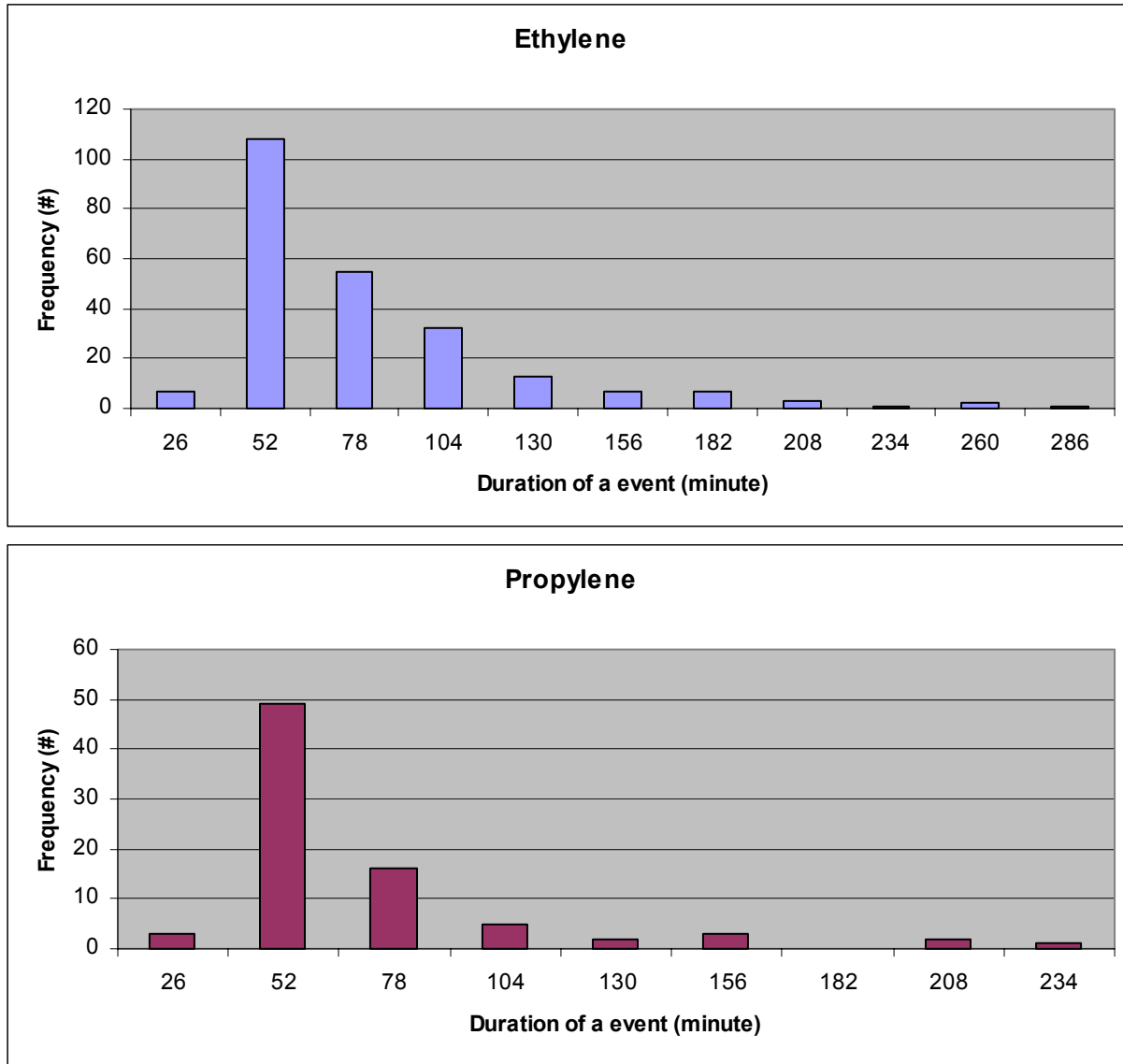
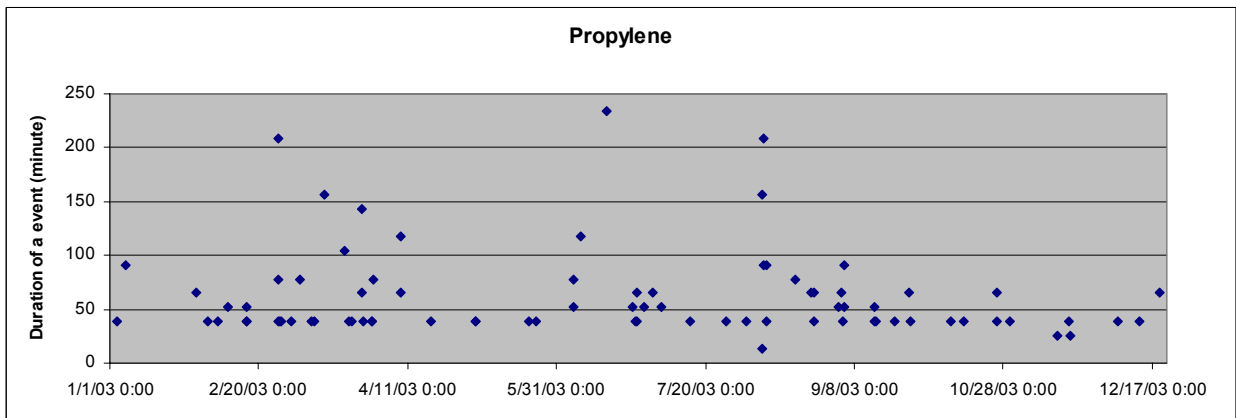
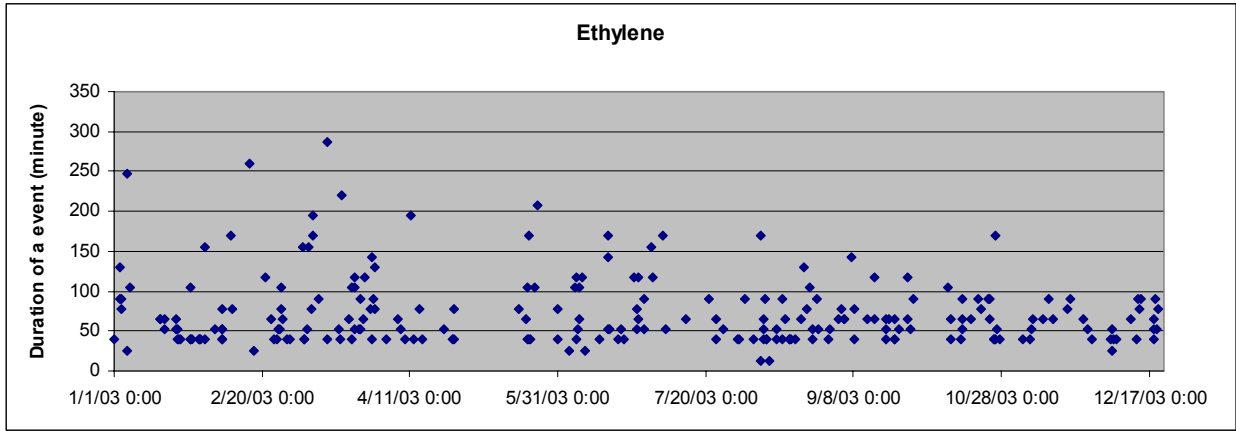


Figure 37 shows, for ethylene and propylene, the duration of individual events, where the duration is defined as the length of time between the start of detection and the return to a no-detect level (10 ppb for ethylene and 20 ppb for propylene). The data clearly show that some events persisted for up to half a day, and some events were very short, but most lasted approximately an hour (4-6 measurement periods). These data are qualitatively consistent with the durations of emission events reported in Section IVa.

Draft

**Figure 38.** Time series pattern of the duration of individual hydrocarbon detection events for ethylene and propene, where the duration is defined as the length of time between the start of detection and the return to a no-detect level (10 ppb for ethylene and 20 ppb for propylene).



**Figure 39.** Time series of hexane concentrations (in this case note that a concentration of 50 ppb corresponds to 300 ppbC) detected at the Seabrook FTIR monitor.

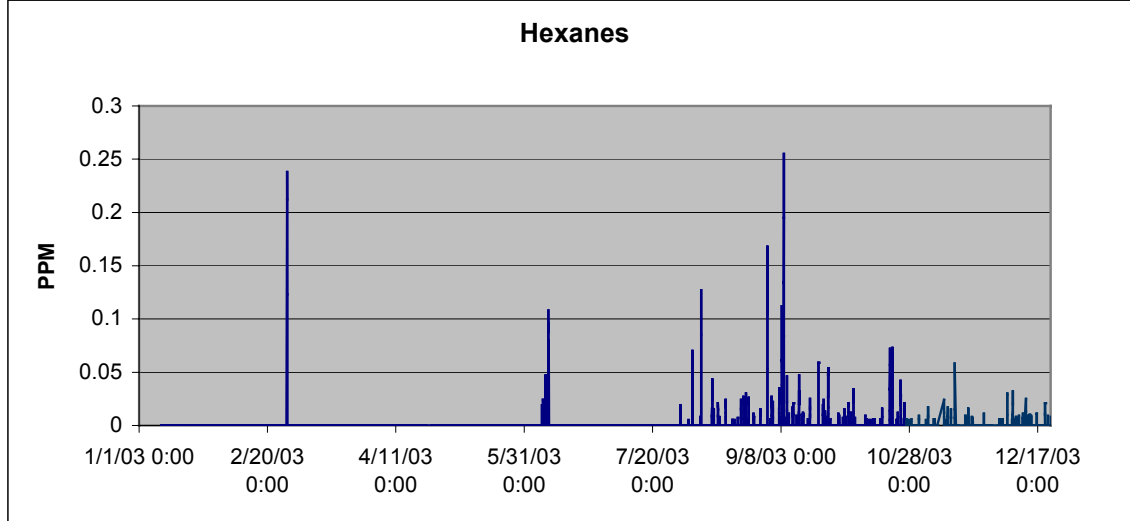
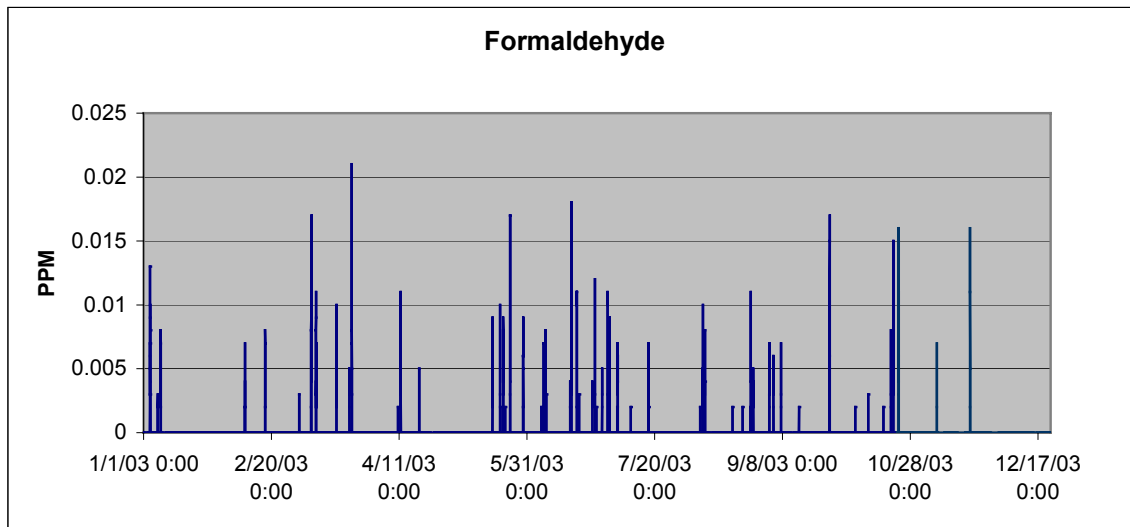


**Figure 40.** Time series of formaldehyde concentrations detected at the Seabrook FTIR monitor.



Figures 39 and 40 provide some additional insights from the Seabrook site FTIR dataset. Figure 39 shows a time series of hexane concentrations (in this case note that a concentration of 50 ppb, or 0.05 ppm, corresponds to 300 ppbC). This time series shows that the detection of very high (more than 1 ppmC) concentrations of some compounds can occur as isolated instances, while other, similar magnitude instances, can occur as part of a recurring pattern of lower concentration measurements. Figure 40 shows a time series of formaldehyde concentrations. While there are some formaldehyde emissions in the Houston-Galveston area, most is formed due to the reactions of hydrocarbons. Thus, the formaldehyde concentration can be viewed as a qualitative surrogate for total hydrocarbons reacted. The data in Figure 40 show that concentrations of formaldehyde exceed the detection limit and reach 5-10 ppb on a roughly weekly basis during the ozone season at this site, with roughly monthly excursions to 15 ppb or above.

To summarize, while the ambient ground data are suggestive of emission variability, it is difficult, based only on ambient ground data, to separate out the effects of atmospheric conditions from the effects of emission variability. Nevertheless, the combined evidence of industrial process upsets and variability in ambient concentrations is consistent and indicative of significant variability in point source VOC and HRVOC emissions. Aircraft data provide additional supporting evidence.

**V a. Observational data Aircraft VOC Measurements**

Figure 41 provides a summary of measurements made by one of the aircraft operating during the Texas Air Quality Study during the summer of 2000. The data are compared to data collected in other U.S. cities by the same aircraft/measurement system. The Houston data reported in Figure 41 are based on the hydrocarbon concentrations observed by the aircraft, during the August and September 2000 sampling program, when ozone was forming very rapidly (ozone formation rates in the top 10% of those observed during the study). The hydrocarbon concentrations are weighted by their atmospheric reactivity (for details, see Kleinman, et al., 2002), so the data are reported in reactivity units. The aircraft data clearly show that the high hydrocarbon concentrations are due to human activities and that Houston has more extreme values of hydrocarbon reactivity (caused by elevated highly reactive hydrocarbon concentrations) than cities that do not have Houston's concentration of industrial facilities. If the elevated concentrations were due strictly to meteorology instead of emission variability, elevated concentrations carbon monoxide would also be expected.

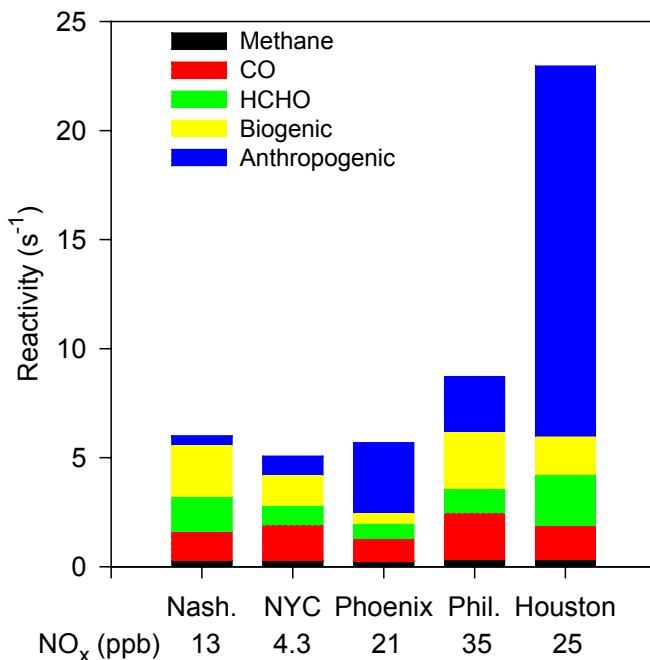


**Figure 41.** VOC reactivity for 5 cities, averaged over a set of samples with ozone formation rate equal or above the 90<sup>th</sup> percentile values. One Houston and one Phoenix VOC sample have been removed as outliers with biogenic reactivity (primarily from terpenes) an order of magnitude greater than the 2<sup>nd</sup> highest value. NO<sub>x</sub> concentration is averaged over near-source samples as defined by Kleinman, et al. (2002)

Additional evidence, supporting the conclusion that the high reactivity of some air samples is caused by industrial point source emissions is shown in Figures 42 and 43. Figure 42a shows that a small percentage of the samples had much higher reactivity than the bulk of the samples collected by aircraft (all of these samples were collected during mid-morning to late afternoon). Figure 42b shows the average composition of the samples that had high reactivity (hydrocarbon concentrations are again weighted by reactivity). The dominant contributors are ethene, propene, and other light alkenes. Figure 43 presents the results of a principal component analysis of the aircraft data collected by Brookhaven National Laboratory. The analysis in Figure 43 indicates that high ozone productivity is most highly correlated with high concentrations of ethene, propene, acetylene, ethane, propane and butane, in the presence of NO<sub>y</sub> (Factor 1). These compounds are commonly associated with emissions from industrial facilities processing light olefins.

**Figure 42.** a.) Distribution of reactivity observed in the samples collected by an aircraft that operated during the Texas Air Quality Study; the distribution is consistent with the ground measurements, showing significant differences between median and high values of reactivity. b.) compounds that contribute to high reactivity in samples collected during rapid ozone formation.

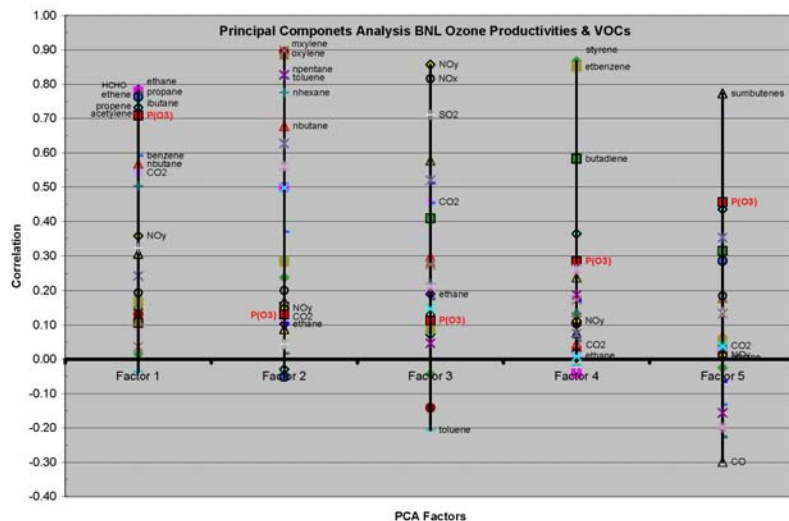
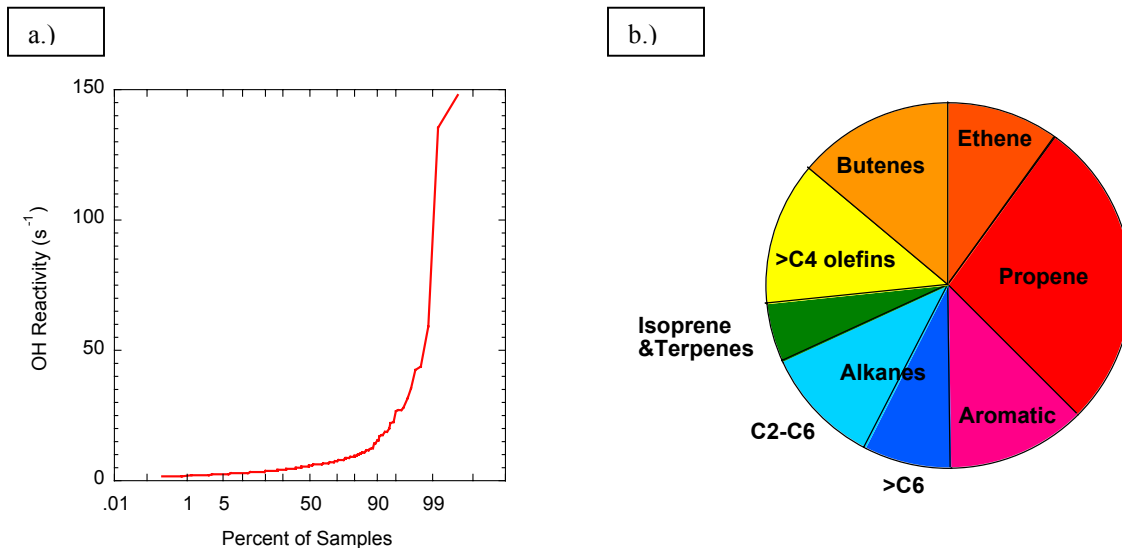


**Figure 43.** Principal component analysis of data collected by Brookhaven aircraft during August and September 2000. Factor 1 is most highly correlated with high ozone formation rate (P(O<sub>3</sub>))

Aircraft data from specific days provide additional supporting evidence for variability in emissions and hydrocarbon concentrations. Hydrocarbon concentrations, measured on sequential days at the same locations, show large variations.

Shown in Figure 44 are comparisons between the observed and predicted concentrations of paraffins (PAR) ethylene (ETH) the sum of higher olefins (OLE, propylene and other terminal olefins), and the sum of internal olefins and higher aldehydes (both represented as ALD2 in the Carbon Bond IV mechanism). The measurements, for August 30, 2000, were taken from aircraft operated by NCAR and NOAA during the Texas Air Quality Study, and the data have been processed to be comparable with the modeled species. The predicted values are from TCEQ's gridded photochemical model. Each vertical line in the Figure represents one point of comparison. The modeled values include enhanced ethylene and olefin emissions (emission approximately 600% greater than those reported in the Special Inventory for 2000), but these emissions are assumed to have a uniform temporal distribution.

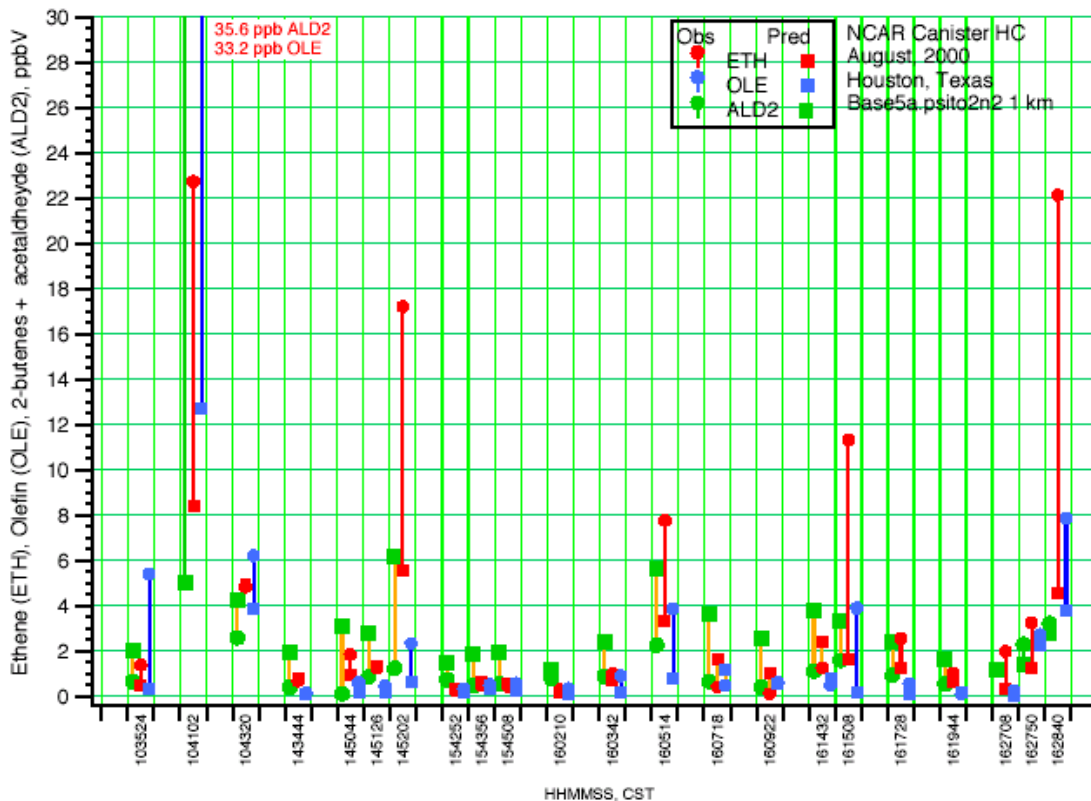


**Figure 44.** Comparisons between the concentrations of ethylene (ETH), sum of higher olefins (OLE, propylene and other terminal olefins) and sum of internal olefins and higher aldehydes (both represented by ALD2) observed by aircraft on August 30, 2000, during the Texas Air Quality Study, and concentrations predicted by a gridded photochemical model. Each vertical line in the Figure represents one point of comparison. The modeled values include enhanced ethylene and olefin emissions, but these emissions are assumed to have a uniform temporal distribution.

The comparison shows a systemic overprediction of hydrocarbon concentrations in the model at low observed concentration levels, but underprediction of the highest observed concentrations.

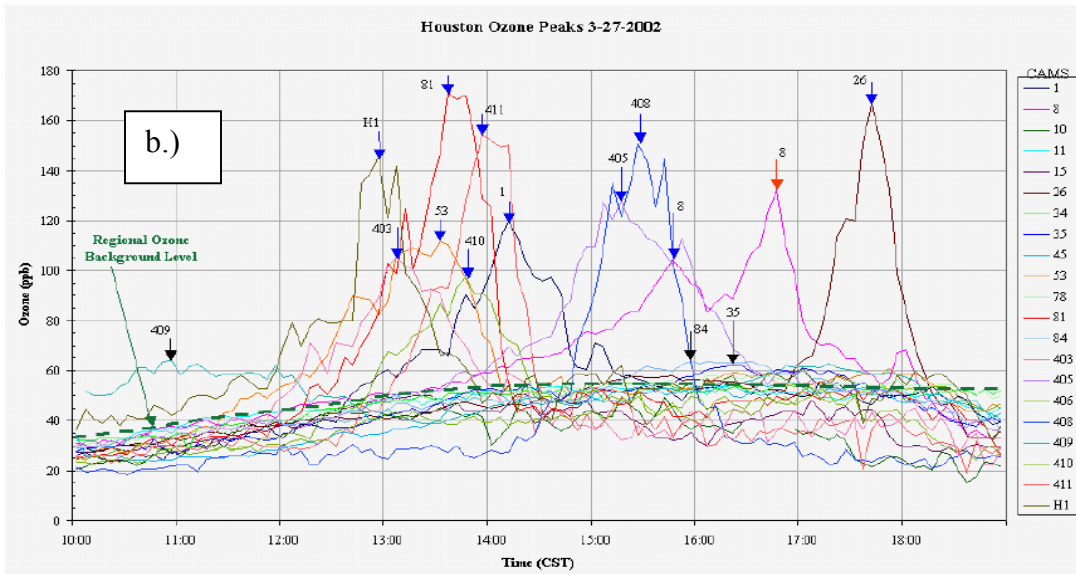
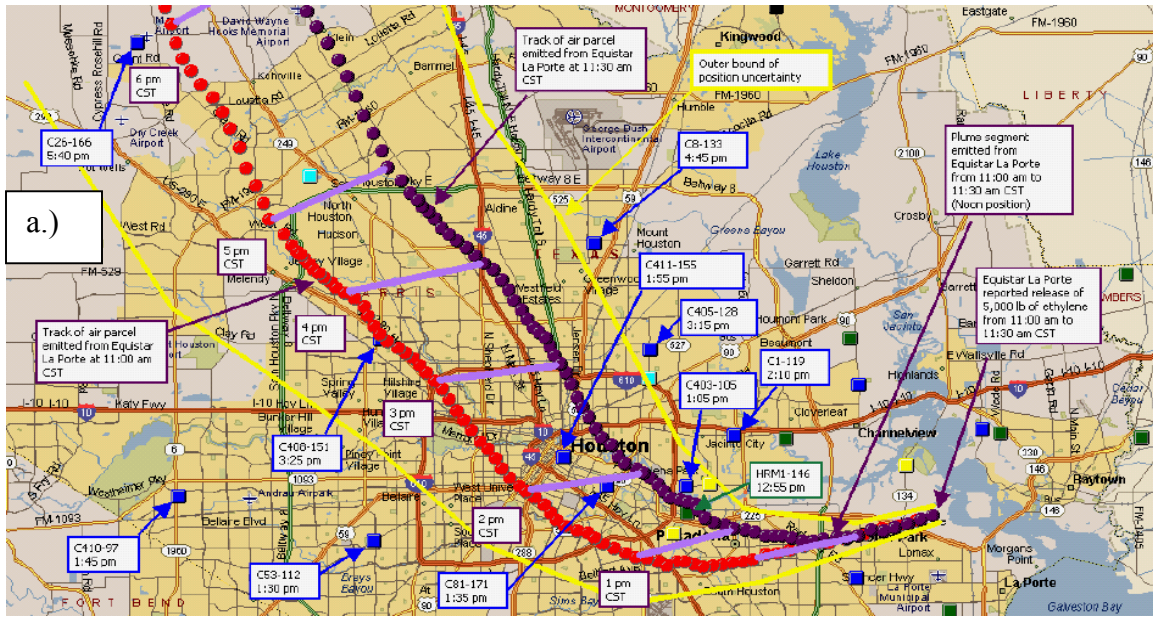
**V a. Observational data** *Ozone measurements*

As will be demonstrated in later sections of this report, only a small fraction of instances where emissions increase substantially above annual averages will lead to changes in the peak ozone concentrations in Houston. In order for emission events and other sources of emission variability to influence peak ozone concentrations, they must occur during times that are conducive to ozone formation and at locations that provide sufficient sources of other emissions (principally nitrogen oxides) that will lead to significant reactions of the emissions.

Later sections of this report will examine the ozone formation consequences of the full range of emission variability, using computationally efficient tools. The goal of that analysis will be to identify the characteristics of the small fraction of instances of emission variability that lead to increases in peak ozone concentrations. In this section, the goal is to document the potential magnitude of changes in peak ozone concentrations, due to emission variability, using data from the ozone monitoring network in Houston. The air quality episodes selected are, of necessity, extreme examples of the impact of emission variability on ozone concentrations, since these are the instances that are most evident in the observational record. While they should be recognized as extreme instances, they are useful to examine since they define the magnitudes of changes in ozone concentrations that air quality models should be able to replicate.

One extreme episode that has been well documented by TCEQ staff occurred on March 27, 2002. In LaPorte, a series of ethylene releases totaling more than 10,000 pounds were released over several hours. One release of approximately 6700 pounds occurred between 11 AM and noon, lasting for approximately 30 minutes. This release was advected initially to the west, then to the northwest, passing over significant highway sources of  $\text{NO}_x$ . Most of the monitors in the Houston area showed peak concentrations of roughly 60 ppb on this day, however, several of the the monitors that were in the path of the plume reached peak ozone concentrations in excess of 160 ppb. The estimated air parcel plume and the data from the ozone monitors are shown in Figure 45.

Figure 45. a.) Estimated trajectory of a 10,000+ lb ethylene release at LaPorte, (6700 lb between 11 and 11:25 AM) on 3/27/2002. b.) Multiple ozone monitors were in the path of the plume; other monitors were outside of the path.



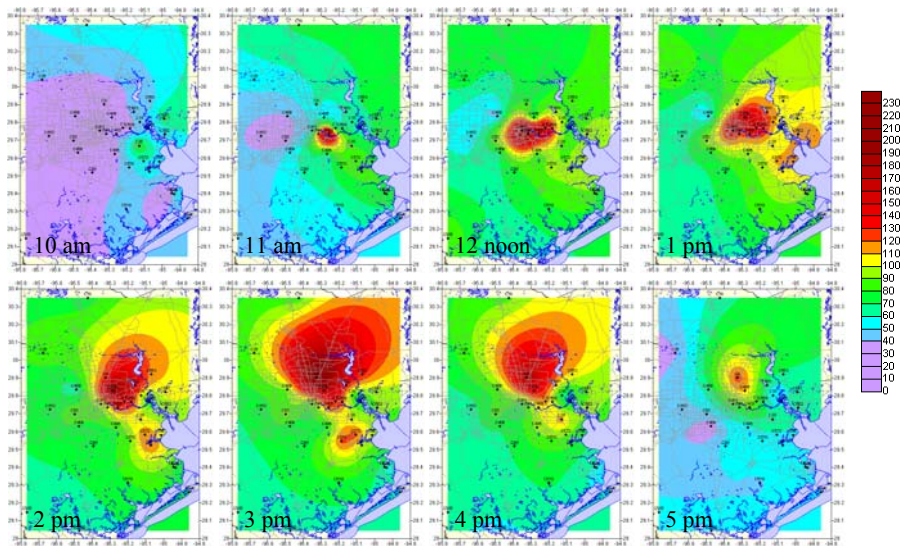
Another ozone episode that appears to be related to a emission variability occurred on October 23, 2003. On this date, ozone monitors detected a large plume of ozone originating in the area near the Clinton Drive monitor, which is located just east of the East 610 Loop where it intersects the 10 Freeway. As shown in Figure 46, peak ozone concentrations eventually reached more than 200 ppb at sites as distant as Aldine (near Bush Intercontinental Airport). Also detected at the Clinton site, were very high concentrations of hydrocarbons. These data are also shown in Figure 46.

**Figure 46.** Data from an ozone episode that occurred on October 23, 2003.

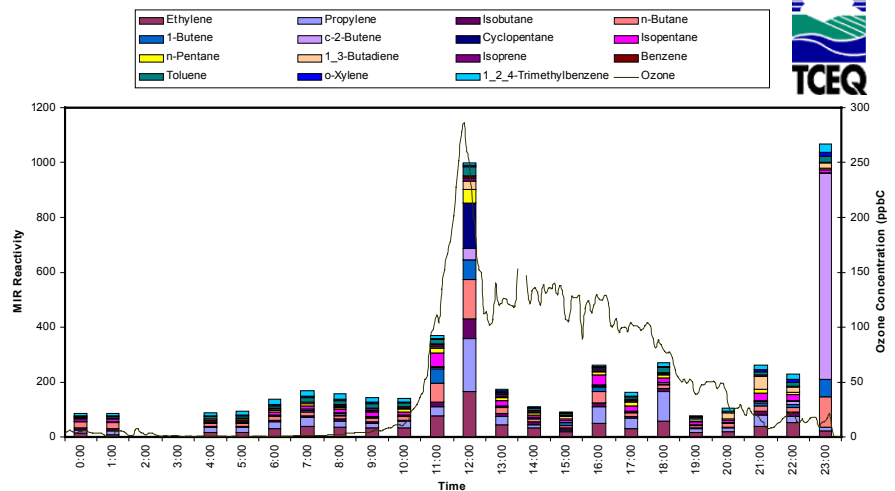
a.) high ozone concentrations, including concentrations in excess of 200 ppb were detected initially near the Clinton monitor at 11AM; high concentrations subsequently spread over a large region

b.) high hydrocarbon concentrations (represented in units of reactivity) were detected at the Clinton site at the start of the event

Contour Maps Showing the Progression of High Ozone on 10-23-03



Ozone Concentration (5 Min. Data) and VOC Reactivity Vs. Time at Clinton C403 for 10-23-03



A systematic analysis has also been done of all days during 2003 when ozone concentrations exceeded 125 ppb (1-hour average) at sites that also recorded hourly hydrocarbon concentrations using an auto-GC (URS, 2004; see Appendix). The analysis identified 31 exceedances of the ozone standard (1-hour average) at the auto-GC sites during 2003. Nine of these exceedances occurred when VOC reactivity exceeded the levels TCEQ considers high; 26 of the exceedances occurred on days when reactivity was high either during or preceding the exceedance. Additional information concerning these analyses is provided in the Appendix.

**V b. Air quality modeling analyses**

Air quality models can be used to assess the effect of instances of emission variability on peak ozone concentrations. One such analysis is shown in Figure 47, which shows the impact of a 10,000 lb/hr, 2 hour release in the region near Deer Park. This modeling was done using a 1-km grid resolution in the region of the release. The difference in peak ozone concentration between the simulation with the release and without the release is more than 50 ppb.

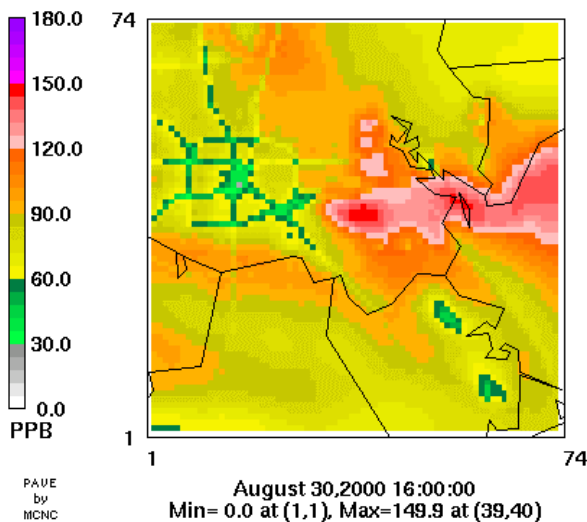
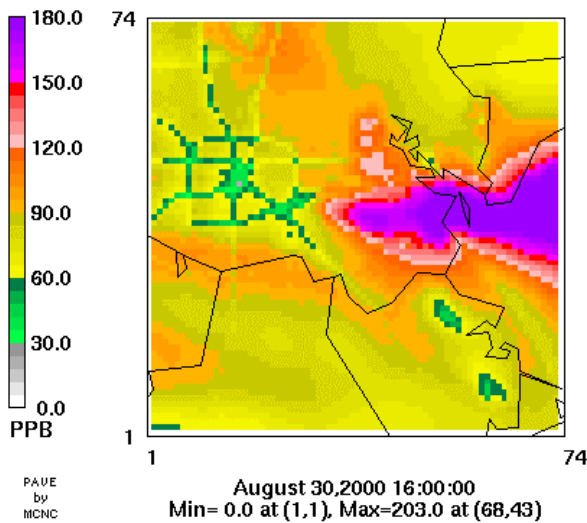


**Figure 47.** 3-D photochemical grid model simulation of an ozone episode on August 30, 2000, performed using the Comprehensive Air Quality Model with extensions (CAMx) at a 1-km grid resolution; the upper plot shows the base case simulation (peak ozone concentration of 150 ppb) with no emission event; the lower plot shows the ozone concentrations predicted if a 10,000 lb/hr, 2 hour reactive olefin release is added to the base case. The peak ozone concentration in the simulation with the release is in excess of 200 ppb, more than 50 ppb higher than in the base case.



Simulations of the type shown in Figure 47 could, in principle, be used to simulate the impacts of a wide variety on instances of emission variability on peak ozone concentrations. The computational requirements of this approach, however, are extremely demanding. It would be difficult, if not impossible, to consider thousands of potential emission variability scenarios in full 3-D photochemical grid models. Therefore, in this work, an alternative modeling approach was employed, which is described in the next section.

## **VI. Modeling tools for characterizing the ozone formation potential of ozone formation**

As outlined in Section V, it would be difficult, if not impossible, to consider thousands of instances of emission variability in full 3-D photochemical grid models. Yet, consideration of many different emission “snapshots” or scenarios is necessary, because of the emission variability outlined in previous sections of this report. Therefore, in this work, an alternative to full 3-D modeling was employed, which will be referred to as sub-domain modeling.

The sub-domain modeling approach recognizes that the emission variability occurs in the Ship Channel and other industrialized regions of the Houston Galveston area and that much of the photochemistry leading to increased ozone formation will be confined to relatively small sub-domains near the industrial source regions. Computationally efficient sub-domain models can be built to examine the effect of emission variability in these sub-domains. The sub-domain models can be used as screening tools to identify the types of emission variability (time, location and magnitude of emission) that would have the greatest impact on ozone formation. Once a small number of emission scenarios are identified, they can be more precisely simulated in a full 3-D photochemical model.

### **VI a.) Computationally efficient sub-domain models**

The steps involved in developing computationally efficient sub-domain models are:

- Identify sensitive sub-domains based on full 3-D photochemical model simulations
- Match 3-D photochemical model to computationally efficient sub-domain model using Process Analysis
- Run scenarios in computationally efficient sub-domain model
- Evaluate sensitive scenarios in full 3-D photochemical model

Each of these steps is described in more detail below.

*Identify sensitive sub-domains based on full 3-D photochemical model simulations* The 3-D gridded photochemical model that was used in this work is the same model that is being used to develop revisions to the air quality plan for the Houston-Galveston area. The Comprehensive Air Quality Model with extensions (CAMx) was used in the simulations and the historical ozone episode used in the analysis spanned the period from August 22-September 1, 2000.

The first step in the analysis was to use the full 3-D photochemical model to identify the locations of critical sub-domains. This was done by identifying areas upwind of peak ozone concentrations in the base case episode and in a number of future year, control strategy simulations. Figure 48 shows results from the simulation labeled FY07i CS03\_harCap GOES2. This simulation has the meteorology for the August 25-September 1, 2000 historical episode modified by GOES satellite data, and emissions projected to future year 2007 (FY 07), reduced using the suite of controls labeled as Control Strategy 3 (CS03) with a cap on HRVOC emissions. Figure 48 shows the locations of peak ozone concentrations on August 25 and August 30, two of the days that had high ozone concentrations for this simulation. Also shown in Figure 48 are industrialized sub-domains upwind of the locations where peak ozone concentrations were predicted.

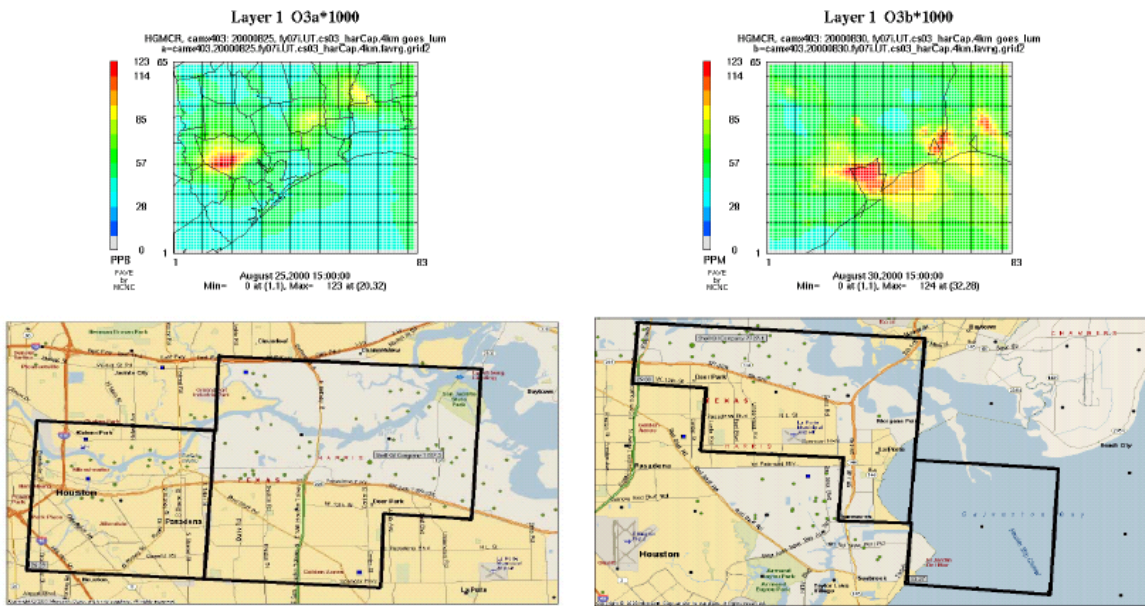


**Figure 48.** Locations of peak ozone concentrations on August 25 and August 30, two of the days that had high ozone concentrations for this simulation (upper plots), and industrialized sub-domains upwind of the locations where peak ozone concentrations were predicted (lower plots).

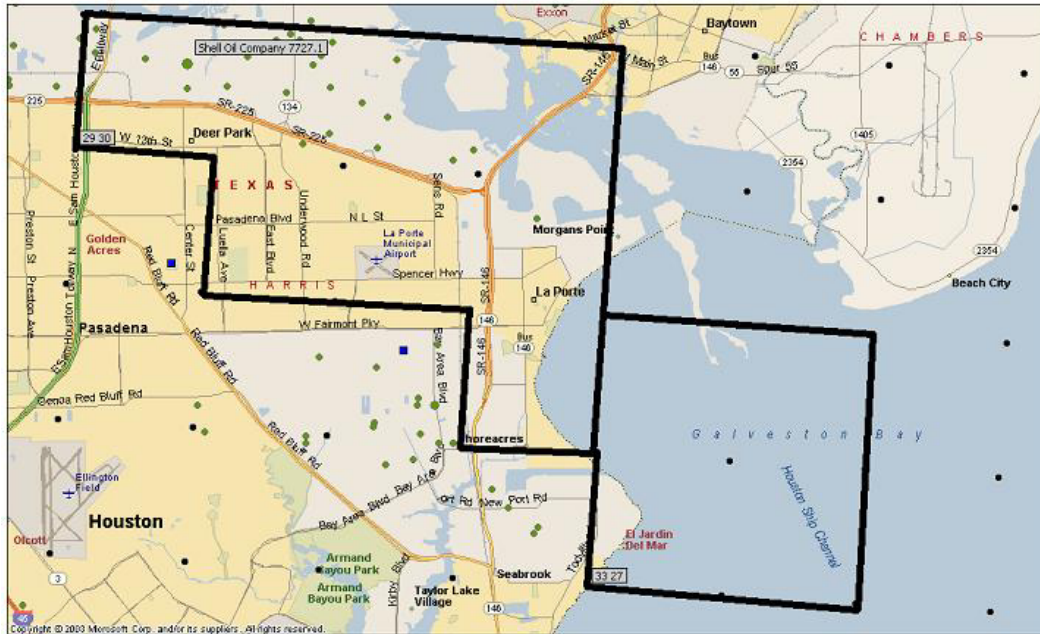
Figure 49 shows, in more detail, the sub-domain for August 25. Wind trajectories on this date, during the time period preceding the peak ozone concentration, were out of the east. Therefore, the peak ozone concentration is most sensitive to emissions beginning near Deer Park and advecting to the west-southwest over industrial and urban NOx sources. The area outlined in Figure 49 captures this source region.



8\_25\_00 Process Analysis Box outlined in black. Black Dots represent lower left hand corner of 4 km grid cells

**Figure 49.** Sub-domains for August 25. Wind trajectories on this date, during the time period preceding the peak ozone concentration, were out of the east. Therefore, the peak ozone concentration is most sensitive to emissions beginning near Deer Park and advecting to the west-southwest over industrial and urban NOx sources. For an explanation of the two areas outlined, see text.

Figure 50 shows, in more detail, the sub-domain for August 30. Wind trajectories on this date, during the time period preceding the peak ozone concentration, were out of the northwest. Therefore, the peak ozone concentration is most sensitive to emissions beginning near Deer Park and advecting to the southeast over industrial NO<sub>x</sub> sources, and out over Galveston Bay. The areas outlined in Figure 50 capture this source region.



8\_30\_00 Process Analysis Box outlined in black. Black Dots represent lower left hand corner of 4 km grid cells

**Figure 50.** Sub-domain for August 30. Wind trajectories on this date, during the time period preceding the peak ozone concentration, were out of the northwest. Therefore, the peak ozone concentration is most sensitive to emissions beginning near Deer Park and advecting to the southeast over industrial NO<sub>x</sub> sources, and out over Galveston Bay. The areas outlined in capture this source region. For an explanation of the two areas outlined, see text.

Figures 49 and 50 identify two sub-domains, one in the upwind region that contains the added emission source, and a second, downwind area. To understand why two sub-domains are used, it is necessary to understand the conflicting goals that are involved in selecting sub-domains.

One goal in sub-domain selection is to make the area of the sub-domain sufficiently large so that the area includes both the source and the location of the peak ozone concentration. A conflicting goal is imposed because the computationally efficient sub-domain model assumes that the sub-domain is well mixed, as described later in this section. Since the sub-domain is assumed to have homogeneous concentrations (the sub-domain is well-mixed), the sub-domain should be kept as small as possible to preserve information about localized peak ozone concentrations.

A method for dealing with these conflicting demands on the spatial scale of the sub-domain is to create two sub-domains – a source sub-domain and a down-wind sub-domain. Figures 49 and 50

## Draft

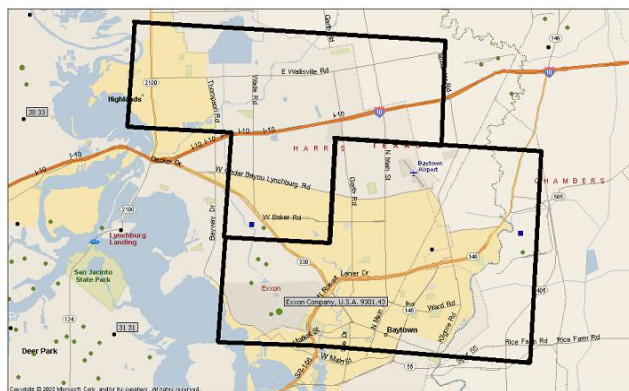
show these two-sub-domains for the region upwind of the peak ozone concentration on August 25 and 30.

Figure 51 shows additional sub-domains used in this analysis. These sub-domains were selected because they are in regions that are not near the locations of peak ozone concentrations. They were selected to provide a contrast to the sub-domains shown in Figures 49 and 50.

**Figure 51.** Sub-domains originating near Chocolate Bayou and Baytown. The lower boxes are the source regions; the upper boxes are the downwind regions. These sub-domains were selected because they are in regions that are not near the locations of peak ozone concentrations.



8\_28\_00 Process Analysis Box outlined in black. Black Dots represent lower left hand corner of 4 km grid cells



8\_28\_00 Process Analysis Box outlined in black. Black Dots represent lower left hand corner of 4 km grid cells

*Match 3-D photochemical model to computationally efficient sub-domain model using Process Analysis* Once the sub-domain locations are selected, a computationally efficient sub-domain model is constructed. The goal of the sub-domain model is to mimic the predictions of the full

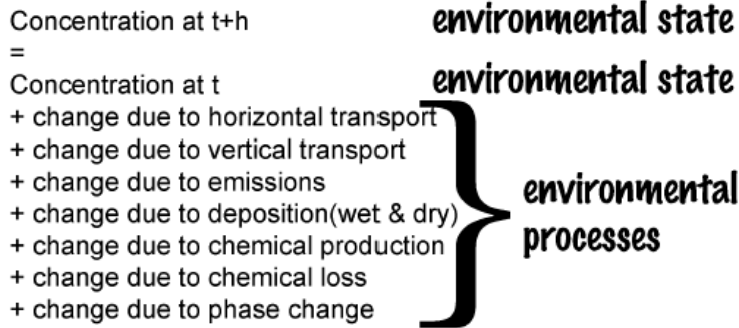
## Draft

3-D simulation, as accurately as possible, within the sub-domain. The sub-domain model achieves its computational efficiency by assuming that all of the concentrations within the sub-domain are homogeneous (the sub-domain is well mixed). Clearly, this is an approximation, therefore, the sub-domain model will not precisely replicate the spatial sensitivity of the 3-D simulation. Completely replicating the full 3-D simulation is not the goal, however. The goal is to create a computationally efficient sub-domain model that will show the same relative sensitivity to added emissions as the full 3-D model. The sub-domain model is used as a screening tool to identify emission times and locations that will most affect peak ozone concentrations in the full 3-D model.

To make the sub-domain model an effective screening tool for evaluating the impact of added emissions on ozone formation, the atmospheric processes used in the sub-domain model to calculate ozone and other pollutant concentrations are matched to the predictions of the full 3-D model using a tool referred to as Process Analysis.

Gridded, 3-D photochemical air quality models calculate the rates of atmospheric processes that control air pollutant concentrations. These processes include chemical formation, chemical consumption, advection, diffusion, and deposition. In the photochemical model, these processes are coupled into a system of mass continuity equations used to predict the species concentrations in each grid cell (Russell and Dennis, 2000). Many models output only the spatial and temporal distribution of species concentrations. The magnitudes of the individual processes (advection, diffusion, deposition, and chemical formation and destruction) that lead to these changes in species concentrations are not typically recorded.

# Conceptual Model



**some changes are positive and some are negative**

**Figure 52.** Conceptual model explaining processes that contribute to changes in pollutant concentrations.

Figure 52 illustrates the conceptual basis of a “process-based” photochemical grid model. Concentrations of pollutants at every time step are determined by a set of processes that describe the physical and chemical changes that are occurring. Various physical and chemical processes that affect the species concentrations are represented in the model by fluxes, flows of mass, momentum, and energy. When these processes are allowed to operate simultaneously for a small amount of time, changes in species concentrations over a time step are predicted. This “marching in time” technique can be used to advance a given initial concentration to a future time by repeating many incremental steps.

This conceptual model is implemented in a photochemical grid model as “well-mixed” environmental volumes, or grid cells as shown in Figure 53. These grid cells are subjected to a mass balance at each time step. The air quality model utilized in the analyses reported here applied grid cells of different sizes, ranging from 1 km by 1 km to 4 km by 4 km, or larger, in horizontal resolution. The grid cells can extend vertically from 20 to 1000 meters.

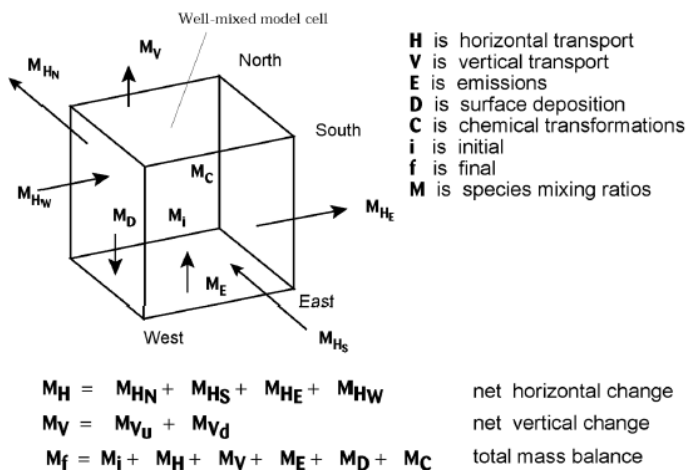


**Figure 53** Models are formulated using “well-mixed” chemical reactor cells that hold concentration information and are subject to a collection of processes that modify those concentrations over short time steps.

Figure 54 shows that many well-mixed grid cells are coupled together via cell-to-cell transport through all faces in common with other adjacent cells. This cell-to-cell transport can either be by advection or by diffusion. In air quality models, the rates of all these processes for each cell are added together and the combined effect is integrated and added to the initial state to predict the subsequent state. In most 3-D gridded models, only the resulting species concentrations are saved and all information concerning how these concentrations were achieved is lost.

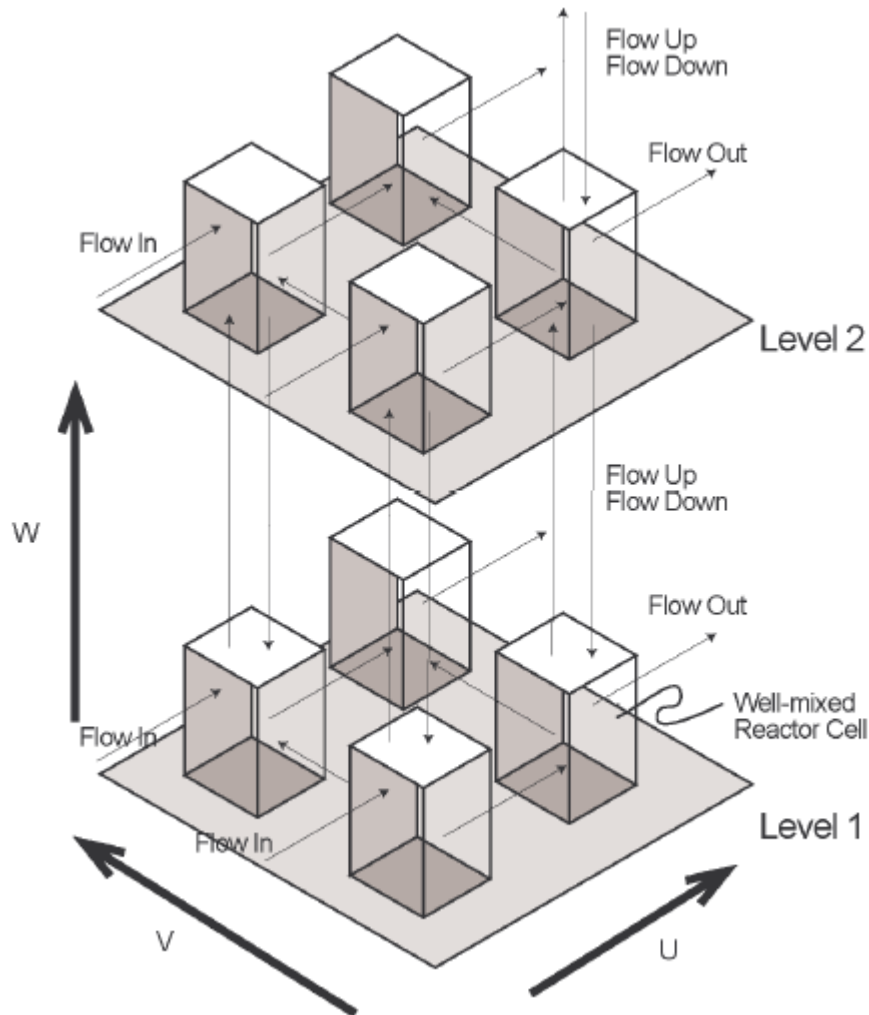


**Figure 54** Conceptual drawing of the CAMx grid cell network of many “well-mixed cells” coupled together via cell to cell transport through all faces in common with other adjacent cells. This cell-to-cell transport can either be by advection or by diffusion.

Process analysis techniques permit displaying the roles of individual processes that contribute to ozone formation in a complex model. These methods were developed at the University of North Carolina by Jeffries and his graduate students beginning in the 1990s (Crouse, 1990; Jeffries, 1993, Tonnesen and Jeffries, 1994; Jeffries and Tonnesen, 1994; Jang et. al, 1995; Jeffries, Keating, Wang, 1997; Jeffries and Wang, 1997). The Comprehensive Air quality Model with

extensions (CAMx) photochemical air quality model includes the option to output process analysis data (Environ 2004).

As part of this project, the existing Process Analysis tools were modified and expanded at the University of Texas by Jeffries, Kimura and Vizuete to function with the existing output of CAMx and additional post processing codes were written. (Tesche, et al., 2004; Vizuete *et al.* 2004). These were needed to permit a dynamic vertical analysis box that was a new feature of the University of Texas version of the Process Analysis code. The process analysis tool produces a significant amount of information that ultimately leads to the creation of spreadsheets entitled “time series” and “cycles”. In the time series, a series of graphs show the magnitudes of the various processes that are used to determine species concentrations, as a function of time of day. In the cycles spreadsheet, the initialization, propagation, and termination processes in the chemistry are illustrated and distributions of competitive pathways in the chemistry are shown.

Figure 55 shows an example of a time series plot that illustrates the process rates and model concentrations versus time (Jeffries, et al., 1997). This graph closely follows the concepts shown in Figure 53, where the model concentration is given for each hour and the magnitudes of the various processes are shown as different colored lines. In these graphs the chemistry change is the net change due to multiple reaction pathways, so time series plots alone are not capable of explaining the contributions of specific reaction pathways to the net change. A different type of analysis detailed in the cycle spreadsheet is required to characterize the magnitudes of particular reaction pathways.

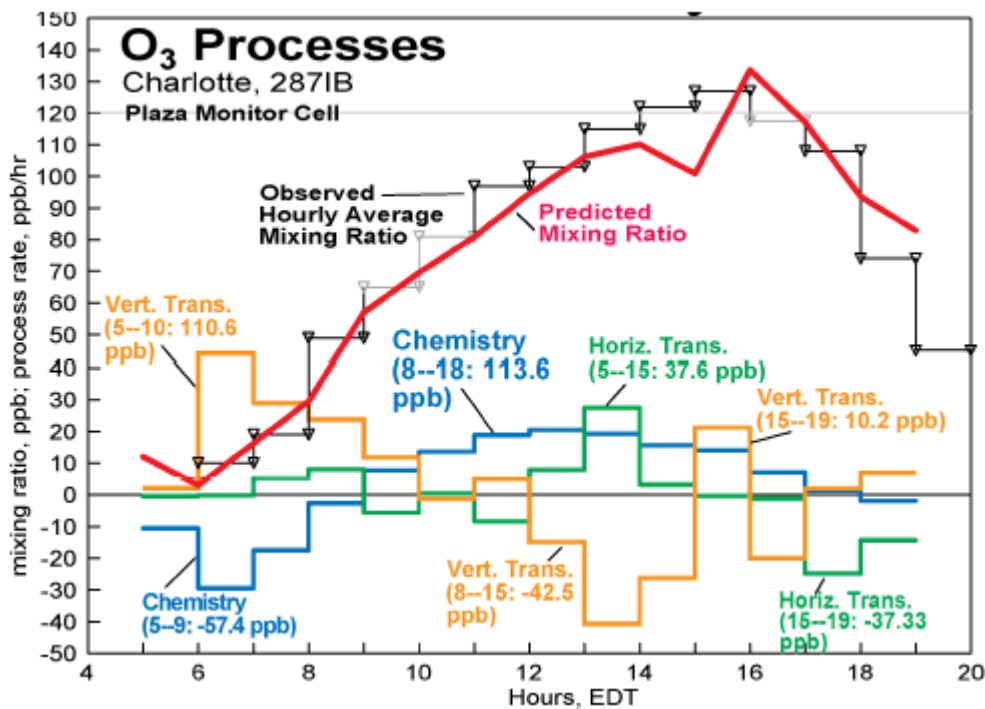


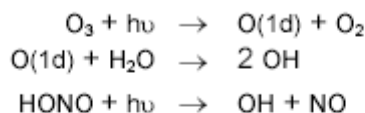
**Figure 55.** Example Process Analysis time series plot with observed hourly averaged observations. The change in the red line (predicted mixing ratio or concentration) is the sum of all of the individual processes represented by the green, blue and yellow lines ( $\Delta\text{O}_3$  mixing ratio in any hour =  $\Sigma$  net vertical transport + net horizontal transport + net chemical production)

## Draft

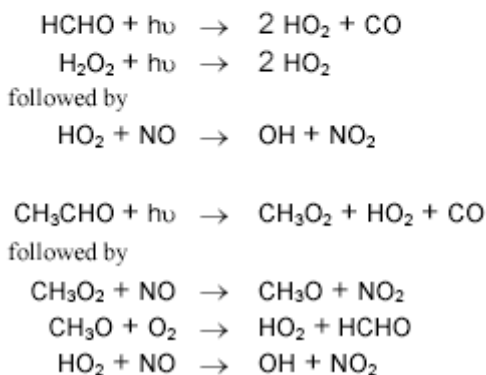
In order to describe the data provided by the cycles spreadsheet, which describes reaction cycles in the atmosphere responsible for generating ozone, it is useful to briefly review ozone formation pathways. Ozone ( $O_3$ ) is not emitted directly from sources, but is formed by chemical reactions in the atmosphere (Seinfeld 1995). Combustion processes emit mostly NO, which is rapidly oxidized to  $NO_2$  in the ambient air. In sunlight, the  $NO_2$  is photolyzed to produce NO and atomic oxygen,  $O(^3P)$ . The atomic oxygen then reacts with molecular oxygen to form  $O_3$ . Therefore, the photolysis of  $NO_2$  is the major source of  $O_3$  in the troposphere. This ozone can immediately react with NO to produce  $NO_2$  again. In the absence of competing reactions, NO,  $NO_2$ , and  $O_3$  reach equilibrium and the amount of  $O_3$  never exceeds the amount of  $NO_x$  ( $NO+NO_2$ ). However, if volatile organic compounds (VOCs) are present in the system then free radicals, generated from the oxidative degradation of VOCs, oxidize NO to  $NO_2$ . This oxidation results in accumulation of the  $O_3$  formed in the  $NO_2$  photolysis, causing a net increase in  $O_3$ . The NO can be reused several times under these conditions (NO is oxidized by a hydrocarbon radical, converted to  $NO_2$ ; the  $NO_2$  photolyzes to form NO and  $O(^3P)$ ; the  $O(^3P)$  reacts to form ozone and the NO starts the cycle again). Thus, the amount of  $O_3$  can now be many times the amount of  $NO_x$ . The hydrocarbon radicals are products of the reactions involving hydroxyl radicals, OH, with VOC and CO. Each time a radical oxidizes an NO, an  $O_3$  accumulates and another  $NO_2$  is generated. This  $NO_2$  can again photolyze to create yet another  $O_3$ . Eventually the reaction of  $NO_2$  with several of the radicals forms nitrogen products such as nitric acid ( $HNO_3$ ) and organic nitrates terminating the production of  $O_3$  from that particular NO molecule. In the Carbon Bond IV mechanism used by the model in this study, new OH radicals are produced directly and indirectly by the following reactions (Jeffries, 1995):

### Radical Initiation Reactions

#### Direct OH:



#### Indirect OH:

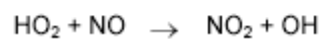
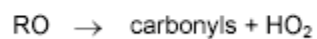
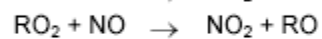
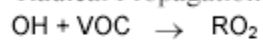


Following radical initiation, VOCs are oxidized and NO-to- $NO_2$  conversion occurs in radical propagation steps. The following reaction steps illustrate a propagation chain where a VOC molecule is converted to one or more carbonyl molecules and two molecules of NO are

## Draft

converted to two molecules of  $\text{NO}_2$ . Note that the free radical emerges as OH again at the end of the chain. In these chains, the initial OH could be either a new OH or a re-created OH.

### Radical Propagation Reactions



The radical propagation stops when the reacting radicals are incorporated into stable products. The following are the radical termination steps.

### Radical Termination Reactions



Figure 56 shows a schematic in which the OH initiation, propagation, and termination and the NO emissions, oxidation, and photolysis cycles are combined. Here the NO<sub>x</sub> and radical cycles which show the re-creation of OH and of NO, are made explicit.

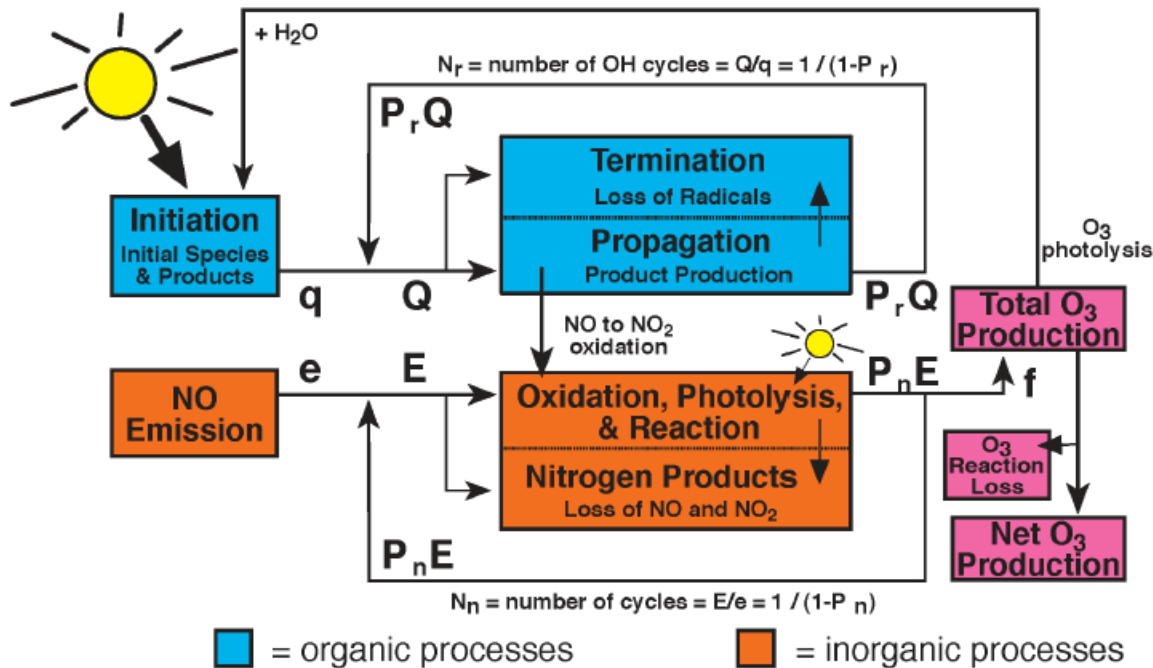


**Figure 56** Conceptual model of the radical and nitrogen oxides chemical cycles resulting in ozone production (Jeffries, 1995)

The named quantities in the figure are:

- $q$  = "new OH" radicals produced by photolysis, ppb
- $Q$  = "total OH" radicals reacting, ppb:  $Q = q + q P_r + q P_r^2 + \dots = q / (1 - P_r)$
- $P_r$  = OH propagation factor,  $< 1.0$  due to termination
- $e$  = "new NO" from emissions, ppb
- $E$  = "total NO" reacting, ppb:  $E = e + e P_n + e P_n^2 + \dots = e / (1 - P_n)$
- $P_n$  = NO propagation factor,  $< 1.0$  due to termination
- $f$  = net O<sub>3</sub> yield from NO<sub>2</sub> photolysis

The term  $P_r$  represents the fraction of OH that propagates via reactions with VOC, and  $1 - P_r$  is essentially the fraction of OH that reacts with NO<sub>2</sub> to make HNO<sub>3</sub>. Similarly, the term  $P_n$  represents the fraction of NO<sub>2</sub> that is photolyzed, and  $1 - P_n$  symbolizes the fraction of NO<sub>2</sub> that is converted to termination products (HNO<sub>3</sub>, RNO<sub>3</sub>) or is lost by physical processes like deposition and horizontal or vertical transport.

An example of an application of a cycle diagram is shown in Figure 57, which is for a UAM application in Charlotte, NC over a 6 x 6, 5-km aggregated cell area covering the downtown region (Jeffries *et al.* 1997). The numerical values in this figure are typical of conditions that led to ozone near the one-hour standard. Charlotte is in general NO<sub>x</sub> limited, but the core city are near the optimum ozone production conditions. This is evident in that the NO<sub>x</sub> is nearly completely consumed by the end of the daylight period.

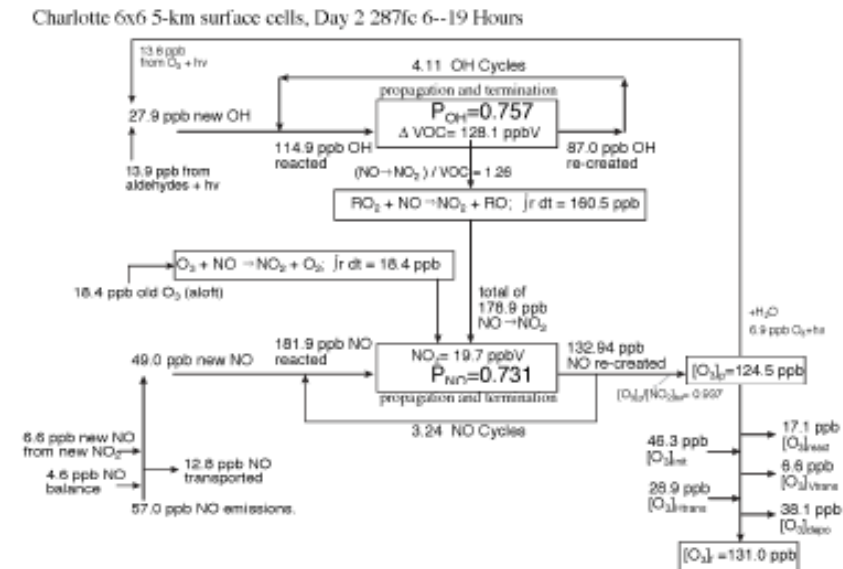


Figure 57 Example of the Process Analysis Radical and Nitrogen Cycles diagram (Jeffries, 1995)

For NO<sub>x</sub> limited conditions, new O<sub>3</sub> is explained by the following:

$$\text{new O}_3 = E * P_n * f$$

where

$$E = (\text{new NO}) [1/(1 - P_n)] = \text{total NO oxidized to NO}_2$$

$$P_n = \text{fraction of all NO}_2 \text{ that is photolyzed}$$

$$f = \text{fraction of all NO}_2 \text{ photolysis reactions that make ozone}$$

Using the values in Figure 57, new NO = 49.0 ppb, P<sub>n</sub> = 0.731, f = 0.937. Therefore (new O<sub>3</sub>)/(new NO) = 2.54

For radical limited conditions, new O<sub>3</sub> is explained by the following:

$$\text{new O}_3 = (\text{VOC reacted}) * R * P_n * f$$

where

$$(\text{VOC reacted}) = (\text{new OH}) * [1/(1 - P_r)] + (\text{VOC photolyzed})$$

$$R = (\text{NO} \rightarrow \text{NO}_2) / (\text{VOC reacted}) \text{ essentially a type of "mixture reactivity"}$$

$$P_n = \text{fraction of all NO}_2 \text{ that photolyzes}$$

$$f = \text{fraction of all NO}_2 \text{ photolysis reactions that make ozone}$$

Using the values in Figure 57, new OH = 27.9 ppb, P<sub>r</sub> = 0.757, R = 1.26  
(new O<sub>3</sub>)/(new OH) = 4.46

These two values are the “gain” or “chemical amplification” of the system. If there is sufficient NO<sub>x</sub>, then for 1 ppb of new OH radical created, there will be 4.4 ppb ozone created. From the NO<sub>x</sub> viewpoint, if there are sufficient sources of peroxy radicals, then for every 1 ppb of NO emitted, there will be 2.5 ppb ozone created.

Returning to the sub-domains of Figures 49 to 51, time series and cycle analyses can be extracted from the full 3-D model for these subdomains, as shown in Figure 58. Figure 58 (analogous to Figure 55) reports the horizontal transport, vertical transport and chemical production/destruction of ozone for the August 25 sub-domain (source region). The results shown in Figure 58 are for the full 3-D simulation. From the full 3-D simulation, the following data are extracted for use in the computationally efficient sub-domain model:

- Hour by hour emissions into the sub-domain
- Hour by hour concentrations of individual chemical species entering the sub-domain, horizontally and vertically
- Hour by hour wind fields causing vertical and horizontal advection
- Hour by hour changes in mixing heights, based on changes in vertical diffusivity as a function of elevation
- Hour by hour deposition rates and photolysis rates

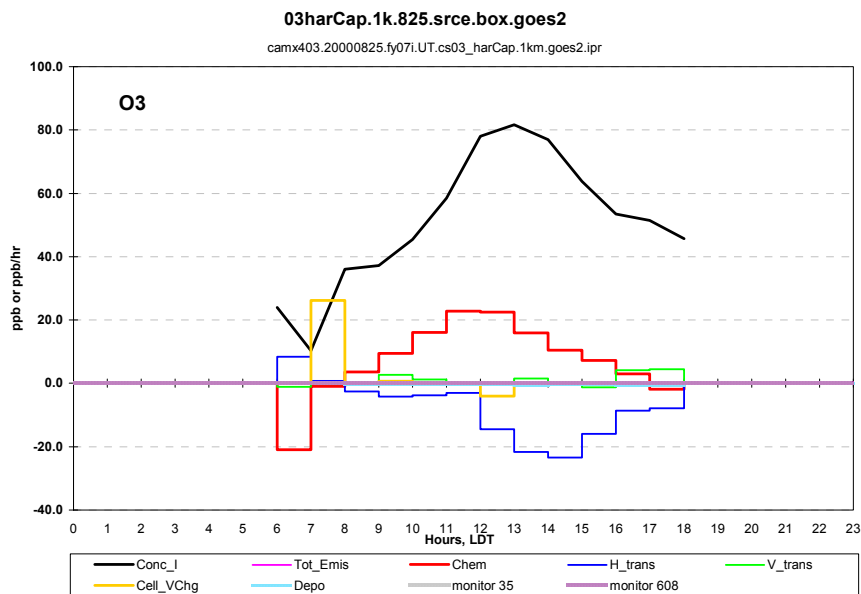


**Figure 58.** Time series process analysis from the full CAMx simulation for the sub-domain shown in Figure 49 (source region)

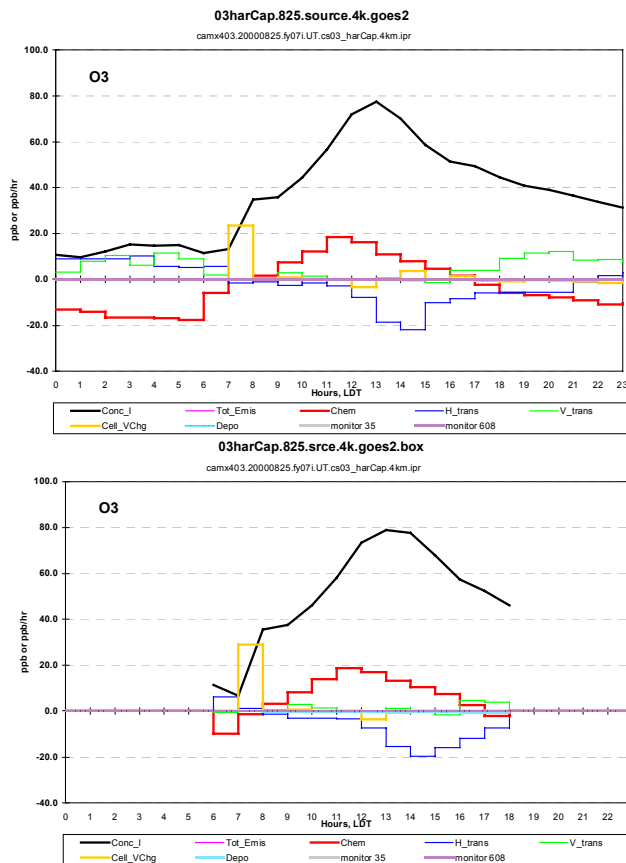
Based on these inputs, the sub-domain model calculates:

- Hour by hour chemical formation and destruction of species in the sub-domain
- Hour by hour concentrations of individual chemical species leaving the sub-domain due to advection and diffusion
- Hour by hour net (entering – leaving) vertical and horizontal advection
- Hour by hour concentrations of chemical species

# Draft

These quantities, calculated by the sub-domain model, can be represented in time series and compared to the time series of the same quantities calculated by the full gridded simulation. If the two time series match, then the computationally efficient sub-domain model is an effective tool for characterizing the spatially averaged performance of the full 3-D simulation. Figures 59, 60 and 61 compare time series generated by the full 3-D simulation, and the computationally efficient sub-domain model. Many more comparisons could be presented, but all show comparable performance. More complete documentation is available in the Appendix.

**Figure 59.** Comparison of process analysis time series (See Figure 55 for definitions) for ozone in the sub-domain defined in Figure 49 (8/25, source region); sub-domain processes (lower diagram) match the analogous processes for the full 3-D, gridded model (upper diagram) in the sub-domain.



Draft

Figure 60. Comparison of process analysis time series (See Figure 55 for definitions) for NO in the sub-domain defined in Figure 49 (8/25, source region); sub-domain processes (lower diagram) match the analogous processes for the full 3-D, gridded model (upper diagram) in the sub-domain.

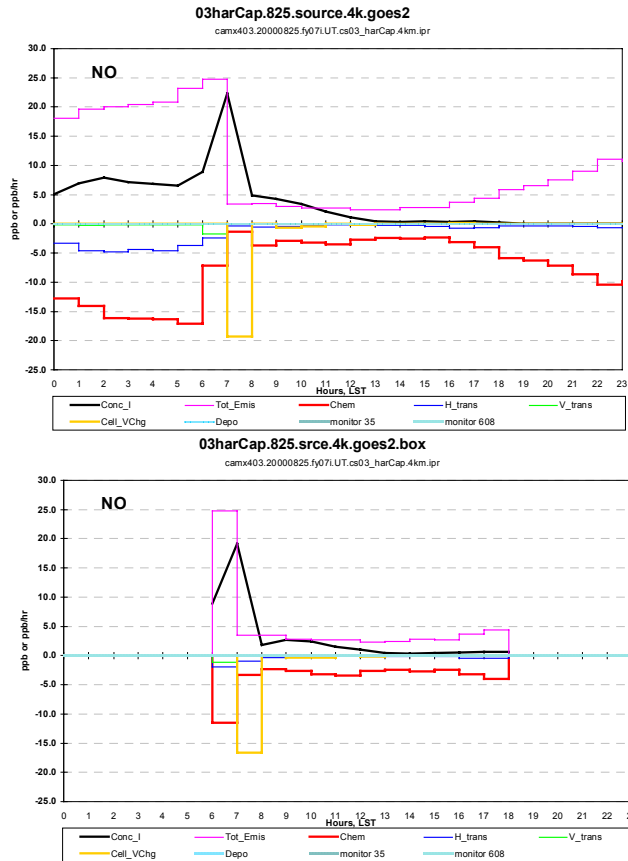
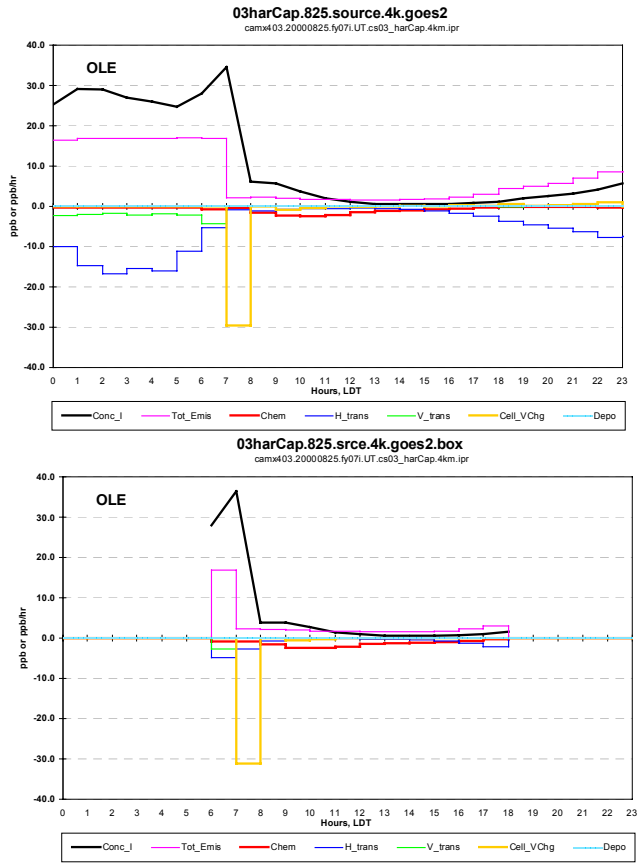
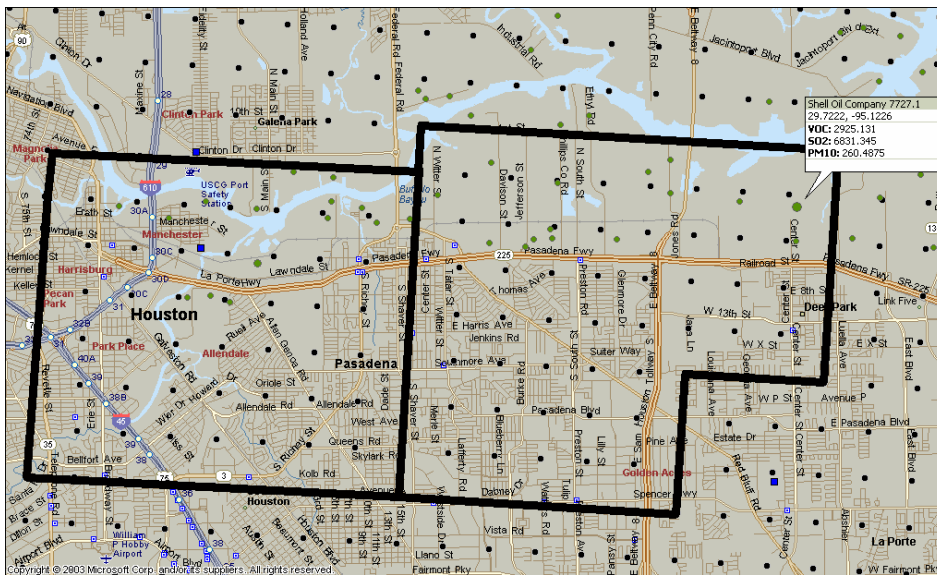


**Figure 61.** Comparison of process analysis time series (See Figure 55 for definitions) for ozone in the sub-domain defined in Figure 49 (8/25, source region); sub-domain processes (lower diagram) match the analogous processes for the full 3-D, gridded model (upper diagram) in the sub-domain.



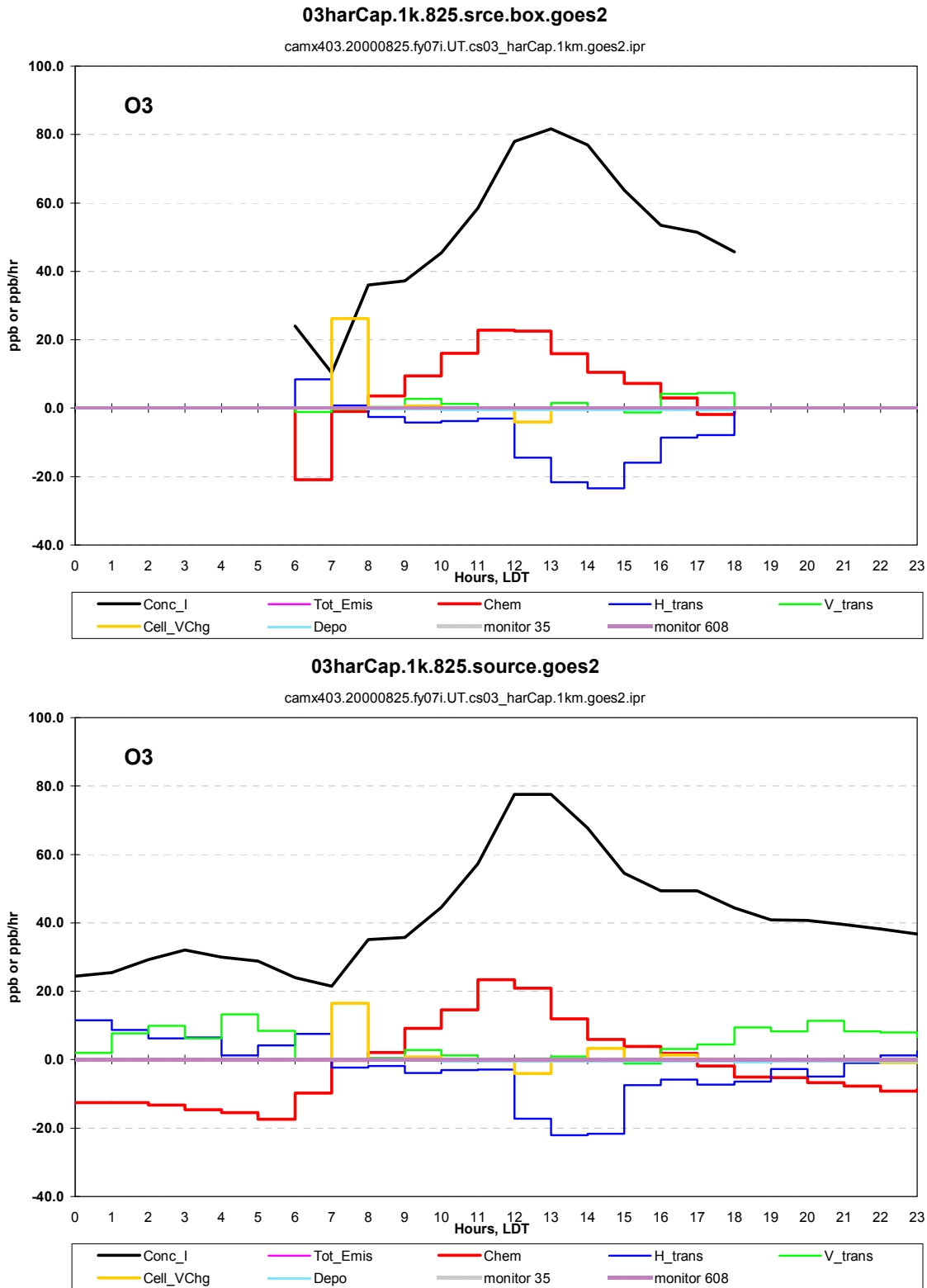
Figures 59-61 have demonstrated that the sub-domain model can be matched to the full 3-D simulation. Since, the next step in the use of the sub-domain model will be to evaluate the impact of many emission scenarios in the sub-domain model, it is also useful to demonstrate that the sub-domain model will generate the same response to added emissions as the full 3-D model. To perform this comparison, the 8/25 subdomain with a source region (Figure 62) was used. The sub-domain model was created using the full 3-D simulation, without added emissions. A 2900 lb release of a reactive olefin in the Deer Park region was then simulated independently in the sub-domain model and in a full 3-D simulation with a 1 km by 1 km horizontal grid cell dimension in the region of the event (Simulation FY 07 CS04). The results from those independent analyses were compared using the Process Analysis tool. Figures 63, 64 and 65 show time series comparisons for selected species before and after addition of the emissions. Figure 65 shows a comparison of reaction cycles analyses before and after the addition of the emissions. Overall, the results indicate that the sub-domain model shows the same response to added emissions as the full 3-D model, averaged over the same spatial area.

**Figure 62.** Sub-domain used to compare full CAMx simulation (FY 07i CS03\_harcap GOES2, 1 km grid resolution in source area) to sub-domain model; data for 8/25 used in the comparison; source region is to the right (including Deer Park); downwind region is to the left.

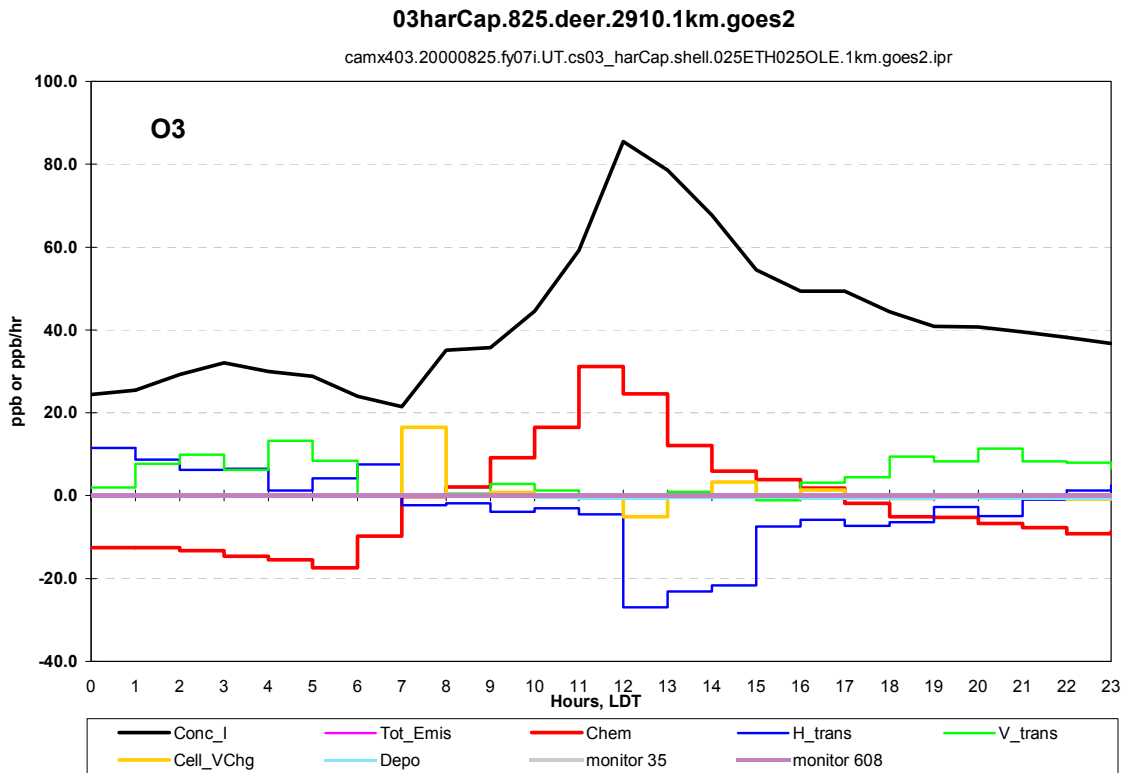
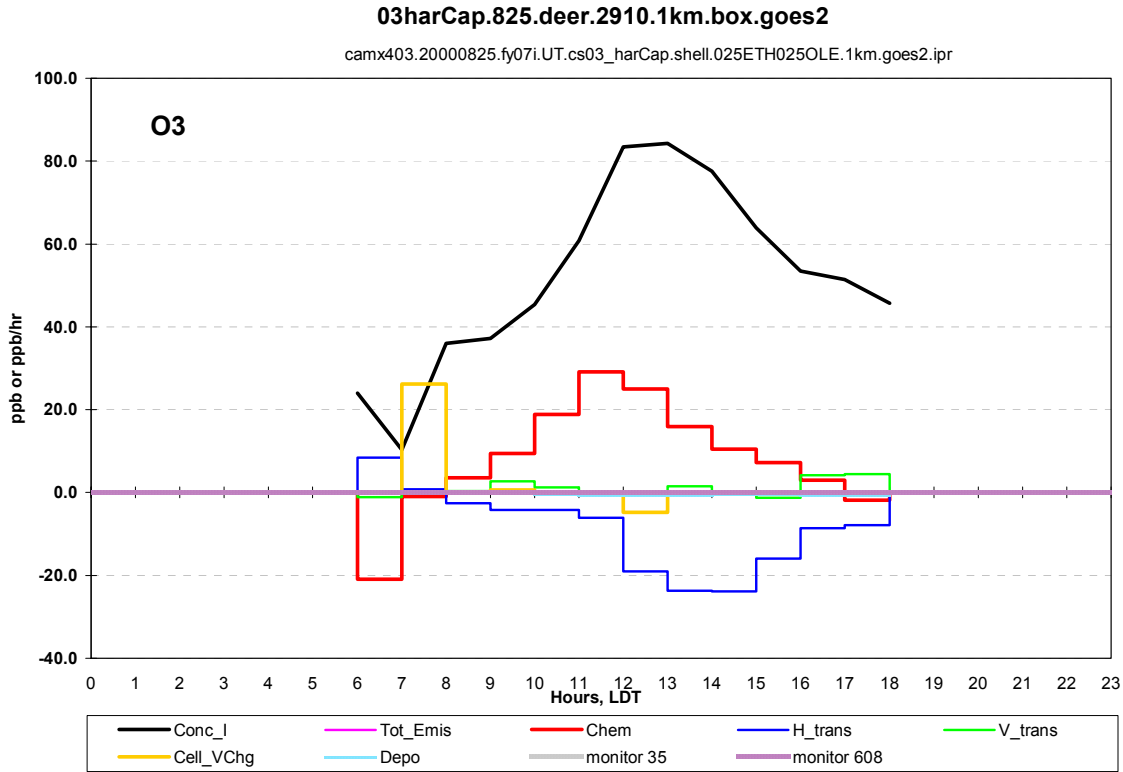


8-25\_00 Process Analysis Box outlined in black. Black Dots represent lower left hand corner of 1 km grid cells

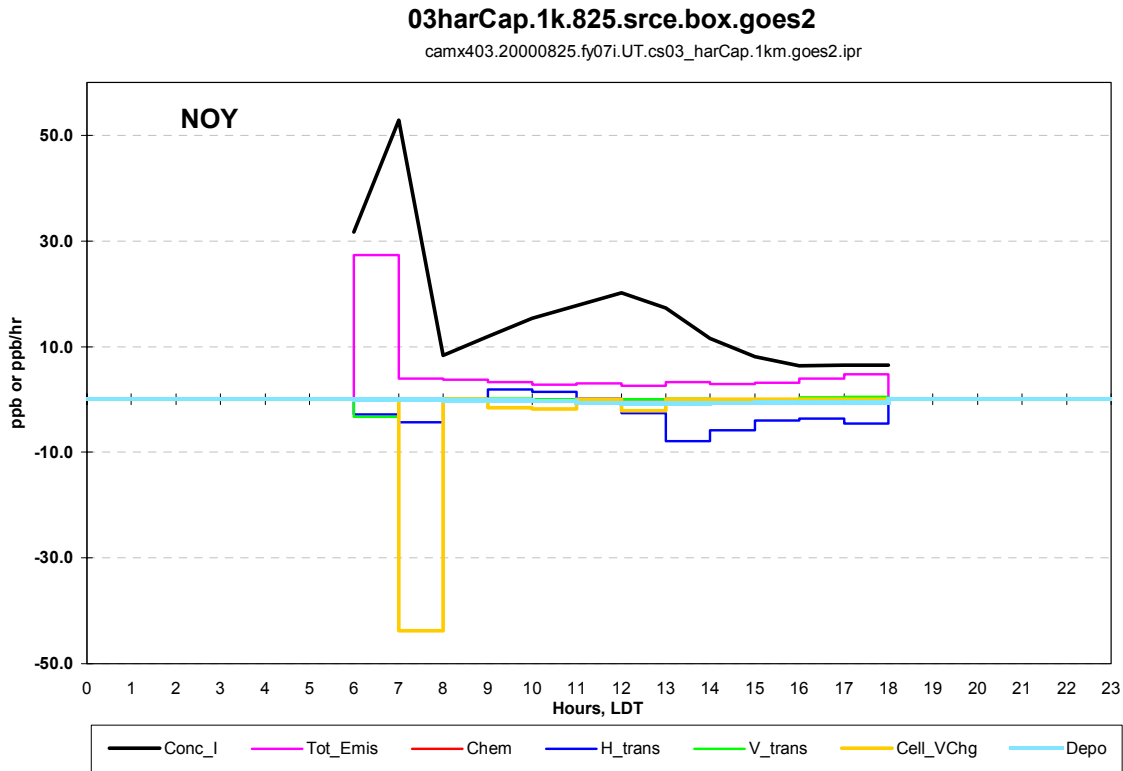
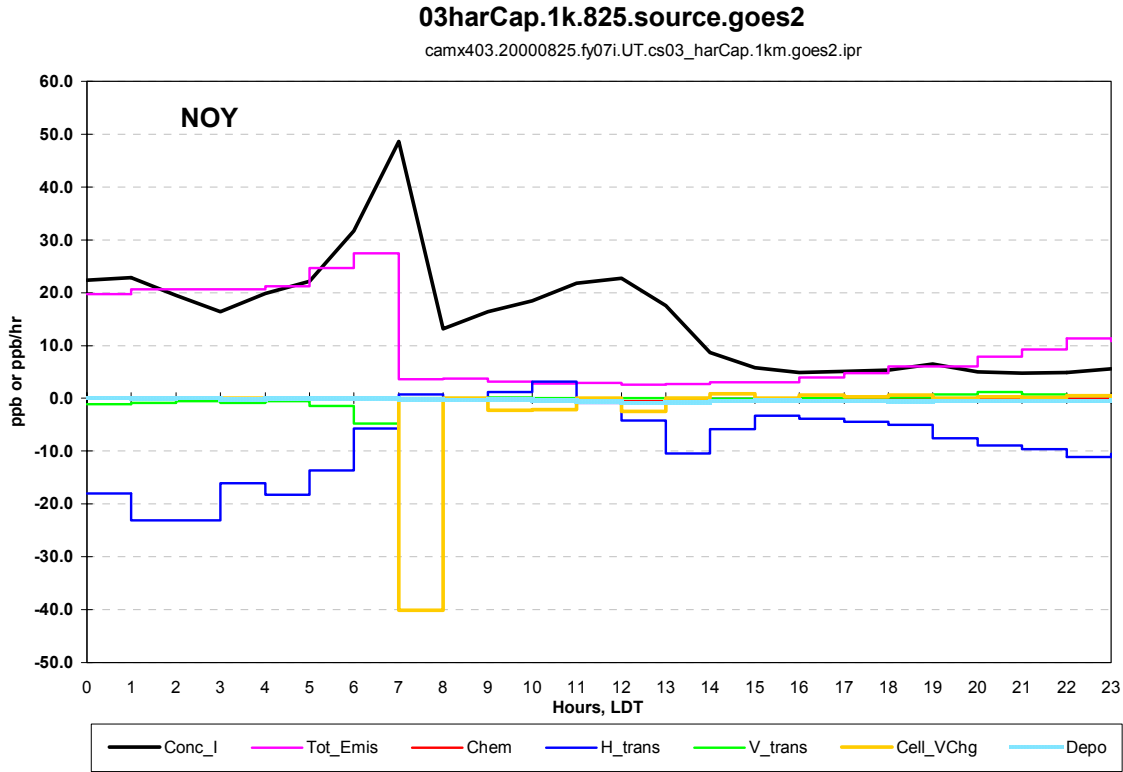
**Figure 63a.** Comparison of process analysis time series (See Figure 55 for definitions) for ozone in the sub-domain defined in Figure 62 (8/25, source region) before emissions are added; sub-domain processes (lower diagram) match the analogous processes for the full 3-D, gridded model (upper diagram) in the sub-domain.



**Figure 63b.** Comparison of process analysis time series (See Figure 55 for definitions) for ozone in the sub-domain defined in Figure 62 (8/25, source region) after emissions are added; sub-domain processes (lower diagram) match the analogous processes for the full 3-D, gridded model (upper diagram) in the sub-domain.

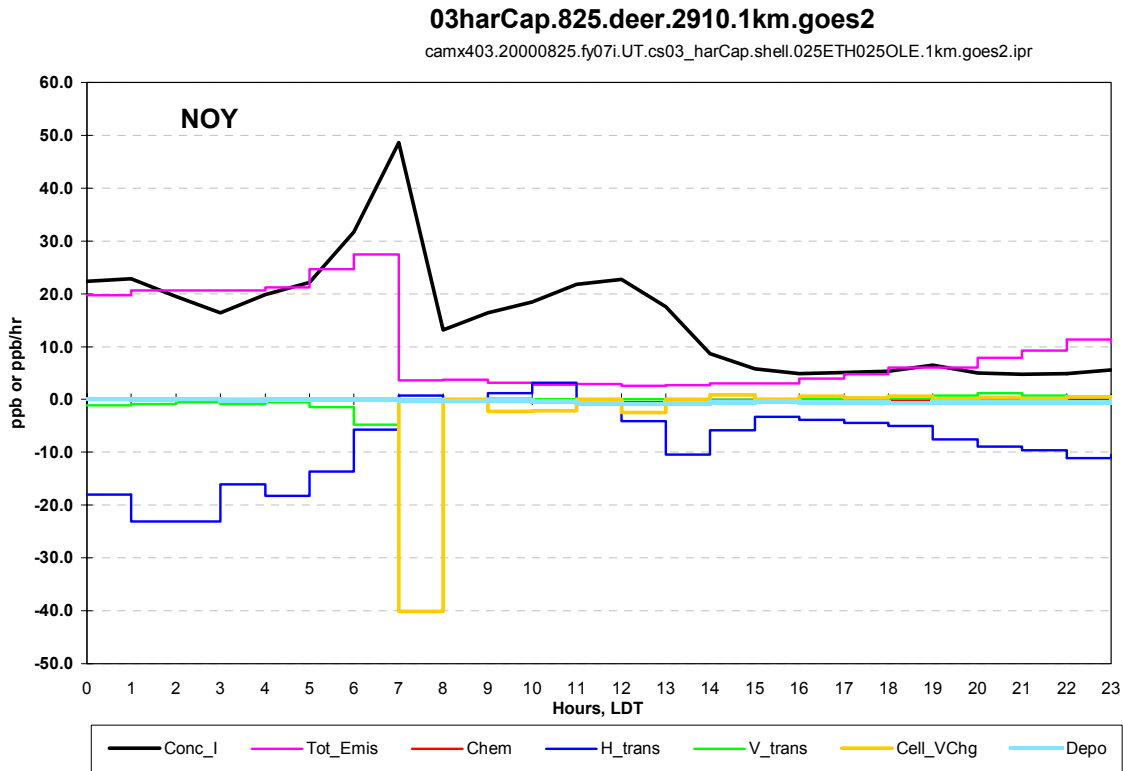
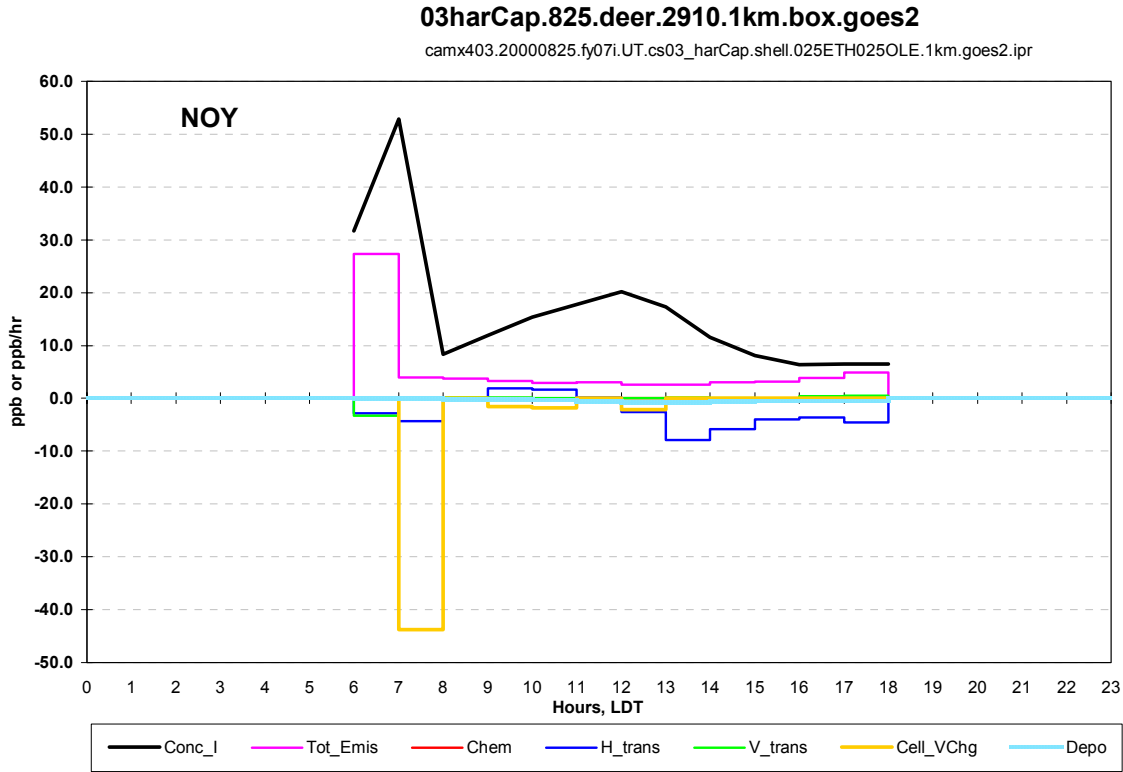


**Figure 64a.** Comparison of process analysis time series (See Figure 55 for definitions) for NO<sub>y</sub> in the sub-domain defined in Figure 62 (8/25, source region) before emissions are added; sub-domain processes (lower diagram) match the analogous processes for the full 3-D, gridded model (upper diagram) in the sub-domain.



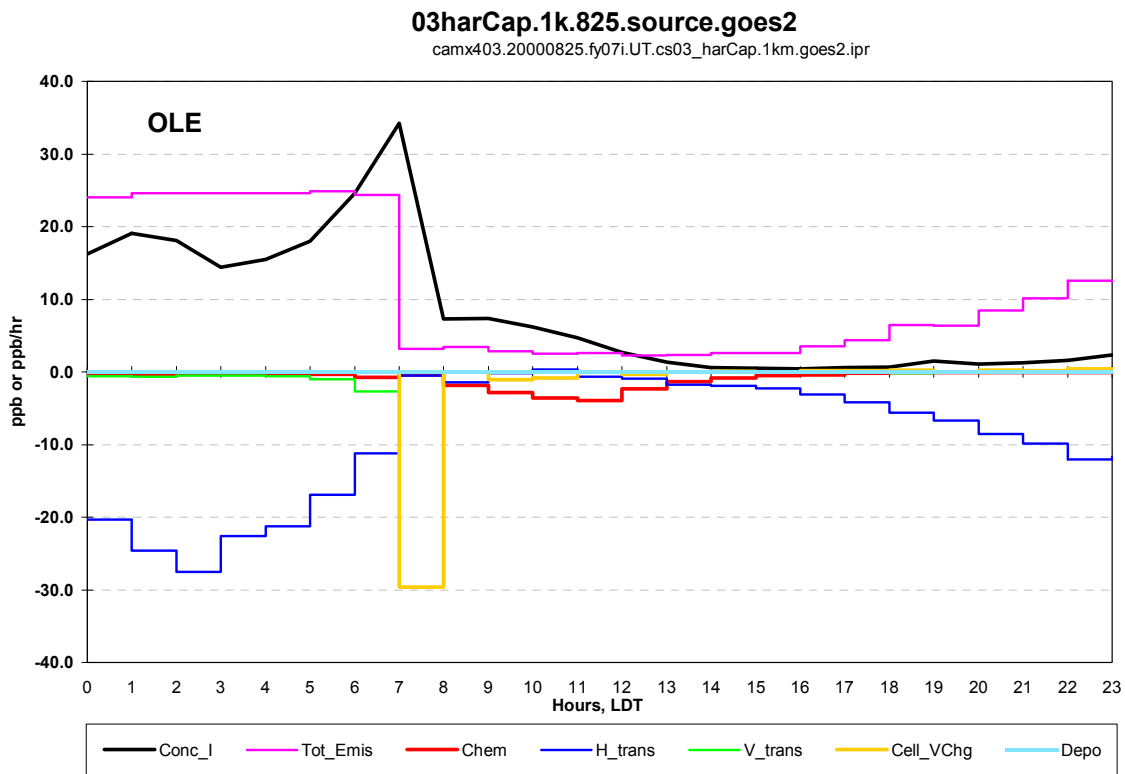
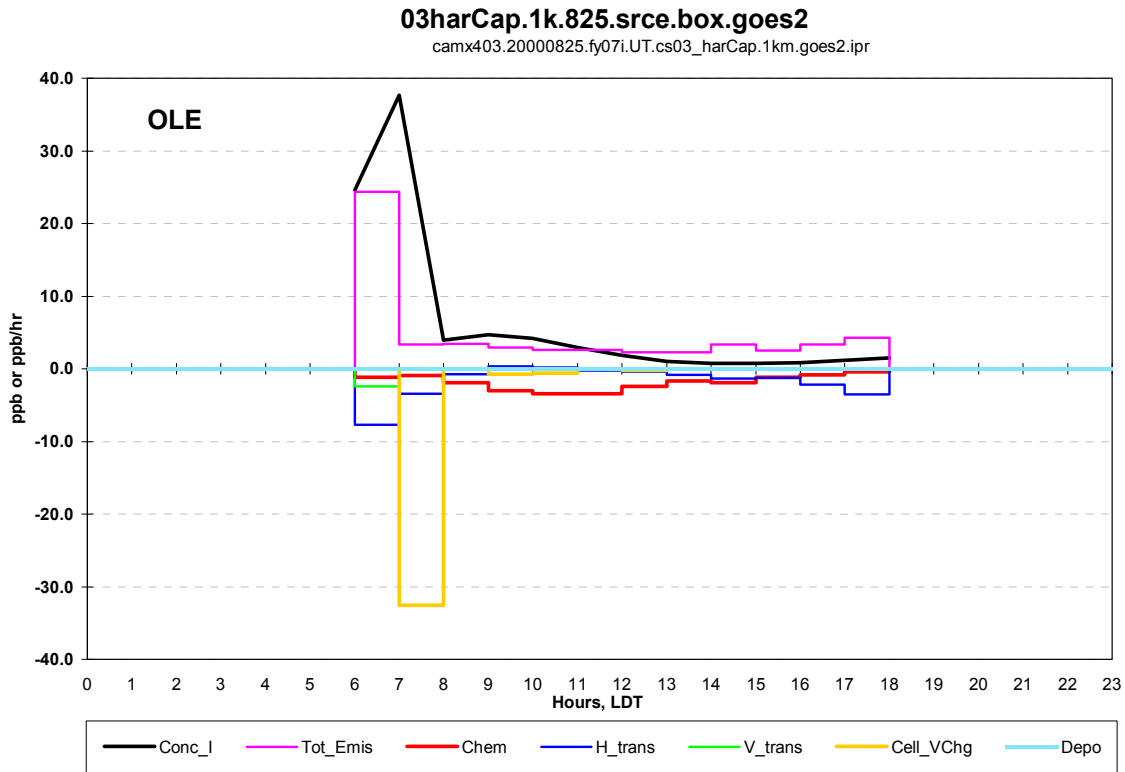
Draft

Figure 64b. Comparison of process analysis time series (See Figure 55 for definitions) for NO<sub>y</sub> in the sub-domain defined in Figure 62 (8/25, source region) after emissions are added; sub-domain processes (lower diagram) match the analogous processes for the full 3-D, gridded model (upper diagram) in the sub-domain.



Draft

Figure 65a. Comparison of process analysis time series (See Figure 55 for definitions) for reactive olefins in the sub-domain defined in Figure 62 (8/25, source region) before emissions are added; sub-domain processes (lower diagram) match the analogous processes for the full 3-D, gridded model (upper diagram) in the sub-domain.



**Figure 65b.** Comparison of process analysis time series (See Figure 55 for definitions) for reactive olefins in the sub-domain defined in Figure 62 (8/25, source region) after emissions are added; sub-domain processes (lower diagram) match the analogous processes for the full 3-D, gridded model (upper diagram) in the sub-domain.

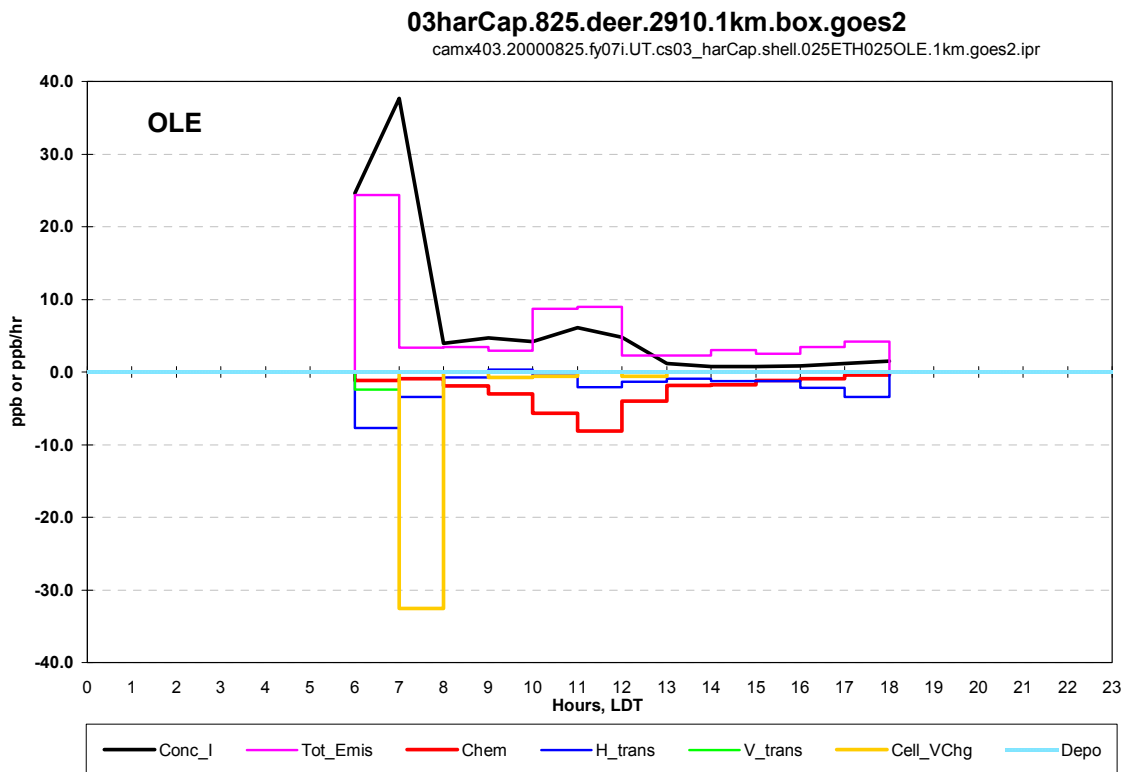
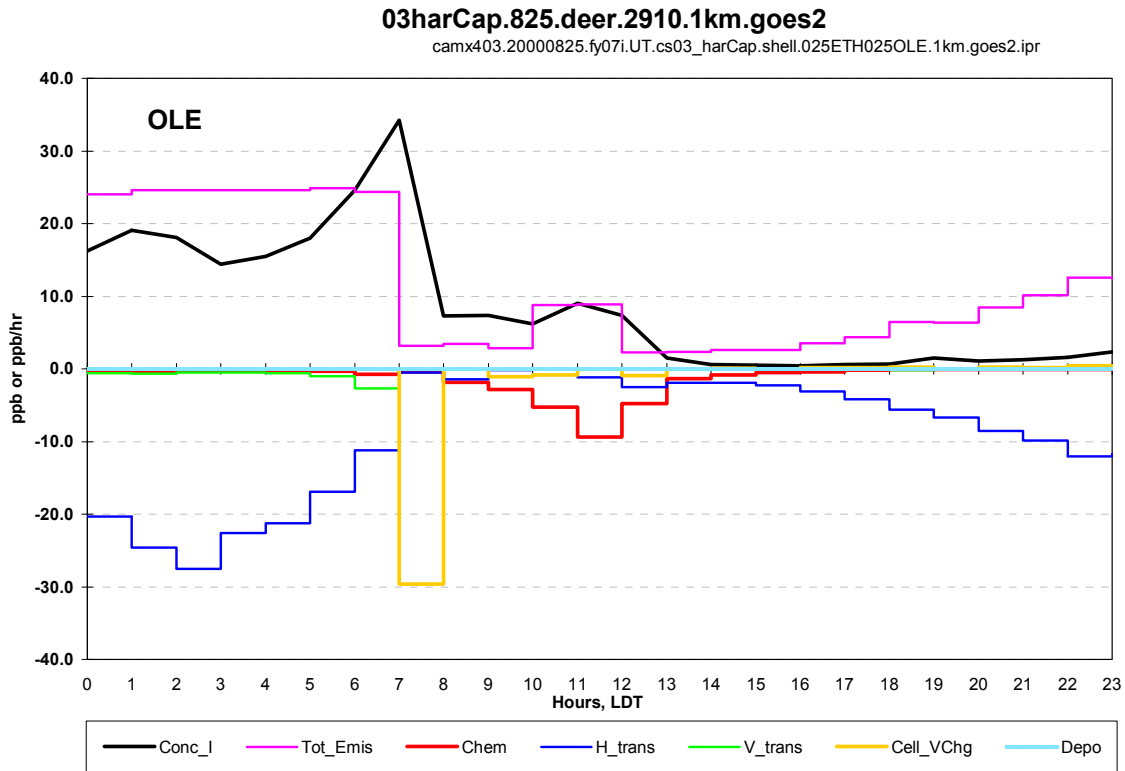


**Figure 66a.** Comparison of process analysis reaction cycle diagram (See Figures 56 and 57 for definitions) in the sub-domain defined in Figure 62 (8/25, source region) before emissions are added; sub-domain processes (next page) match the analogous processes for the full 3-D, gridded model (this page) in the sub-domain.

camx403.20000825.fy07i.UT.cs03\_harCap.1km.goes2.ipr  
 camx403.20000825.fy07i.UT.cs03\_harCap.1km.goes2.irr  
 825.source.1km.goes2.cycles

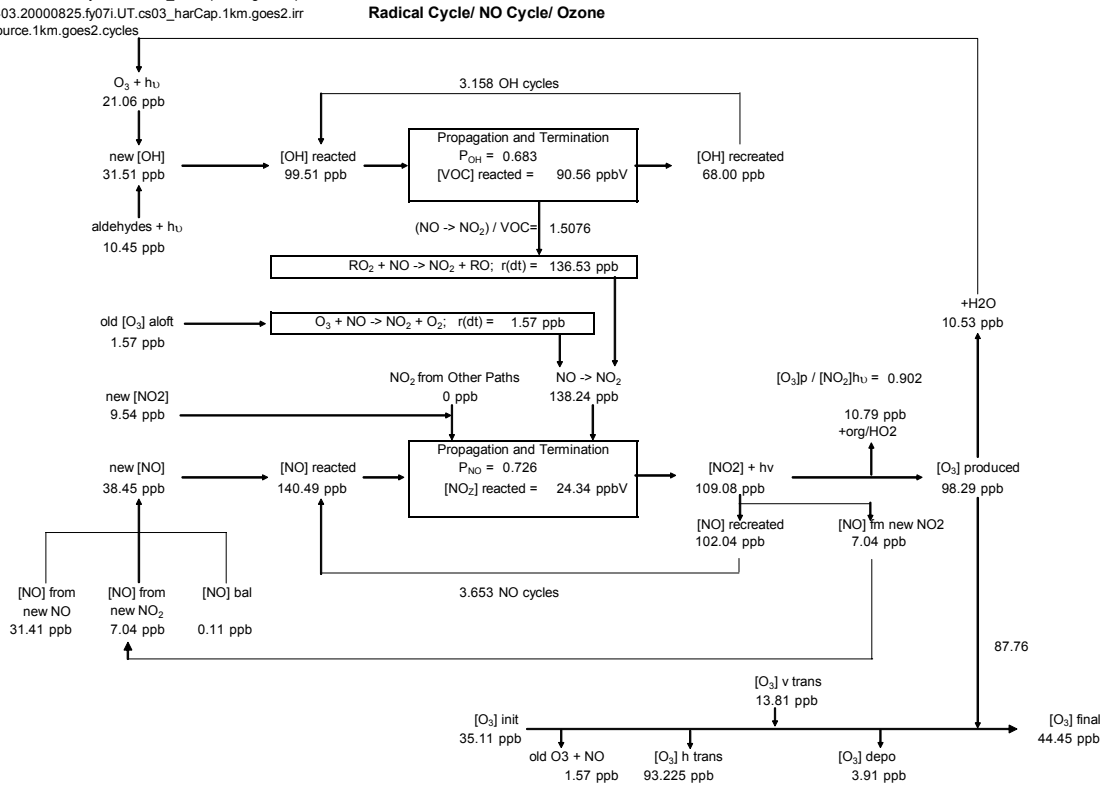
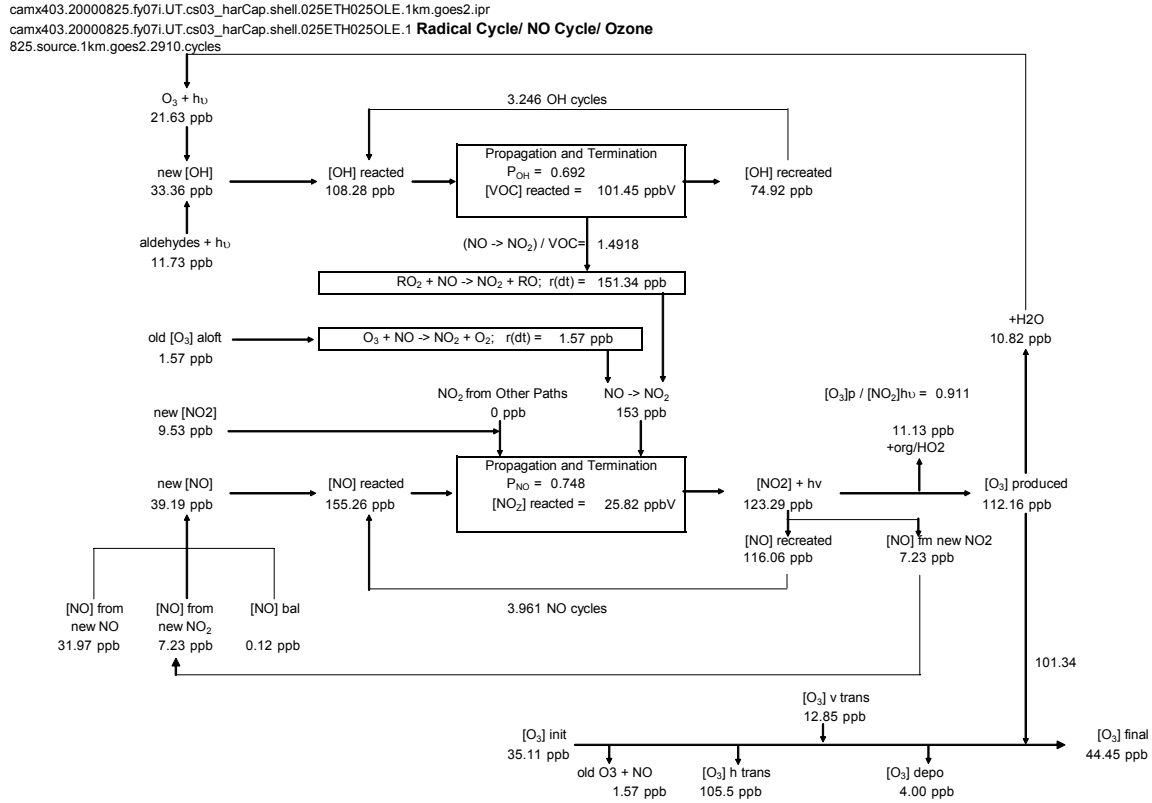
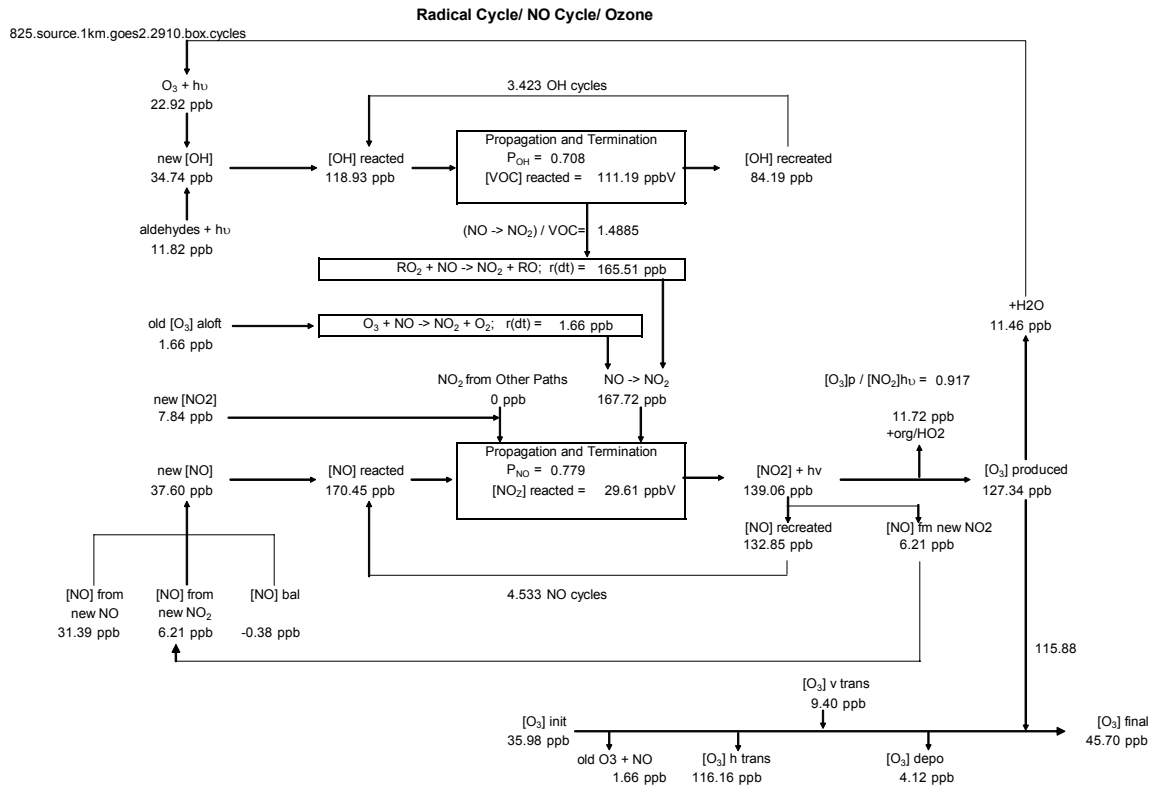




**Figure 66b.** Comparison of process analysis time series (See Figure 55 for definitions) for reactive olefins in the sub-domain defined in Figure 62 (8/25, source region) after emissions are added; sub-domain processes (next page) match the analogous processes for the full 3-D, gridded model (this page) in the sub-domain.



Draft



## Draft

### *Run scenarios in computationally efficient sub-domain model*

Figures 59-66 have demonstrated that computationally efficient sub-domain models can be constructed that replicate the behavior of a full 3-D model and that replicate the 3-D model's response to added emissions.

The sub-domains defined in Figures 49-51 were used in evaluating the ozone formation implications of added emissions. Specifically, the sub-domain modeling tool was used to address the following questions:

1. *What is the response of peak ozone concentration to different magnitudes of HRVOC added emissions?*
2. *Does the time of day when the emission occurs influence the response of peak ozone concentration?*
3. *Does the length of the added emission influence peak ozone concentration?*
4. *Does the location of the added emission influence peak ozone concentrations?*

Each of these questions is addressed below, however, before describing the results it is useful to present a brief summary of the sub-domains that were used in the analysis.

One set of sub-domains (corresponding to the areas shown in Figures 49, 50 and 51) was matched to CAMx simulation FY07i CS03\_harCap GOES1 (Future Year 2007, Control Strategy 3 with additional highly reactive VOC reductions, with meteorology modified using GOES data, but not including the mixing height correction, simulation at 4 km horizontal resolution). These sub-domains will be referred to as FY 07i CS03\_harcap GOES1 Deer Park 8/25, FY 07 CS03\_harcap GOES1 Deer Park 8/30, FY 07 CS03\_harcap GOES1 Baytown 8/28 and FY 07 CS03\_harcap GOES1 Chocolate Bayou 8/28. Upwind and downwind sub-domains in each of these areas will be denoted by the suffix source and plume, respectively.

Another set of sub-domains (corresponding to the areas shown in Figures 49, 50 and 51) was matched to CAMx simulation FY07i CS03\_harCap GOES1 (1 km) (Future Year 2007, Control Strategy 3 with additional highly reactive VOC reductions, with meteorology modified using GOES data, but not including the mixing height correction, simulation at 1 km horizontal resolution). These sub-domains will be referred to as FY 07i CS03\_harcap GOES1 1km Deer Park 8/25, FY 07 CS03\_harcap GOES1 1km Deer Park 8/30, and FY 07 CS03\_harcap GOES1 1km Baytown 8/28. Upwind and downwind sub-domains in each of these areas will be denoted by the suffix source and plume, respectively.

A third set of sub-domains (corresponding to the areas shown in Figures 49, 50 and 51) was matched to CAMx simulation FY07i CS03\_harCap GOES2 (Future Year 2007, Control Strategy 3 with additional highly reactive VOC reductions, with meteorology modified using GOES data, including the mixing height correction, simulation at 4 km horizontal resolution). These sub-domains will be referred to as FY 07i CS03\_harcap GOES2 Deer Park 8/25, and FY 07 CS03\_harcap GOES2 Deer Park 8/30. Upwind and downwind sub-domains in each of these areas will be denoted by the suffix source and plume, respectively. This is the set of sub-domains most consistent with the attainment demonstration.

## Draft

A fourth set of sub-domains (corresponding to the areas shown in Figures 49, 50 and 51) was matched to CAMx simulation FY07i CS03\_harCap GOES2 (1 km) (Future Year 2007, Control Strategy 3 with additional highly reactive VOC reductions, with meteorology modified using GOES data, including the mixing height correction, simulation at 1 km horizontal resolution). These sub-domains will be referred to as FY 07i CS03\_harcap GOES2 1km Deer Park 8/25, and FY 07 CS03\_harcap GOES2 1km Deer Park 8/30. Upwind and downwind sub-domains in each of these areas will be denoted by the suffix source and plume, respectively.

None of these different simulations led to significantly different relative sensitivities of source areas and time of day. Therefore, the focus will be on the simulations matched to CAMx simulation FY07i CS03\_harCap GOES2 (Future Year 2007, Control Strategy 3 with additional highly reactive VOC reductions, with meteorology modified using GOES data, including the mixing height correction, simulation at 4 km horizontal resolution), since this is the case most closely related to the attainment demonstration. Full results, including some additional sub-domains not described above, are presented in the Appendix, for the sake of completeness.

# Draft

Consider first the FY 07i CS03\_harcap GOES2 Deer Park 8/25 scenario. The sub-domain model was used to systematically examine the impact, on peak ozone concentrations, of added emissions of different magnitudes. Emission additions beginning at 100 lbs were considered, in 100 pound increments, ranging up to 5000 pounds. Additions of ethylene emissions and additions of propylene emissions were considered separately. All emission additions were assumed to occur over a 1-hour period, beginning at 10 AM. The results are shown in Figure 67.

nhour|1|bhr|11

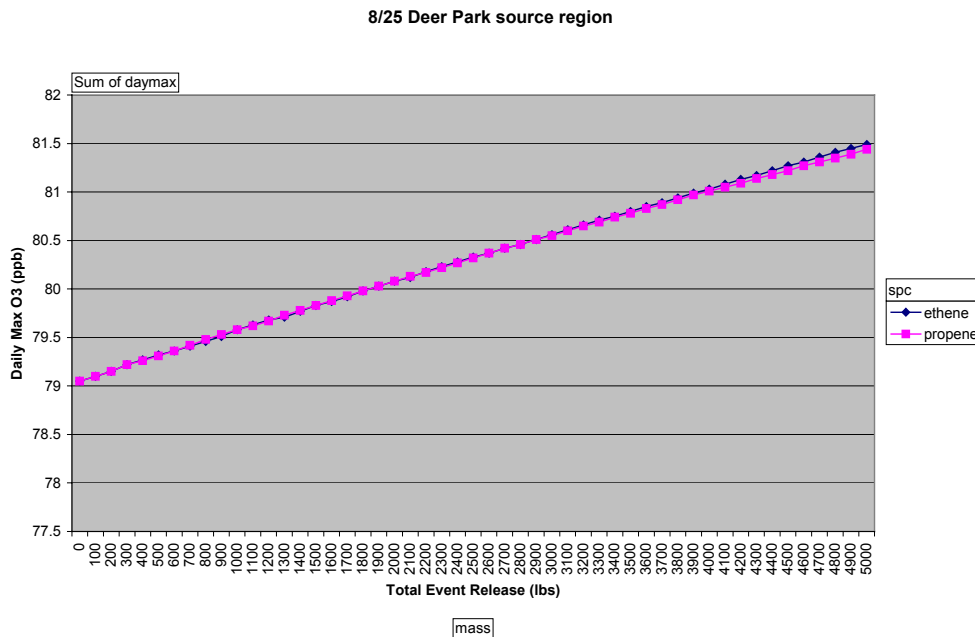


**Figure 67.** Sensitivity of ozone formation in the FY 07i CS03\_harcap GOES2 8/25 Deer Park domain (shown) to emission events of ethylene and propylene, ranging from 100 to 5000 lbs. The events were assumed to occur at 11 AM and to last for an hour. The peak ozone concentration in the sub-domain was a linear function of the size of the event. A one thousand pound event led to an increase in peak ozone concentration of approximately 0.5 ppb.



8\_25\_00 Process Analysis Box outlined in black. Black Dots represent lower left hand corner of 4 km grid cells

As shown in Figure 67, the peak ozone concentration in the sub-domain was a linear function of the size of the added emission. A one thousand pound added emission led to an increase in peak ozone concentration of approximately 0.5 ppb. As shown in the Appendix, similar sensitivities of peak ozone concentration to event size were seen for the 8/30 Deer Park subdomain.

Since the goal of the sub-domain modeling is to determine relative response of peak ozone concentrations to various emission addition magnitudes, the key feature of Figure 67 is that the responses are linear. As described in the Appendix, many other sub-domain scenarios were examined and the sub-domain models consistently yielded a linear relationship between peak ozone concentration and emission magnitude. Details of the other sub-domain results are provided in the Appendix.

The sub-domain models were also used to examine the sensitivity of peak ozone formation to time of day of the added emissions. As shown in Figure 68, the response of peak ozone concentration to time of day was strongly dependent on the time of day of the release. As shown in Figure 68a, releases of ethylene, lasting one hour, have maximum impact on peak ozone concentration if they occur at 11 AM. Impact falls off either before or after this time window. Figure 68b shows that for propylene releases lasting one hour, the maximum changes in peak ozone concentration result if the emissions are added at 11AM. Note that in all cases, the relationship between change in peak ozone concentration and magnitude of the release is linear, as was observed in Figure 67.

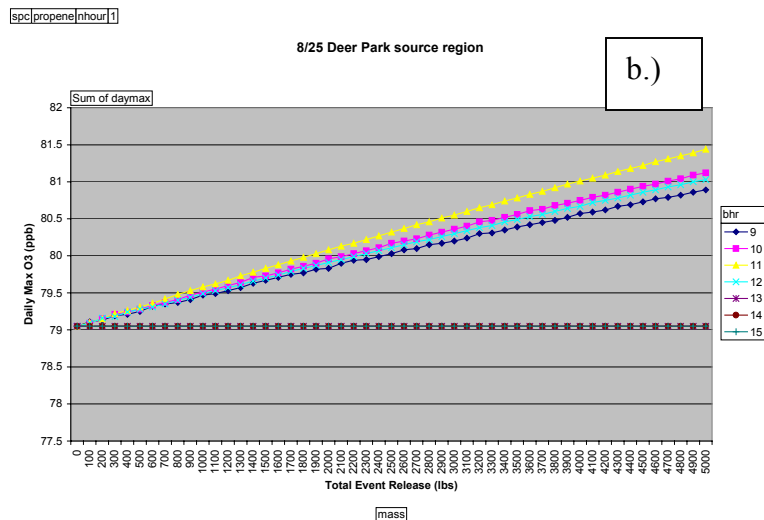
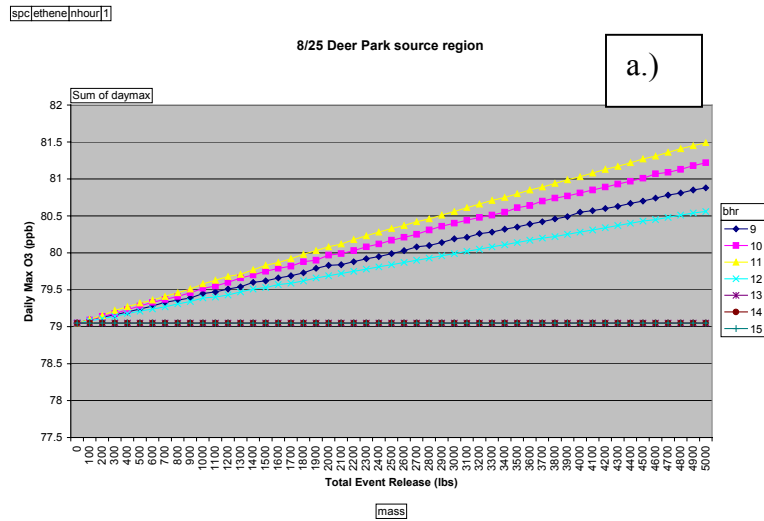


**Figure 68.** Sensitivity of ozone formation in the FY 07i CS03\_harcap GOES2 8/25 Deer Park domain, source region to emission events of ethylene (a.) and propylene (b.). The events ranged from 100 to 5000 lbs. The events were assumed to last for an hour, beginning at various times of day. The peak ozone concentration in the sub-domain was a linear function of the size of the event, and was sensitive to the time of day of the event.

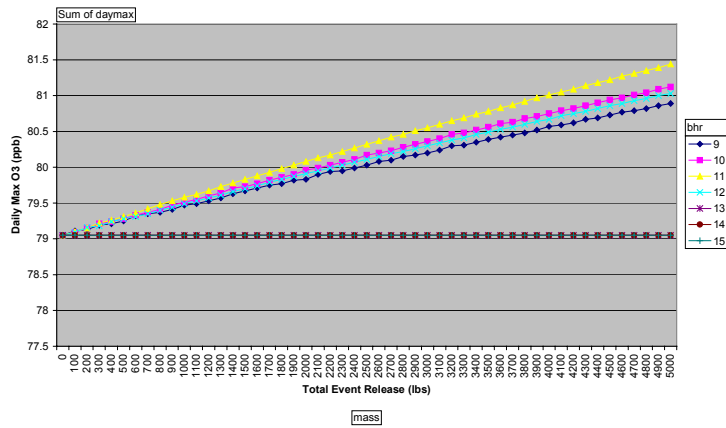
## Draft

The sub-domain models can be further used to examine the sensitivity of peak ozone formation to the duration of the emission addition. To examine the sensitivity to added emission duration, each added emission was divided over 1, 2 or 3 hours. Thus, a one thousand pound emission addition was evaluated as a 1 hour/1000 lb/hr addition, a 2 hr/500 lb/hr addition and a 3 hour/333 lb/hr addition. As shown in Figure 69, the response of peak ozone concentration was somewhat dependent on the duration of the emission addition, but the sensitivity could have largely been predicted from the results shown in Figure 68, which indicated that the response of peak ozone concentration was sensitive to the time of day of the release. At the most sensitive times of day, added emissions spread over one, two, or even three hours have comparable impacts on peak ozone concentrations, if they have the same magnitude. If the added emissions begin to fall outside of the time window of peak sensitivity, the impact on peak ozone concentration decreases. Note that in all cases, the relationship between change in peak ozone concentration and magnitude of the release is linear, as was observed in Figures 67 and 68.

Scenarios similar to those reported in Figures 67-69 were examined for other sub-domains, with analogous results. The results from those analyses are provided in the Appendix.

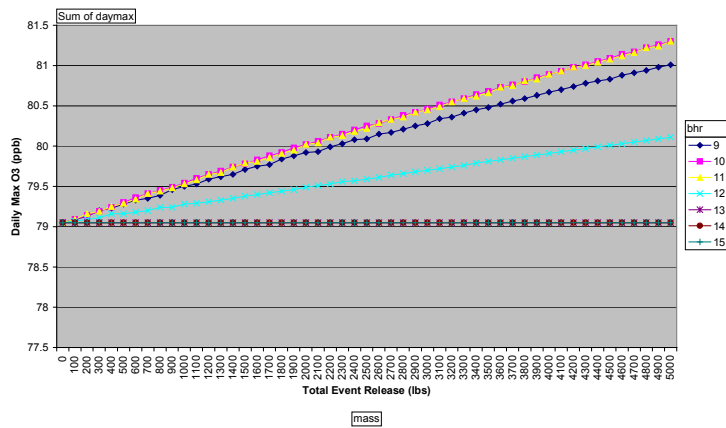
spc:propene|nhour|1

8/25 Deer Park source region



spc:propene|nhour|2

8/25 Deer Park source region



spc:propene|nhour|3

8/25 Deer Park source region

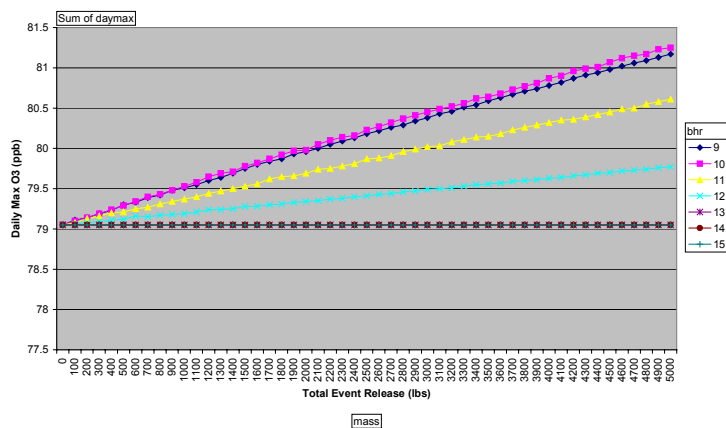


**Figure 69.** Sensitivity of ozone formation in the FY 07i CS03\_harcap GOES2 8/25 Deer Park domain, source region to emission events of propylene. The events ranging from 100 to 5000 lbs. The events were assumed to last for one (top diagram), two (middle diagram) or three hours (bottom diagram), beginning at various times of day. For multiple hour events, the emissions were distributed evenly over the length of the event (e.g., a 1000 lb event over 2 hours had an emission rate of 500 lb/hr). The peak ozone concentration in the sub-domain was a linear function of the size of the event, and was sensitive to the time of day of the event. At the most sensitive times of day, emission events spread over one, two, or even three hours have comparable impacts on peak ozone concentrations, if they have

**VI b. Combining 3-D photochemical and sub-domain models**

*Evaluate sensitive scenarios in full 3-D photochemical model*

The results from the sub-domain models indicated that the peak ozone concentration is a linear function of the magnitude (mass) of the emission addition up to emission addition masses of at least 5000 pounds; the peak ozone concentration response to emission additions is greatest during a time window of approximately 2-4 hours on ozone conducive days, and the length of the emission addition (e.g., 1000 lbs over one hour or 500 lbs/hr over 2-4 hours) does not impact peak ozone concentration, as long as all of the releases occur during the sensitive time window of approximately 2 hours.

Using these findings as a starting point, multiple full 3-D CAMx simulations of the FY 07i CS03\_harcap GOES2 (1 km) simulation were conducted. The results are summarized in Figure 70. The CAMx simulations confirm that the response of change in peak ozone concentration to the magnitude of the emission addition is linear up to emission addition magnitudes much larger than 5000 pounds.

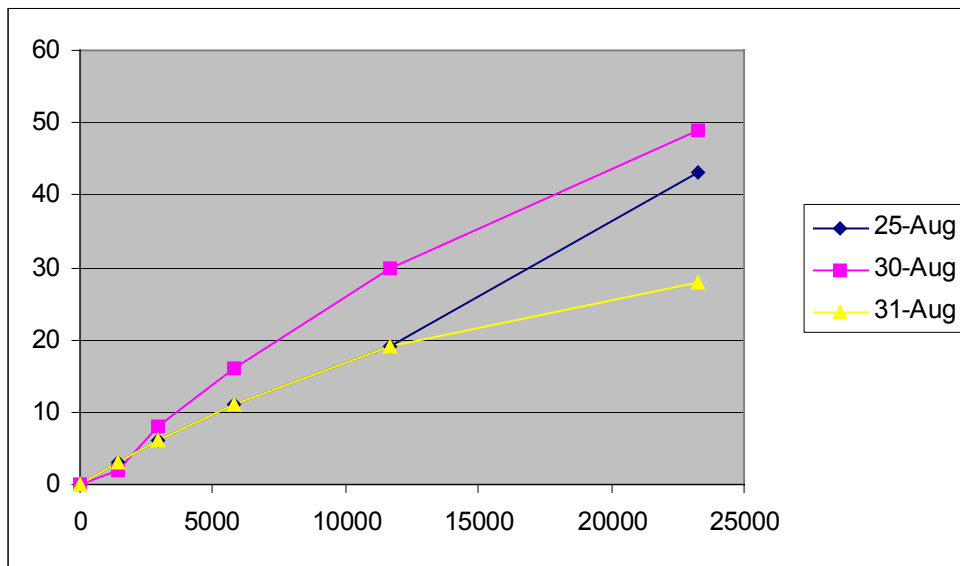


**Figure 70.** Response of full CAMx simulations (FY 07i CS03\_harcap GOES2 (1 km) ) to emission additions at the time of day identified as most sensitive in the sub-domain simulations. The CAMx simulations confirm that the response of change in peak ozone concentration to the magnitude of the emission addition is linear up to emission event magnitudes much larger than 5000 pounds

The full 3-D CAMx simulations provide an assessment of the magnitude of the impact of emission additions on peak ozone concentration. At the most sensitive locations, the magnitude of change in peak ozone concentration ranges from 2-3 ppb per 1000 lbs of HRVOC emission addition, depending on the date of the release.

**Finding 2: HRVOC emission variability in the range of 100-1000 lb/hr, which has been reported daily in the Houston-Galveston area, can increase peak, region-wide ozone concentrations, if the emission variability occurs in regions upwind of the location of the peak, region-wide ozone concentration.** *The magnitude of the increase in ozone concentration depends on the location of the emission variability, the time of day when the emission variability occurs and the magnitude of the non-variable ozone precursor emissions. Increases of 1-4 ppb in peak ozone concentration per 1000 lb/hr of HRVOC emission variability are expected at times and locations that are sensitive to emission variability. This sensitivity may increase as non-variable HRVOC emissions decrease and NOx emissions increase.*

## VII. Characterizing the impact of variable emissions on attaining the NAAQS for ozone

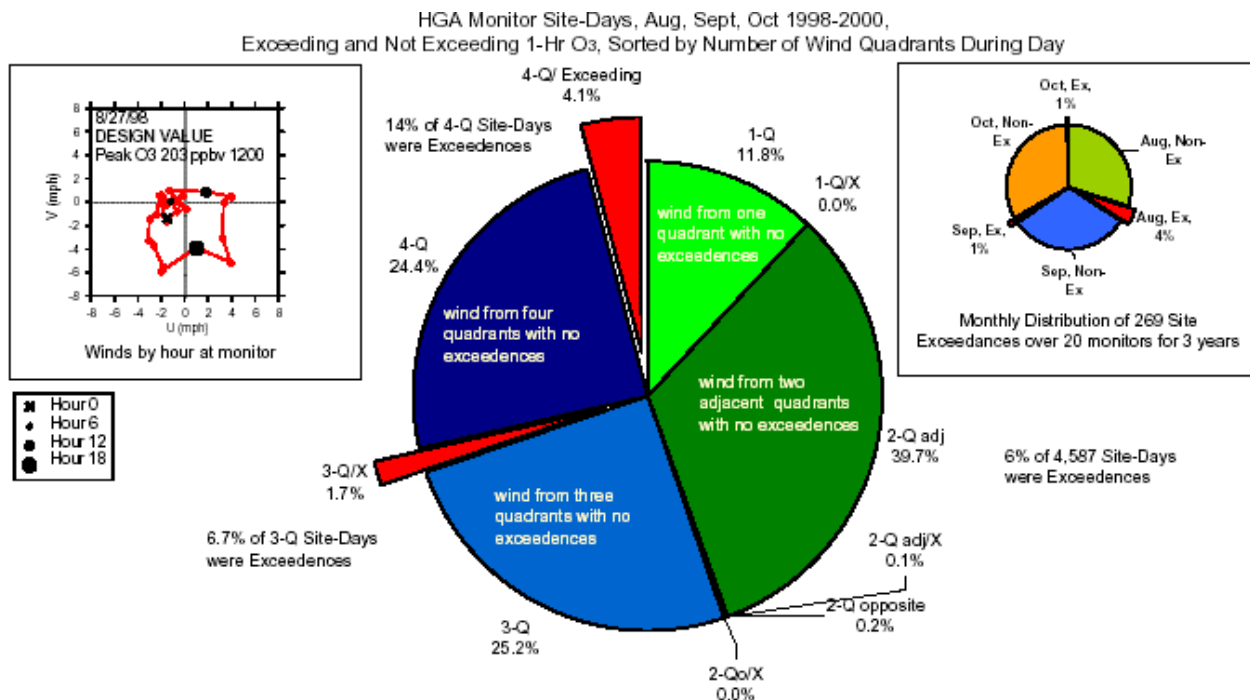
### VIIa. Estimating the probability of emission events and impacts on peak ozone concentrations

In order to characterize the impact of variable emissions, particularly emission events, on attainment of the National Ambient Air Quality Standard (NAAQS) for ozone (concentrations averaged over 1-hour), it is necessary to combine the information presented in the previous section with additional analyses.

Section VI demonstrated that the effect of emission additions on peak ozone concentration depends on the magnitude, location and time of day of the release. Stated differently, for emission variability to have an impact on peak ozone concentration, added emissions must occur at a particular time and a particular location.

Consider first the issue of the time window for added emissions to impact peak ozone concentration. For peak ozone concentration to be impacted, the added emissions must occur on an ozone conducive day, during a time window of approximately 2-4 hours. Figure 71 shows that approximately half of all days in the months of August, September and October are ozone conducive in the Houston-Galveston area. The frequency of ozone conducive days is expected to be lower in other months, leading to a very rough estimate of one day in 4 being ozone conducive, on an annual basis.

**Figure 71.** Analysis of the degree to which flow circulations (rotating wind directions) occur that are conducive to ozone formation occur during August-October. Roughly half of the days during this period have wind fields that rotate through 3 or 4 quadrants and virtually all of the exceedances occur during these periods.



## Draft

If one day in 4, and 2-4 hours of each of those days are conducive to emission events impacting peak ozone concentration, then roughly 1 hour in 25-50 has the potential for an added emissions to impact peak ozone concentration if the emission occurs in the correct location.

Analyses are still underway for assessing the impact of event location, but for the moment assume that events in Harris County are most likely to impact peak ozone concentration, and that within Harris County, roughly one in two to one in four significant additions of emissions will occur at a location that will impact peak ozone concentration.

Taken together, this suggests that only one instance of added emissions in one hundred will occur at the right location and the right time to impact peak ozone concentration. A key question to answer then, is what is the expected magnitude of added emissions that would impact peak ozone concentration.

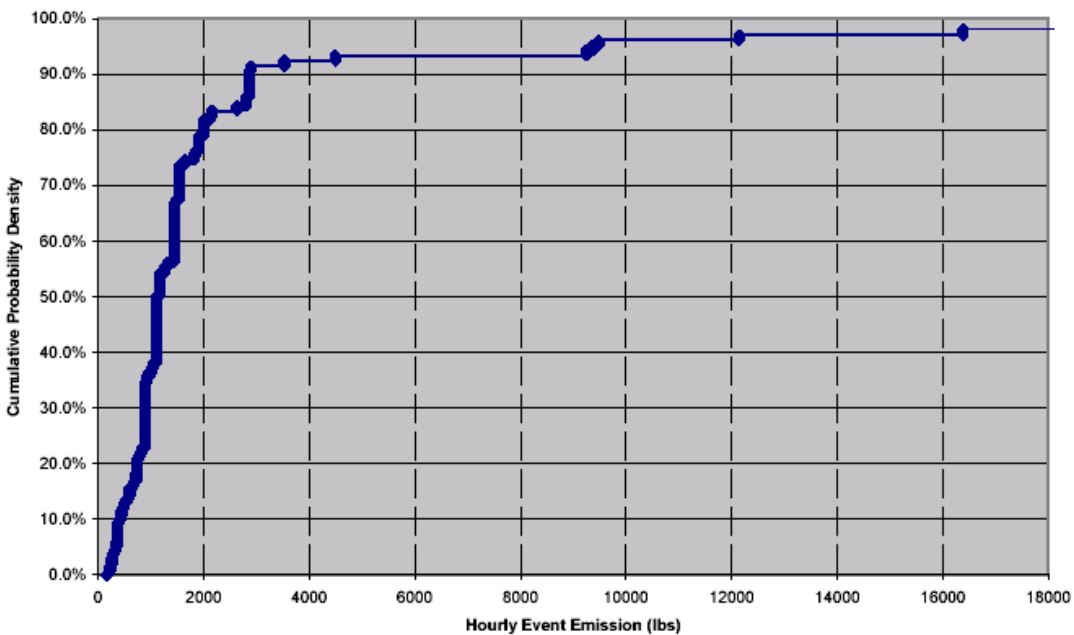
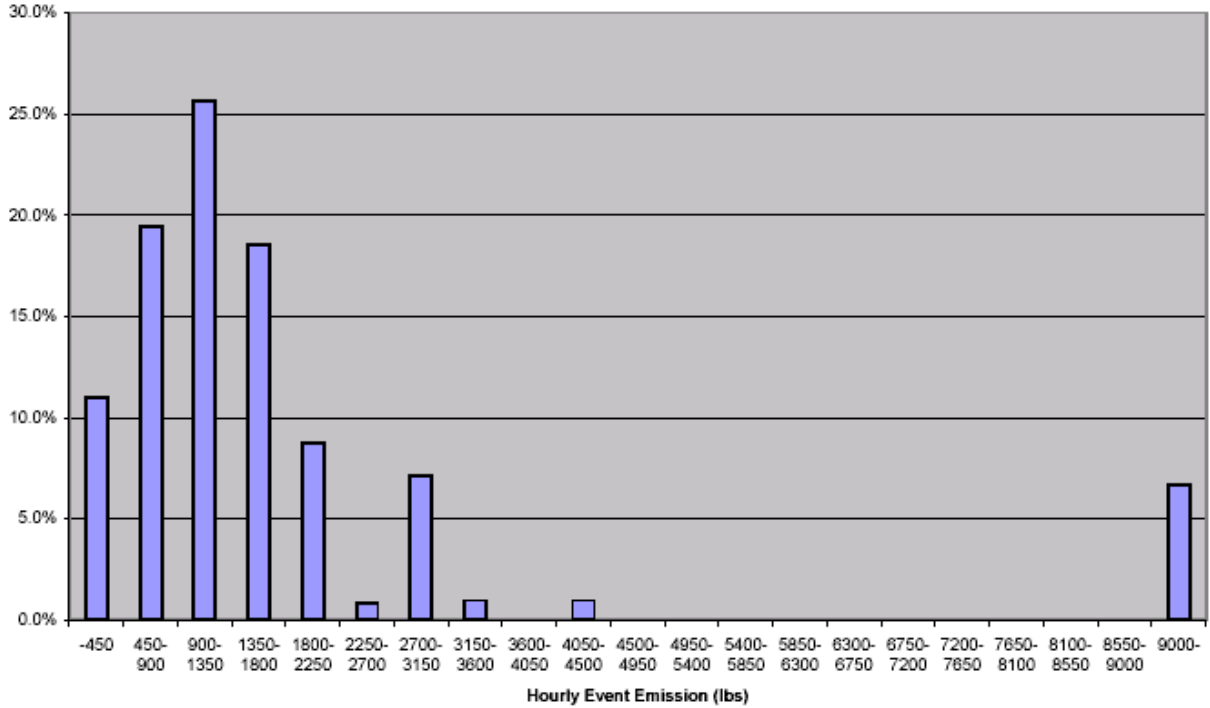
To answer this question, the emission event database examined in Section IV was analyzed using a Monte Carlo simulation. The Monte Carlo simulation followed the following process:

1. For any emission event occurring in Harris County over a one hour period, roughly one event in one hundred (one hour in one hundred) has the potential to impact peak ozone; therefore for the 11 months of data available (roughly 8000 hours), randomly select 80 hours
2. Identify the worst case emission event. This event corresponds to the worst emission event that would impact peak ozone concentration in a hypothetical year.
3. Repeat steps 1 and 2 ten thousand times to generate a distribution of worst case emission events in potential years. From this distribution of worst case emission events select the median (an event of this magnitude is more likely than not to occur) or the 90<sup>th</sup> percentile emission event (only for one in 10 hypothetical years would an event larger than this, impacting peak ozone concentration, occur)

The results of the Monte Carlo analysis are shown in Figure 72. Figure 72 shows the distribution of worst case emission events in Harris County for total HRVOCs that would be expected if 1 hour in one hundred, on average, has the potential for an emission event to impact peak ozone concentration. The median value is approximately 1000 pounds and the 90<sup>th</sup> percentile value is roughly 3000 pounds. This would suggest that, if no actions were taken to reduce event emissions, it would be necessary to plan for an event of 1000 to 3000 pounds in the attainment demonstration, at a location that would influence peak ozone concentrations. As noted in Section VI, this level of emission event, would likely increase peak ozone concentrations by 2-3 ppb.

Draft

**Figure 72** Distribution of annual worst case emission events in Harris County for total HRVOCs that would be expected if 1 hour in one hundred, on average, has the potential for an emission event to impact peak ozone concentration. The median value is approximately 1000 pounds and the 90<sup>th</sup> percentile value is roughly 3000 pounds.



## Draft

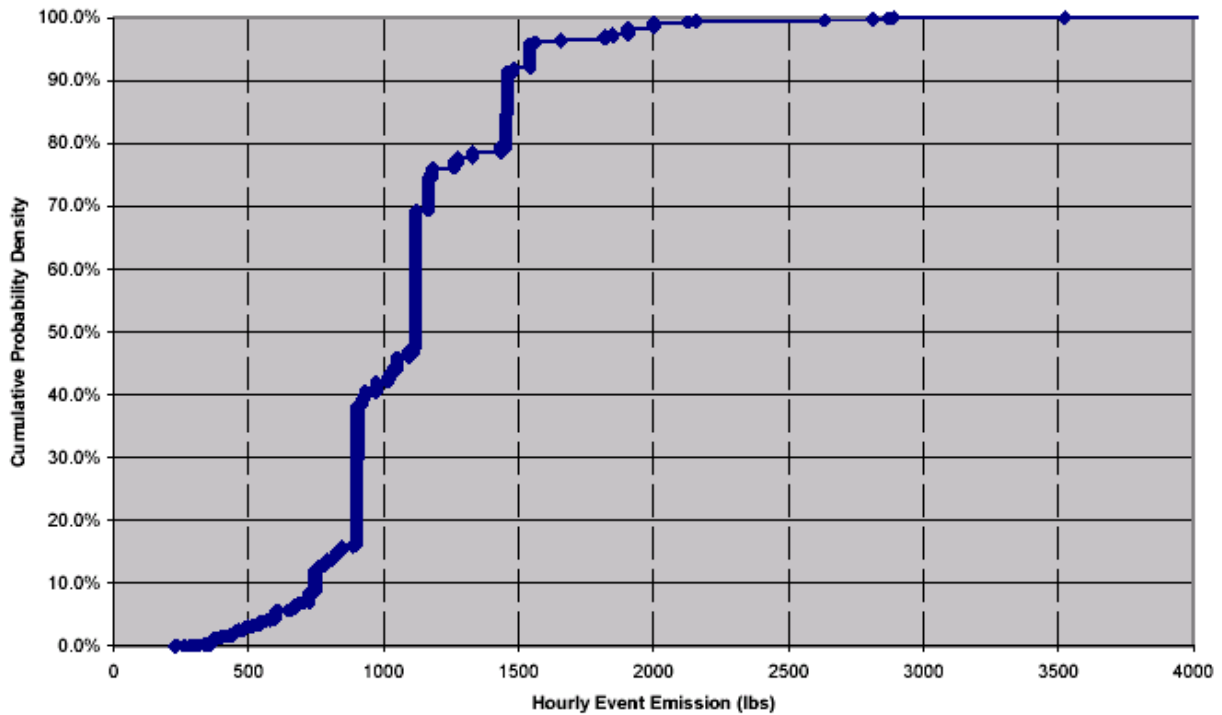
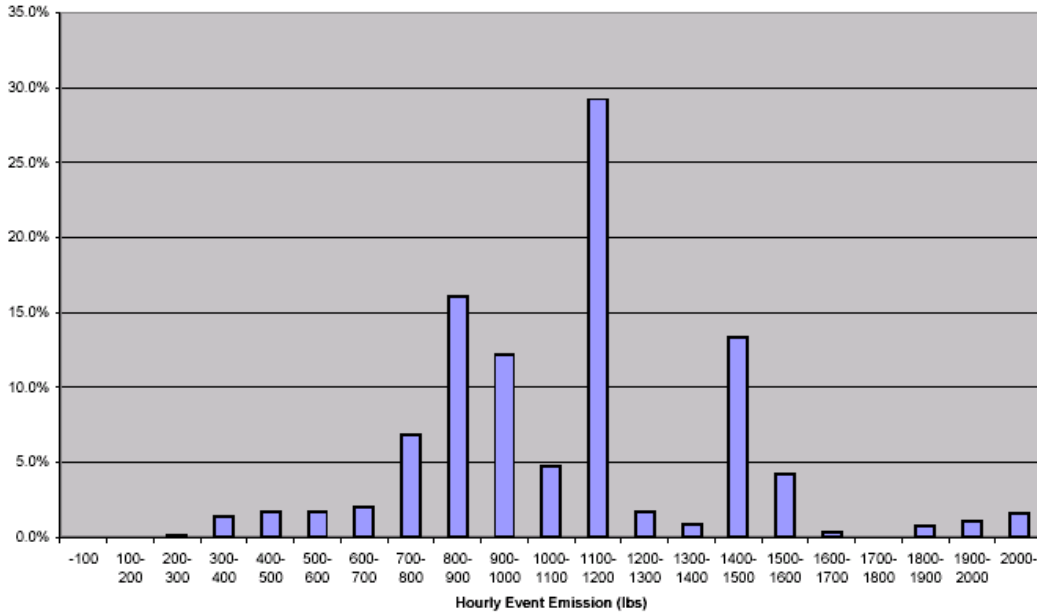
There are multiple assumptions inherent in the Monte Carlo analysis. These include the probability that an emission event will lead to a change in peak ozone concentration (currently set at 1 in 100), the assumption that only one hour of emissions should be considered (instead of one, hour, two hour, and three hour blocks), and the assumption that the worst case event should be chosen in any given year.

The impacts of all of these assumptions on the analysis could be examined. Figure 73 shows the results of an analysis using an alternative to considering the worst case event in any year. Since the NAAQS for ozone is based on the 4<sup>th</sup> highest ozone concentration observed over 3 years, an alternative is to examine the 4<sup>th</sup> highest ozone concentration over 320 randomly selected hours (equivalent to 3 years). The median value is again 1000 pounds, but in this case the 90<sup>th</sup> percentile value for a worst case emission event is 1500 pounds.

It is important to note that this finding assumes that emission events are merely adding a marginal enhancement to peak ozone concentrations and are not the sole cause of the emission event.

# Draft

**Figure 73** Distribution of fourth highest HRVOC emission event magnitudes, over 3 years, in Harris County, that would be expected if 1 hour in one hundred, on average, has the potential for an emission event to impact peak ozone concentration. The median value is approximately 1000 pounds and the 90<sup>th</sup> percentile value is roughly 1500 pounds.



## VII b. Impact of short-term limits and other control scenarios on emission event magnitudes

The worst case emission event distributions shown in Figures 72 and 73 are based on current event magnitudes and frequencies. If control practices are put in place to reduce event emissions, then expected worst case emission events in future years would be reduced. For example, if a short term limit of 500 lb/hr were placed on HRVOC emissions, then the expected value of the worst case emission event would decrease from 1000 pounds/hr to less than 500 pounds/hr.

The goal of this section is to apply several possible control strategies to the event emissions to determine the approximate impact on expected worst case emission event magnitudes.

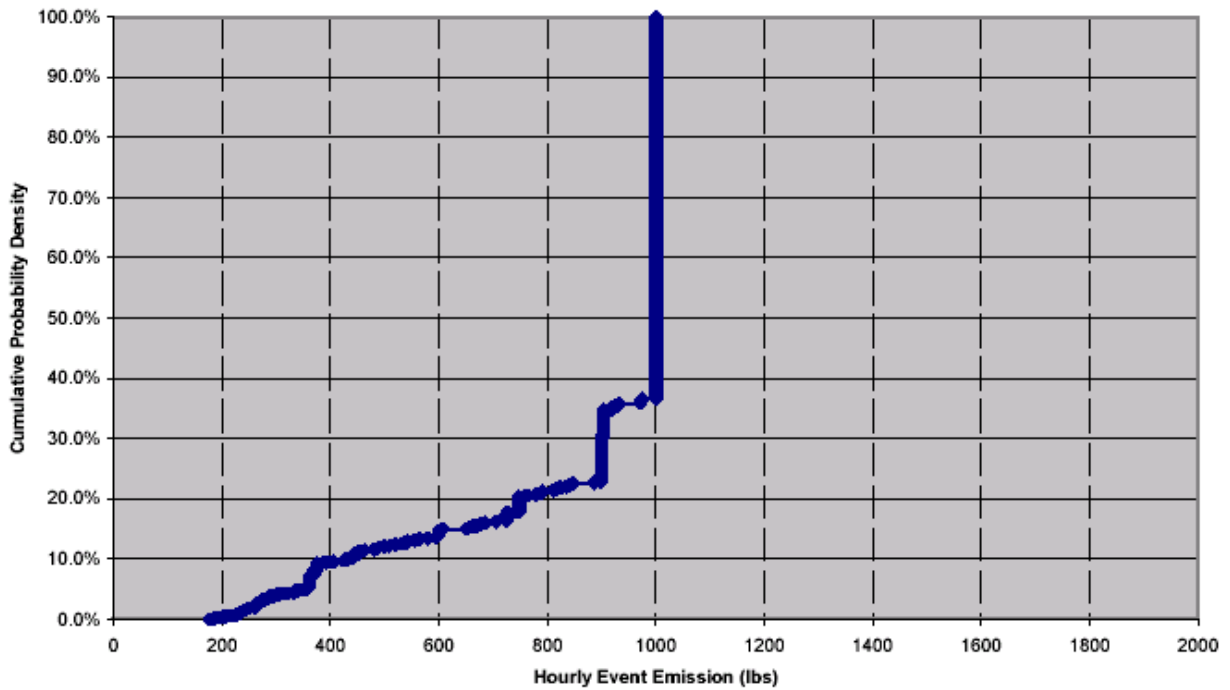
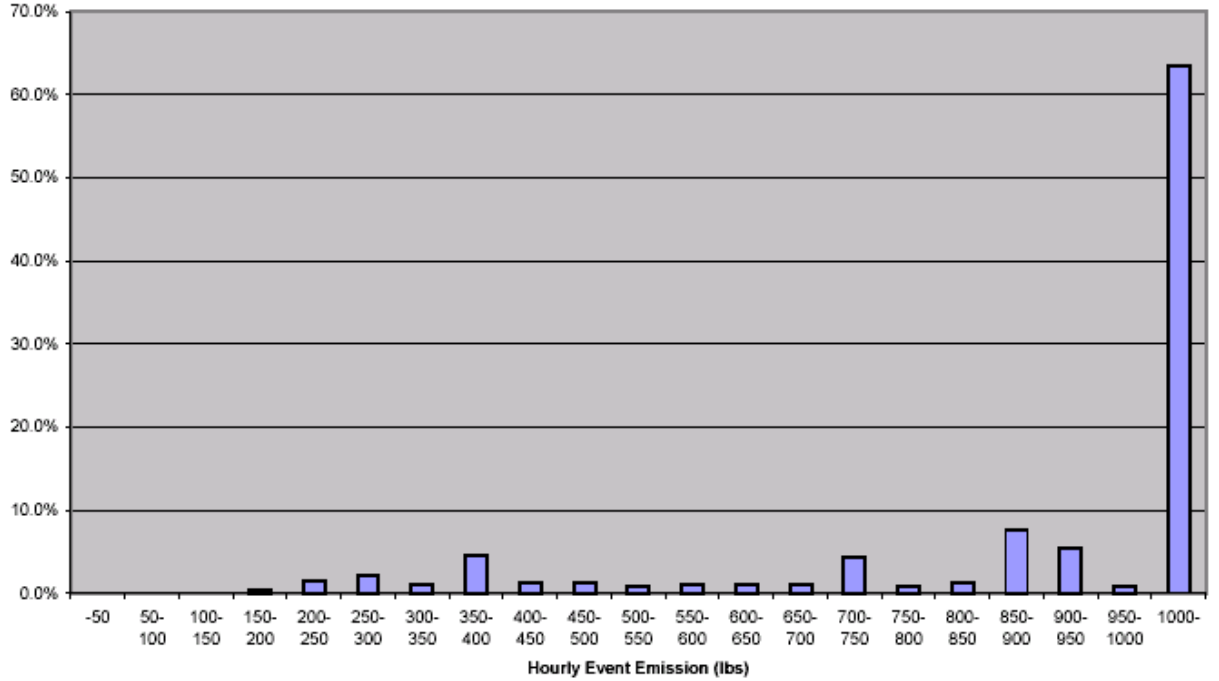
The first control strategy assumes that there is a short term limit such that the maximum event magnitude is 100, 500 or 1000 pounds/hr. Note that there is no assumed effect on event frequency – all events still occur but are limited in maximum magnitude. The results of this analysis are shown in Figure 74. The new median values of worst case emission events are 100, 500 and 1000 pounds/hr, respectively, for emission limits of 100, 500 and 1000 pounds/hr.

The second control strategy assumes that there is a short term limit of 100, 500 or 1000 pounds and that the control strategy has the effect of preventing events over 100, 500 or 1000 pounds (these events are set to zero in the controlled event emission database). In effect, the number of events, or frequency, is reduced because events in excess of the limit are zeroed-out and therefore are assumed to no longer occur. The results of this analysis are shown in Figure 75. The new median values of worst case emission events are 97, 360 and 747 pounds, respectively, for emission limits of 100, 500 and 1000 pounds.

**Finding 3: Emission variability of roughly 1000 lb/hr should be expected in the regions upwind of peak, region wide ozone concentration at least once per year in the Houston-Galveston area.** *This finding is based on estimates of the frequency of ozone conducive conditions and the frequency and magnitude of HRVOC emission events reported through a TCEQ database. This expected value could potentially be decreased by imposing short term limits on HRVOC emission variability.*

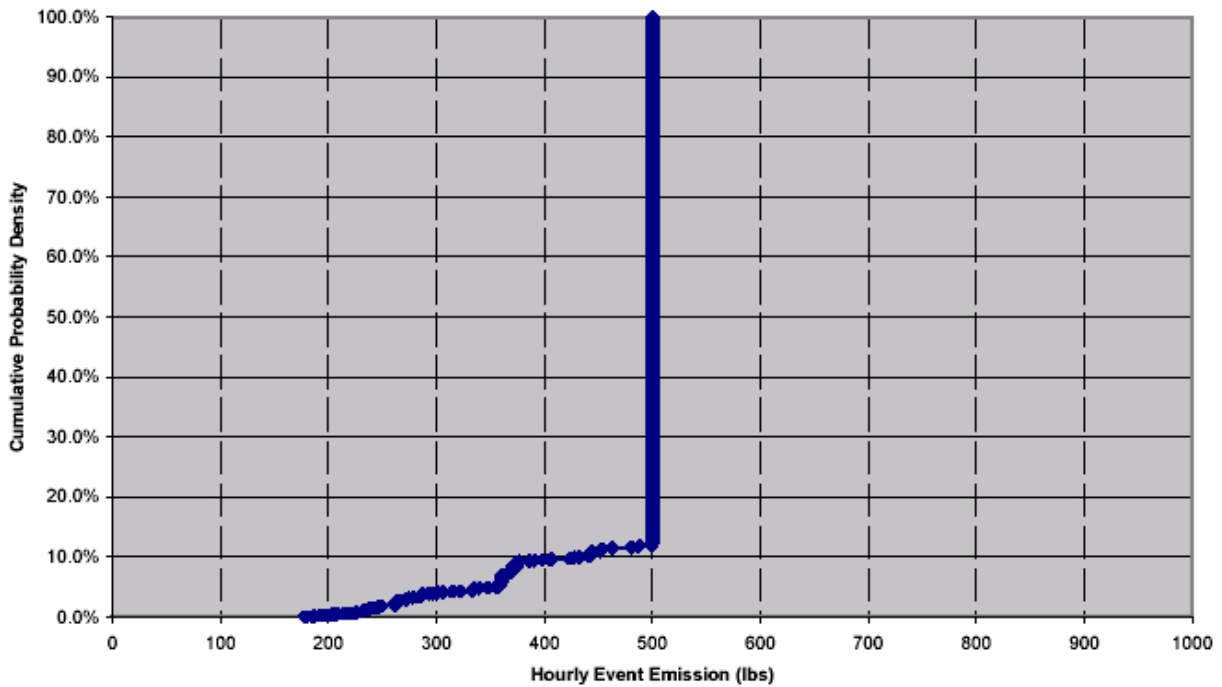
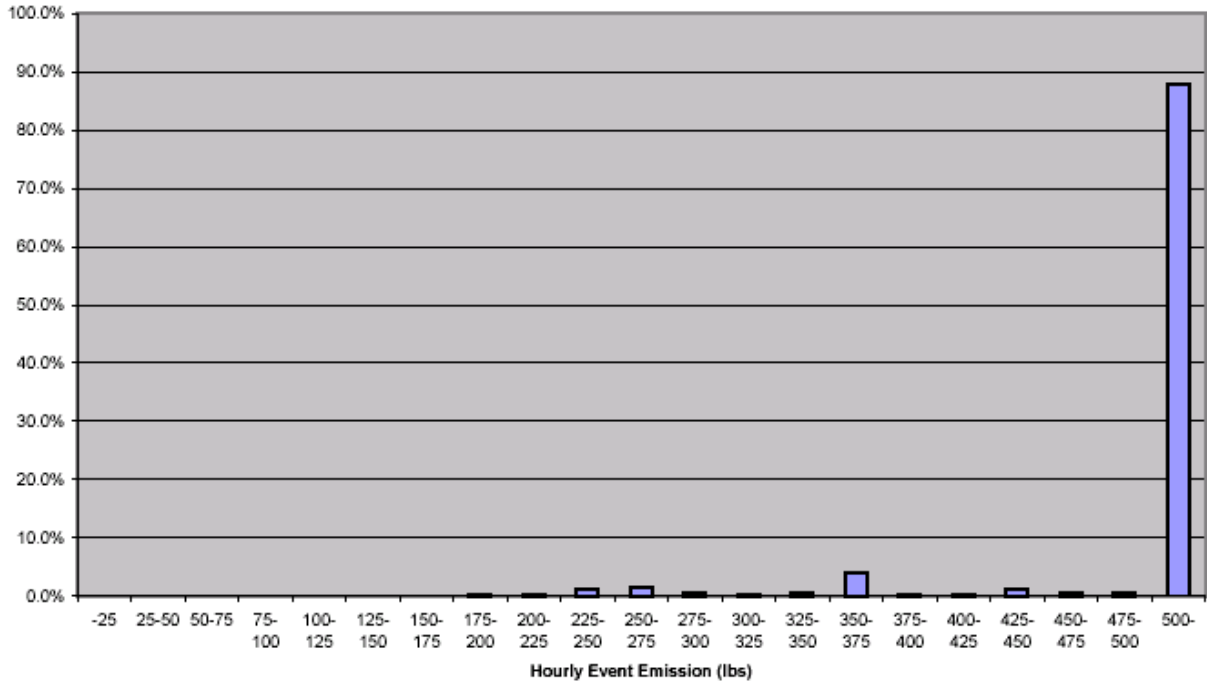
# Draft

**Figure 74a** Distribution of annual worst case emission events in Harris County for total HRVOCs (with a 1000 lb/hr short term limit, but no change in event frequency) that would be expected if 1 hour in one hundred, on average, has the potential for an emission event to impact peak ozone concentration. The median value is 1000 pounds and the 90<sup>th</sup> percentile value is 1000 pounds.



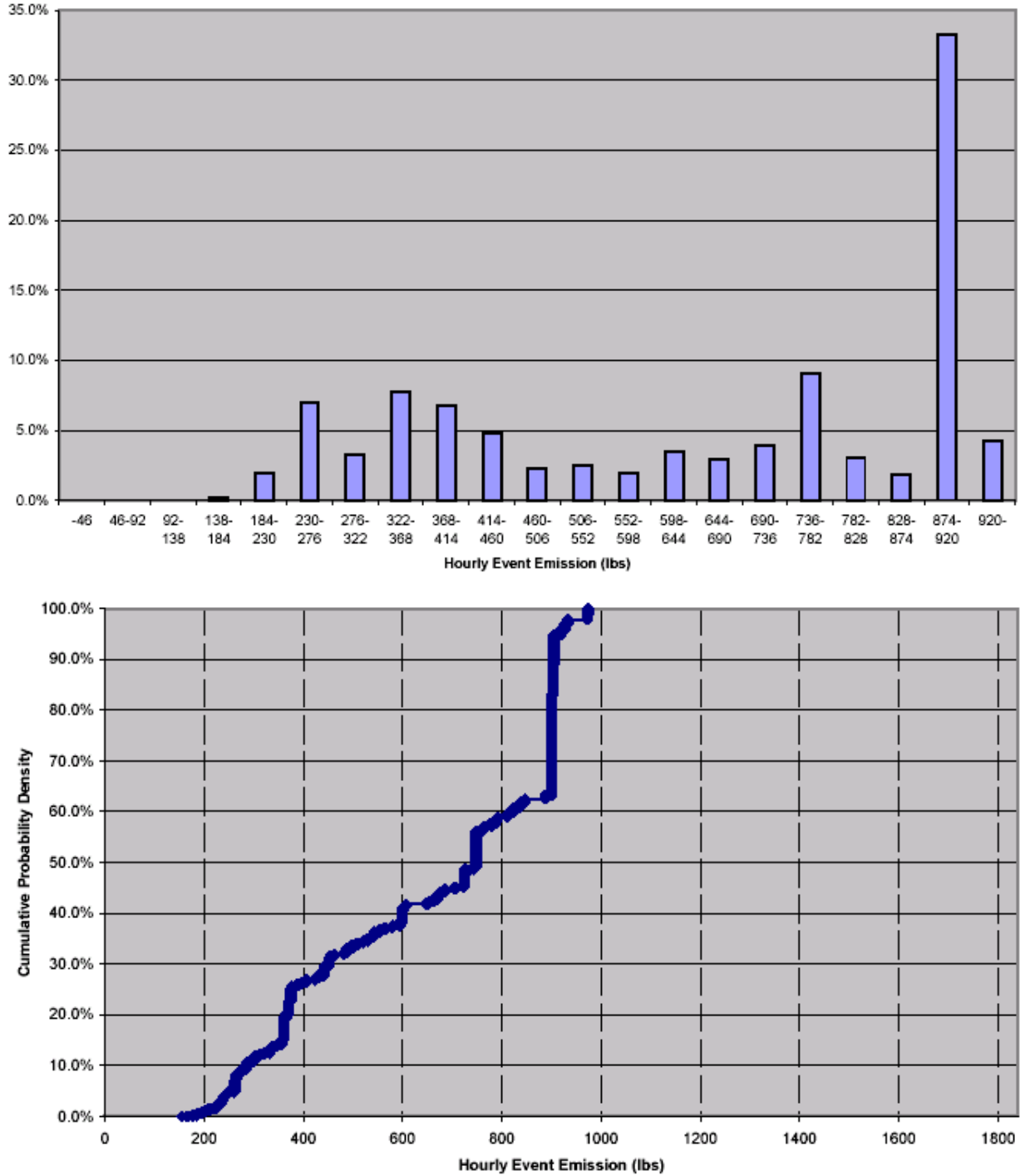
Draft

**Figure 74b** Distribution of annual worst case emission events in Harris County for total HRVOCs (with a 500 lb/hr short term limit, , but no change in event frequency) that would be expected if 1 hour in one hundred, on average, has the potential for an emission event to impact peak ozone concentration. The median value is 500 pounds and the 90<sup>th</sup> percentile value is 500 pounds



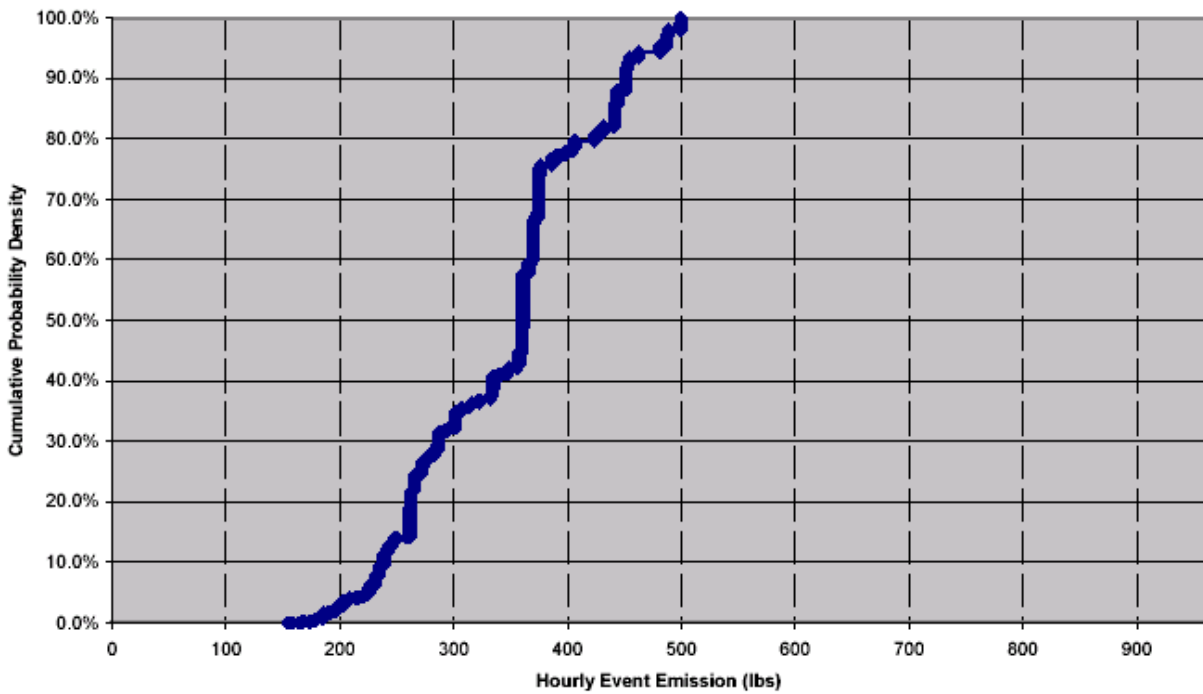
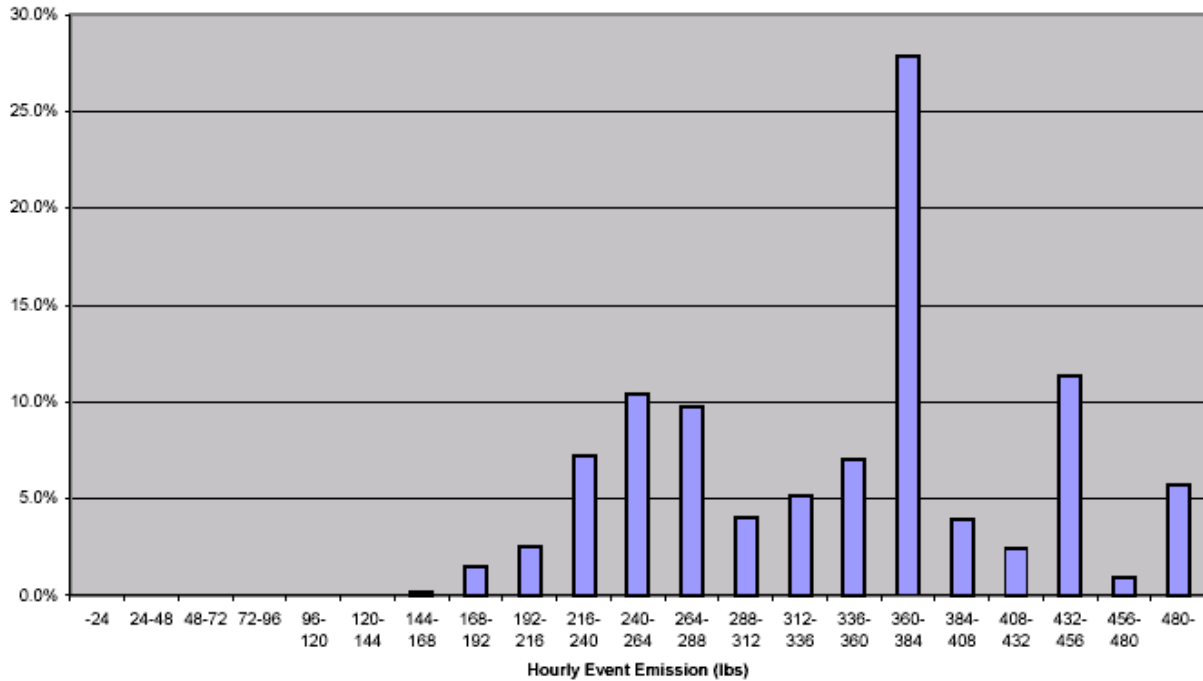
# Draft

**Figure 75a** Distribution of annual worst case emission events in Harris County for total HRVOCs (with a 1000 lb/hr short term limit, which causes events larger than 1000 lb to be prevented) that would be expected if 1 hour in one hundred, on average, has the potential for an emission event to impact peak ozone concentration. The median value is approximately 750 pounds and the 90<sup>th</sup> percentile value is roughly 900 pounds



# Draft

**Figure 75b** Distribution of annual worst case emission events in Harris County for total HRVOCs (with a 500 lb/hr short term limit, which causes events larger than 500 lb to be prevented) that would be expected if 1 hour in one hundred, on average, has the potential for an emission event to impact peak ozone concentration. The median value is approximately 350 pounds and the 90<sup>th</sup> percentile value is roughly 450 pounds



## Draft

## References

- Allen, D., Durrenberger, C. and Texas Natural Resource Conservation Commission, Technical Analysis Division (2003) "Accelerated Science Evaluation of Ozone Formation in the Houston-Galveston Area: Emission Inventories" Version 3, February, 2003, available at <http://www.utexas.edu/research/ceer/texaqsarchive/accelerated.htm>
- Cantu, G. Technical Analysis Division, Technical Support Section "*Point Source Modeling Inventory Development*" presentation at Houston Modeling Workshop, April 1, 2004, available at [http://www.tnrcc.state.tx.us/air/aqp/airquality\\_techcom.html#section5](http://www.tnrcc.state.tx.us/air/aqp/airquality_techcom.html#section5)
- Crouse, R.R. (1990). "Integrated Reaction Rate Analysis of Ozone Production in a Photochemical Oxidant Model," Master's
- ENVIRON, 2004. CAMx Users Guide, v4.00. [www.camx.com](http://www.camx.com).
- Jang, J.C., Jeffries, H.E., Byun, D., Pleim, J.E., 1995a. Sensitivity of Ozone to Model Grid Resolution: Part I. Application of High Resolution Regional Acid Deposition Model, *Atmos. Environ.*, 29(21)3085.
- Jang, J.C., H. E., Jeffries and S. Tonnesen, 1995b. Sensitivity of Ozone to Model Grid Resolution: Part II. Detailed Process Analysis for Ozone Chemistry, *Atmos. Environ.*, 29(21)3114.
- Jeffries H., T. Keating, and Z. Wang, 1997. "Integrated Process rate analysis of the effect of nitrogen oxides emission height on peak ozone concentration predicted by the urban airshed model." Department of Environmental Sciences and Engineering, School of Public Health, The University of North Carolina - Chapel Hill, <http://airsite.unc.edu>. Contract No. 5094-250-3069.
- Jeffries, H. E., 1993. A Different View of Ozone Formation, Fuel Reformulation, 3(1):57; ISSN:1062-3744.
- Jeffries, H.E., 1995. Photochemical Air Pollution, Chapter 9 in *Composition, Chemistry, and Climate of the Atmosphere*, Ed. H. B. Singh, Van Nostrand-Reinhold, New York.
- Jeffries, H.E., and S. Tonnesen, 1994. A Comparison of Two Photochemical Reaction Mechanisms Using a Mass Balance Process Analysis, *Atmos. Environ.*, 28(18):2991-3003.
- Jeffries, H. and Z. Wang, 1997. Applications of Integrated Process Rate Analysis to the SARMAP Air Quality Model, prepared for the California Air Resources Board, prepared by the Department of Environmental Sciences and Engineering, University of North Carolina, Chapel Hill, NC.
- L.I. Kleinman, P.H. Daum, D. Imre, Y-N. Lee, L.J. Nunnermacker, S.R. Springston, J. Weinstein, Lloyd, and J. Rudolf, 2002 "Ozone Production Rate and Hydrocarbon Reactivity in 5 Urban Areas: A Cause of High Ozone Concentration in Houston, *Geophysical Research Letters*.

## Draft

Russell A. and Dennis R., 2000. "NARSTO critical review of photochemical models and modeling." *Atmospheric Environment*, Volume 34, Issues 12-14, Pages 2283-2324.

Seinfeld J. and S. Panids, 1998. *Atmospheric Chemistry and Physics*. John Wiley and Sons, Eds.

Tesche T. W., D. E. McNally, J. G. Wilkinson, H. E. Jeffries, Y. Kimura, C. Emery, G. Yarwood, and D. R. Souten, 2004. "Evaluation of the 16-20 September 2000 Ozone Episode for use in 1\_hr SIP Development in the California Central Valley." Report prepared for the California Air Resources Board (AG-90/TS201).

Texas Administrative Code, Title 30 Environmental Quality, Part 1 Texas Commission on Environmental Quality, Chapter 101 General Air Quality Rules, 2002. Accessed December 2003 at [http://info.sos.state.tx.us/pls/pub/readtac\\$ext.ViewTAC?tac\\_view=5&ti=30&pt=1&ch=101&sch=A&rl=Y](http://info.sos.state.tx.us/pls/pub/readtac$ext.ViewTAC?tac_view=5&ti=30&pt=1&ch=101&sch=A&rl=Y)

Texas Commission on Environmental Quality (formerly Texas Natural Resource Conservation), *Status of Electronic Reporting of Air Emission Incidents*, 2003a. Accessed December 2003 at <http://www.tnrcc.state.tx.us/e-gov/events.html>

Texas Commission on Environmental Quality (formerly Texas Natural Resource Conservation), *Air Emission Event Reports*, 2003b. Accessed December 2003 at <http://www.tnrcc.state.tx.us/enforcement/fod/eer/>

Texas Commission on Environmental Quality, *2001 Point Source Air Emissions Inventory*, August 2003c, <http://www.tnrcc.state.tx.us/air/aqp/psei.html>

Texas Commission on Environmental Quality 2000 Special Inventory, 2003d, <http://airchem.sph.unc.edu>

Texas Commission on Environmental Quality, *Central Registry Query*, 2003. Accessed December 2003e at <http://www2.tceq.state.tx.us/crpub/>

Texas House Bill (HB) 2912, 77<sup>th</sup> Legislative Session. Accessed December, 2003 at <http://www.capitol.state.tx.us/cgi-bin/tlo/textframe.cmd?LEG=77&SESS=R&CHAMBER=H&BILLTYPE=B&BILLSUFFIX=02912&VERSION=5&TYPE=B>

Tonnesen, S., and J. E. Jeffries, 1994. Inhibition of Odd Oxygen Production in Carbon Bond IV and Generic Reaction Set Mechanisms, *Atmos. Environ.*, 28:(7) 1339-1349.

Tonnesen S., 1995. "Development and application of a process analysis method for photochemical oxidant models." Dissertation, University of North Carolina at Chapel Hill, Environmental Sciences and Engineering, School of Public Health.

**Draft**

URS, Case Studies of 2003 Ozone Events Using HRM and TCEQ PAMS Monitors, URS, February 19, 2004 (personal communication, A. Hendler).

Vizuete W., Y. Kimura, D. Allen, B. U. Kim, H. Jeffries, 2004. "Ozone formation phenomena in Southeast Texas," manuscript in preparation to be submitted to *Atmospheric Environment*.

## Appendices

- A. Event Emissions in the Houston-Galveston Area**
- B. Stochastic Emission Inventories of Continuous Emissions**
- C. Case Studies of 2003 Ozone Events Using HRM and TCEQ PAMS Monitors, URS, February 19, 2003**
- D. Sub-domain modeling case studies**